MD-12-SP109B4N

STATE HIGHWAY ADMINISTRATION

RESEARCH REPORT

THEORETICAL AND FIELD EXPERIMENTAL EVALUATION OF SKEWED MODULAR SLAB BRIDGES

CHUNG C. FU, PH.D., P.E.
TIM L. BRINER
TIGIST GETANEH

THE BRIDGE SOFTWARE AND TECHNOLOGY (BEST) CENTER
DEPARTMENT OF CIVIL & ENVIRONMENTAL ENGINEERING
UNIVERSITY OF MARYLAND
COLLEGE PARK, MD 20742

SP109B4N
FINAL REPORT

DECEMBER 2012

Technical Report Documentation Page

1. Report No.	2. Government Accession No.	3. Recipient's Catalog No.
MD-12-SP109B4N		

4. Title and Subtitle	5. Report Date
Theoretical and Field Experimental Evaluation of Skewed Modular Slab Bridges	December 2012
	6. Performing Organization Code

7. Author/s	8. Performing Organization Report No.
Chung C. Fu, Ph.D., P.E.; Tim L. Briner and Tigist Getaneh	

9. Performing Organization Name and Address	10. Work Unit No. (TRAIS)
University of Maryland College Park, MD 20742	11. Contract or Grant No. SP109B4N

12. Sponsoring Organization Name and Address	13. Type of Report and Period Covered
Maryland State Highway Administration Office of Policy & Research 707 North Calvert Street Baltimore MD 21202	Final Report
	14. Sponsoring Agency Code (7120) STMD - MDOT/SHA

15. Supplementary Notes

16. Abstract

As a result of longitudinal cracking discovered in the concrete overlays of some recently-built skewed bridges, the Maryland State Highway Administration (SHA) requested that this research project be conducted for two purposes: (1) to determine the cause or causes of the reflective cracking on those bridges and (2) to propose additions and/or revisions to the current state bridge design standards concerning the number, orientation, and location of the transverse post-tensioning, specifically in reference to a bridge's skewness. At first, a literature review and a state practices survey were conducted. Then, a bridge with a cracked concrete overlay in the State of Maryland was selected and field tested. Subsequently, the FEM model of the tested bridge was used as a base for further parametric study to gain more complete knowledge of how the skew angle affects transversely post-tensioned adjacent precast prestressed concrete slab bridges. Final summary and conclusions with recommended revisions to the current Maryland bridge design standards were made for the SHA's consideration.

17. Key Words	18. Distribution Statement: No restrictions
Skew bridge, precast beam, posttension	This document is available from the Research Division upon request.

19. Security Classification (of this report)	20. Security Classification (of this page)	21. No. Of Pages	22. Price
None	None	96	

Form DOT F 1700.7 (8-72) Reproduction of form and completed page is authorized.

EXECUTIVE SUMMARY

TITLE: EVALUATION OF SKEWED SIMPLE SPAN TRANSVERSELY POST-TENSIONED ADJACENT PRECAST-CONCRETE SLAB BRIDGES

Adjacent precast, prestressed concrete multi-beam bridges have become more prevalent due to their rapid construction time and cost effectiveness. Over the years, various adjustments and refinements have been made to the design of these bridges to reduce typical deteriorations, including shear key failure, reflective cracking of the overlay, chloride penetration, and freeze/thaw damage. Transverse post-tensioning is a common method that improves a bridge's ability to perform monolithically and reduces the amount of cracking in the overlay. This method has been used with some success. However, longitudinal cracking (possibly caused by insufficient and/or inadequate transverse connection between the beams) has been discovered in the concrete overlays of some skewed bridges that have been built within the past five years. As a result, the Maryland State Highway Administration (SHA) requested that this research project be conducted for two purposes: (1) to determine the cause or causes of the reflective cracking on those bridges and (2) to propose additions and/or revisions to the current state bridge design standards concerning the number, orientation, and location of the transverse post-tensioning, specifically in reference to a bridge's skewness.

To facilitate this study, literature review and a state practices survey were conducted in order to gain a thorough understanding of this problem. The literature review details how each component of this type of bridge affects its performance and is contained within this report. The survey of state practices was accomplished using each state's department of transportation Web site and the associated bridge standards on the beam types, span lengths, transverse ties, maximum skew angle, and transverse reinforcement orientation. Twenty states had some

applicable specifications for adjacent precast-concrete multi-beam bridges, and seventeen states had some reference to how the skew angle of a bridge affected those specifications. Although there were no uniform design specifications, the literature review and state practices survey were used to compile a summary of generally agreed upon design principles for use in this research study.

In order to determine the behavior of skewed bridges under live loads, field trips were conducted and a bridge with a cracked concrete overlay was selected for testing by the research team. The test bridge is in Knoxville, MD, on Route 180 over a tributary of the Potomac River. The test bridge is a transversely post-tensioned precast prestressed concrete solid slab panel bridge built in 2007. It is a two-lane simply supported single span bridge with a 22'-3 1/8" span and a 31.4° skew angle. Eight strain transducers were located on the bridge to acquire the short-term live load strains on the bottom and top surfaces of the bridge when a test vehicle drove over the span. The strain transducer installation and the field test were performed by the research team October 10-11, 2011.

Using the bridge plans, a finite element analysis (FEA) model was created of the bridge. The model was refined and adjusted to reflect the field test data so as to analyze possible causes of the longitudinal cracking found in the bridge deck. The research team further analyzed the performance of this bridge using the FEA model and determined that the transverse stress that the bridge undergoes when subjected to a truck load is one of the key components of the crack propagation and perhaps the crack initiation, also.

The basic model construction and the results from the single FEA model were used to conduct a parametric study using FEA models to gain more complete knowledge of how the skew angle affects transversely post-tensioned adjacent precast prestressed concrete slab bridges

to propose revisions and additions to the Maryland bridge design standards. The parametric study was comprised of twenty-eight FEA models that examined three main components of this type of bridge, in addition to a couple load variations, to produce a set of recommendations about the span length, the skew angle, and the transverse post-tensioning orientation of bridges. Three span lengths were considered: 25'-0", 40'-0", and 55'-0". For each span, two skew angles were considered: 15° and 30°. For each bridge model, three different orientations for the tie rods were considered: parallel to the bridge abutments (skewed tie rods), normal to the slabs (normal or normal and staggered tie rods), and a combination of both (skewed tie rods near the supports and normal tie rods near the midspan of the bridge). For a few of the bridge models, the number of transverse post-tensioning bars for each orientation was varied to examine a fuller range of design possibilities. After a truck load was applied to each FEA model, the transverse, longitudinal, first principal, second principal, and third principal stress distributions were examined. The transverse stress at the slab-deck interface was chosen to be the critical analysis component because this stress predominately contributes to the longitudinal reflective cracking in the concrete overlay observed in the field.

After reviewing the results from the background research, field test and associated FEA model results, and the parametric study, conclusions and recommendations are offered. The study found that temperature effects, shrinkage of the shear key grout, the large skew angle, and the vehicle loads all contribute to the longitudinal crack initiation and propagation. It is recommended that the transverse post-tensioning be constructed parallel to the skewed abutments, with an increasing number of transverse tensioning rods as the span length of the bridge increases because this construction greatly reduces the transverse stresses at the slab-deck interface. Building bridges with as small a skew as is practical is preferred, but a skew angle less

than 30^0 is recommended due to the significant increase in transverse stress as the skew angle increases. The table below summarizes the preliminary recommendations for the SHA bridge design standards.

Span (feet)	Maximum Skew Angle (degrees)	Number of Transverse Tie Rods	Orientation of Transverse Tie Rods	Location of Transverse Tie Rods
< 30	30	2	Parallel to Skew	Third Points (L/3)
30 – 45	30	3	Parallel to Skew	5'-0" from Supports and Midspan (L/2)
> 45	30	4	Parallel to Skew	5'-0" and 20'-0" from Supports

Recommended Skew Particulars for Transversely Post-Tensioned Adjacent Precast-Concrete Slab Bridge Standards in Maryland

A secondary finding from the study is that placing the transverse post-tensioning tie rods normal to the beams instead of parallel to the skew near the midspan of the bridge has a negligible effect on the resulting transverse stress at the slab-deck interface. Additionally, the research team recommends that the SHA bridge design standards include the following: (1) The tie rods closest to the abutment should be constructed parallel to the skew of the bridge; (2) The tie rods near the midspan of the bridge may be constructed normal to the beams as long as the maximum spacing between the ends of adjacent tie rods on both sides of the bridge is less than 25 feet; and (3) should the bridge width require it, transverse post-tensioning may be staggered (i.e., one tie rod does not have to connect all of the beams across the width of the bridge) as long as the tie-rods are overlapped (i.e. the tie rods originating from each exterior beam should overlap at least one interior beam). Furthermore, it is recommended that the construction sequence be changed in the following ways: (1) the transverse tendons should be tensioned to approximately 10% of the total force; (2) the shear keys should be filled with grout; and (3) the transverse tendons should be tensioned to the full post-tensioning force. It is recommended that

full-depth shear key designs be examined further because of their reported effectiveness at transferring shear force between beams and because of the corresponding reduction of shear key-related longitudinal cracking.

Table of Contents

List of Figures

List of Tables

Chapter 1: Introduction

1.1 Background

Short-span concrete bridges have been an integral part of the United States' infrastructure system for more than a century. Yet according to the U.S. Federal Highway Administration's (FHWA) bridge inventory data from 2011, almost 24% of the nation's 605,086 bridges are classified as either structurally deficient or functionally obsolete (Federal Highway Administration, 2011). Approximately a quarter of the nation's bridges are single-span concrete bridges (Menassa et al., 2007). Concrete slab and girder bridges constructed in the 1920s and 1930s have been a reliable component of the Maryland road system so far, but due to time and deterioration, many of these bridges need to be repaired or replaced (Narer, 1997). Adjacent precast-concrete multi-beam bridges have been commonly built as a low-cost, rapid-construction alternative, especially where a shallow superstructure is required (Russell, 2009). One relatively new building technique uses transverse post-tensioning to improve the performance of precast-concrete slab or box girder bridges. These bridges were developed in Europe during the 1960s to: (1) maximize the length of cantilever overhangs, (2) minimize the number of webs, (3) improve the connection between longitudinal girders, and (4) provide better and less congested reinforcement layout at piers (Ramirez & Smith, 2003). Transverse post-tensioning practice in combination with the use of diaphragms was adopted in the United States and has become more prevalent in recent years as states have developed building standards to incorporate this bridge reinforcement technique (Saber & Alaywan, 2011; Schaffer, 1967). The FHWA has also begun to encourage the use of adjacent, precast, prestressed concrete girder bridges in the building of small- and medium-span bridges due to several advantages, which include their simple structure,

standardized production, the in-plant quality control that increases girder durability, and ease of construction (Fu et al., 2011).

A recurring problem in adjacent precast-concrete multi-beam bridges is that longitudinal cracks form along the joints between the adjacent beams, which leads to reflective cracks in the concrete overlay (Russell, 2009). These cracks may be caused by stresses from temperature gradients, the live load, or the post-tensioning. The cracks can result in road chemicals leaking through the concrete, which can corrode the steel reinforcement and, ultimately, lead to full cracks through the joint and the loss of load transfer between beams (Russell, 2009). Longitudinal cracks have recently been found in these types of bridges in Maryland and other states, which led the Maryland State Highway Association (SHA) to request the Bridge Engineering Software and Technology (BEST) Center at the University of Maryland to study the post-tensioning force for the transverse post-tensioning (without regard to the bridge skew and tendon layout) and to propose revisions to the state's standards (Fu et al., 2011). Since that study, cracks have been found in additional skewed bridges of this type, which has led to the current study on the best practice for transversely post-tensioning a skewed concrete slab bridge.

1.2 Research Objectives and Scope of Work

In order to thoroughly investigate the effects of transverse post-tensioning on skewed adjacent precast-concrete multi-beam bridges, the following research objectives were identified:

- To locate, assemble, and document other states' bridge design standards for adjacent precast-concrete multi-beam bridges;
- To identify other states' concerns for this type of bridge and to examine any methods used to mitigate those concerns;
- To identify past or current research that has or is being conducted on this issue;

- To examine bridges that have undergone cracking to determine shared characteristics;
- To conduct live-load testing on a bridge that has longitudinal cracking, and to create a computer model of that bridge for further analysis;
- To determine methods to mitigate the longitudinal cracking by conducting a parametric study using finite element analysis (FEA) methods; and
- To organize, evaluate, and document the information acquired in order to produce a final report that contains recommendations for revising the current Maryland bridge design standards.

The information presented in this report is intended to meet the above-listed objectives. This report discusses the empirical and theoretical behavior of skewed concrete slab bridges and a national survey on current state standards for this type of bridge. The report also summarizes a field test that was conducted on a local bridge that has exhibited longitudinal cracking, the FEA simulating the field test and their corresponding results, and a parametric study conducted to determine the best practices for transversely post-tensioning this type of bridge in Maryland. Conclusions and recommendations are offered as a result of this research

1.3 Research Approach

The following five tasks describe the research approach developed for this project:

Task 1: *Survey Other States' Bridge Construction Designs to Identify Key Design Practices*

The Web sites for each state's department of transportation were reviewed to identify bridge standards. The bridge standards were then compiled, summarized, and compared to find

corresponding practices. A similar survey published in 2009 was used to compare and verify the results.

Task 2: *Conduct Literature Review to Gain Broader Knowledge of Topic*

How skewed modular slab bridge evolved throughout the decades was summarized. Former reports and research was examined to determine the theoretical basis for the behavior of this type of bridge and any empirical results from previous bridge tests. The common issues that have been discovered as well as the most common techniques to repair or mitigate those problems were summarized.

Task 3: *Perform Field Test on Local Cracked Bridge*

A live-load field test was conducted on a local bridge on Rte 180 in Knoxville, MD, that has undergone reflective cracking to provide strain data for a better understanding of the bridge behavior as well as to provide data to create a FEA model.

Task 4: *Create and Analyze FEA Models for the Test Bridge and the Parametric Study*

A FEA model of the test bridge was created, refined using field test data, and then analyzed. Using the same base model, a parametric study was conducted to determine the best practice for transversely post-tensioning this type of bridge based on span length and skew angle. Multiple post-tensioning orientations were considered and compared.

Task 5: *Provide Conclusions and Recommendations*

The information obtained was analyzed and compared to draw a set of conclusions and to provide recommendations to make additions and revisions to the current Maryland bridge design code.

Chapter 2: Literature Review

2.1 Skewed Bridges

2.1.1 Definition of a Skewed Bridge

Non-skewed bridges, also known as straight, normal, or right bridges, are built with the longitudinal axis of the roadway normal to the abutment and therefore have a skew angle of 0°. Similar to the American Association of State Highway and Transportation Officials (AASHTO) Load Resistance Factor Design (LRFD) Bridge Design Specifications (2012), the skew angle of a bridge is defined as the angle between the longitudinal axis of the bridge and the normal to the abutment, or, equivalently, as the angle between the abutment and the normal to the longitudinal axis of the bridge as shown in Figure 2-1. Skewed bridges are often built due to geometric restrictions, such as obstacles, complex intersections, rough terrain, or space limitations (Huang et al., 2004; Menassa et al., 2007).

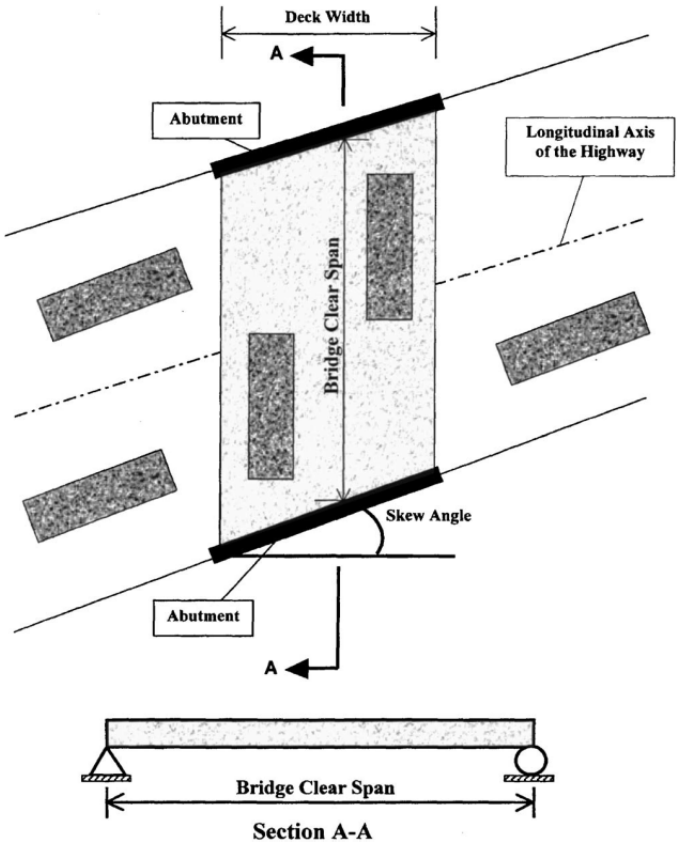

Figure 2-1 Description of a Skew Angle Using a Skewed Bridge over a Highway (Menassa et al., 2007)

2.1.2 General Notes on Skewed Bridges

As early as 1916, design recommendations were made to avoid building skewed bridges because of the many difficulties that arise when designing them, such as complex geometry and load distributions. However, because of increasingly complex site constraints, an increasing number of skewed bridges have been built (Coletti et al., 2011). In addition to the complex geometry and load distributions caused by the skew, the skew angle can affect the performance of the substructure in conjunction with the superstructure, causing a coupling of transverse and longitudinal modes because of wind and seismic loads (Precast/Prestressed Concrete Institute, 2003). Skew angles, in addition to the length to width ratio, also affect whether the bridge

undergoes beam bending or plate action. As the skew increases or the length to width ratio of a bridge decreases, the bridge behaves more similarly to a plate than a beam.

2.2 General Building Practice

2.2.1 Summary of Building Practices

Adjacent precast-concrete slab (or box beam) bridges are built using precast-concrete beams constructed in a factory that are later shipped to the bridge site. The beams are then placed side by side across the abutments and tied together to form an integral structure. The space between the beams is filled with grout material to create a shear key; the beams are also frequently transversely connected using post-tensioning (Fu et al., 2011). A wearing surface, generally cast-in-place concrete, is then poured over the beams. The superstructure of an adjacent precast-concrete multi-beam bridge can often be constructed within two weeks, which is significantly faster than most other alternatives (Narer, 1997). This construction method also satisfies the Accelerated Bridge Construction (ABC) requirement recently promoted by the Federal Highway Administration (FHWA). State standards allow adjacent precast-concrete multi-beam bridges to span 30 to 100 feet, depending on, among other factors, the type of beams and transverse post-tensioning.

2.2.2 Precast-Concrete Beams and Slabs

Precast-concrete box beams or voided slab sections are most commonly used for adjacent precast-concrete multi-beam bridges. However, some states, Maryland included, use only solid slabs because they have proven to be more durable; though they are less structurally efficient. In the past, salt chloride penetration has caused voided slab sections to deteriorate and undergo

punching on the top portion of the slab thus proving a freezing as well as structural problem (Narer, 1997). In this study, only solid slab cases are studied.

2.2.3 Post-Tensioning

After the beams are placed across the abutments, the transverse post-tensioning tendons are inserted through pre-drilled holes. If voided slabs or box beams are used, diaphragms are constructed to contain the transverse post-tensioning tendons. The transverse post-tensioning is provided using either steel strands or rods 0.5 to 1.375 inches in diameter. The ends of the transverse ties are clamped and tensioned to the required force, ranging from 20 to 120 kips depending on each state's bridge design standard, and bolted to the sides of the beams. The recesses where the transverse ties are bolted are then filled in with grout to create a smooth surface with the edge of the beam. On normal bridges, the transverse post-tensioning is placed parallel to the abutment, with the particular locations and number of transverse ties depending on the state standard. On skewed bridges, many states have adopted the practice that transverse ties are placed parallel to the abutment up to 20° or 30° in skew, then, if beyond, placed normal to the girders and staggered, though each state has slightly different standards.

2.2.4 Shear Key Grouting

The shear key, either extending half-depth or full-depth of the beams, depending on the state's bridge design standard, is filled with non-shrink high-strength grout (usually a mixture of sand and mortar) which can be easily vibrated into the gap (Narer, 1997). The construction joint between the beams ties them together to help form an integral unit that distributes stresses more evenly and avoids any differential deflection between the beams (Badwan & Liang, 2007). These shear keys also allow for some fabrication and construction tolerance (Fu et al., 2011).

2.2.5 Cast-in-place Concrete Surface

A cast-in-place concrete overlay is often poured above the beams to further help the structure to perform monolithically, serve as a road surface, and add some protection to keep the beams and joints from deteriorating from the salt chloride road treatments. Some states forgo a concrete overlay and instead use an asphalt road surface or a waterproofing cover in combination with an asphalt road surface.

2.3 Crack Initiation and Propagation

Cracks often occur in adjacent precast-concrete multi-beam bridges, typically as a result of high stresses nearer the supports instead of mid-span. Sharpe (2007) found that these stresses are probably exacerbated by trucks as they pass over the end of the bridge. Results from testing a full-scale member of a multi-beam bridge system showed that cracks in the shear key developed because of thermal strains and were propagated as loads were applied (Badwan & Liang, 2007). This contention, that temperature effects may initiate the cracks, is further supported by observations of cracks on adjacent precast-concrete multi-beam bridges occurring soon after construction was completed but before the bridges were opened for traffic (Russell, 2009). Early parametric finite element studies have also shown that secondary loads from the shrinkage of the shear key and overtopping slab or temperature changes are greater than the applied vehicular loads (Sharpe, 2007). Composite deck slabs, full-depth shear keys, and transverse post-tensioning can reduce the stresses produced in the shear key with varying degrees of effectiveness (Russell, 2009; Sharpe, 2007). Additionally, full-depth shear keys can transfer transverse stresses more evenly between beams, which reduces the stress concentration at the bottom of the shear key (Sharpe, 2007). Full-depth shear keys have been shown to reduce any

hinge behavior that could occur with partial-depth shear keys, helping to transfer moments between beams (Sharpe, 2007). The Maryland state bridge design standards include the use of both composite deck slabs and transverse post-tensioning but do not include full-depth shear keys (MDOT-SHA-OBD, 2006).

Chapter 3: Theoretical Review

3.1 Slab Bridge Behavior

Most American bridges are designed using the AASHTO Standards Specifications for Highway Bridges or the AASHTO LRFD Design Specifications. The AASHTO's simplified design procedure call for reinforced concrete slab bridges to be constructed from a series of beam strips, which use a distribution width for highway loading to form a beam bending problem from a plate bending problem (Menassa et al., 2007). According to Article 4.6.2.2 of the AASHTO LRFD Bridge Design Specifications (2012), if bridge beams are sufficiently connected using a combination of shear keys, transverse post-tensioning, and structural overlay, then the structure will perform as a monolithic unit and may be designed as a whole-width structure. Articles 4.6.2.2.2b, 4.6.2.2.2d, 4.6.2.2.3a, and 4.6.2.2.3b from the AASHTO LRFD Bridge Design Specifications (2012) provide calculations to find the distribution of live loads on a slab bridge for the moments in the interior beams, the moments in the exterior longitudinal beams, the shear in the interior beams, and the shear in the exterior beams, respectively (see Table 3-1).

Load Description	Distribution Factors	Range of Applicability
Moments in Interior Beams	Regardless of Number of Loaded Lanes: S/D Where: $C = K*(W/L) \leq K$ $D = 11.5 - N_L + 1.4 * N_L * (1 - 0.2 * C)^2$ When $C \leq 5$ $D = 11.5 - N_L$ When $C > 5$ $K = \sqrt{\frac{(1+\mu) * I}{J}}$	Skew $\leq 45^{o}$ $N_L \leq 6$
Moments in Exterior Longitudinal Beams	One Design Lane Loaded: $g = e * g_{interior}$ $e = 1.125 + \frac{d_e}{30} \geq 1.0$ Two or More Design Lanes Loaded: $g = e * g_{interior}$ $e = 1.04 + \frac{d_e}{25} \geq 1.0$	$d_e \leq 2.0$

Shear in Interior Beams	One Design Lane Loaded: $\left(\frac{b}{130 * L}\right)^{0.15} * \left(\frac{I}{J}\right)^{0.05}$ Two or More Design Lanes Loaded: $\left(\frac{b}{156}\right)^{0.4} * \left(\frac{b}{12.0 * L}\right)^{0.1} * \left(\frac{I}{J}\right)^{0.05} * \left(\frac{b}{48}\right)$ $\frac{b}{48} \geq 1.0$	$35 \leq b \leq 60$ $20 \leq L \leq 120$ $5 \leq N_b \leq 20$ $25{,}000 \leq J \leq 610{,}000$ $40{,}000 \leq I \leq 610{,}000$
Shear in Exterior Beams	One Design Lane Loaded: $g = e * g_{interior}$ $e = 1.125 + \frac{d_e}{20} \geq 1.0$ Two or More Design Lanes Loaded: $g = e * g_{interior} * \left(\frac{48}{b}\right)$ $\frac{48}{b} \leq 1.0$ $e = 1 + \left(\frac{d_e + \frac{b}{12} - 2.0}{40}\right)^{0.5} \geq 1.0$	$d_e \leq 2.0$ $35 \leq b \leq 60$
Where: S = spacing of beams or webs (feet) D = width of distribution per lane (feet) C = stiffness parameter K = constant for different types of construction W = edge-to-edge width of bridge (feet) L = span of beam (feet) NL = number of design lanes as specified in Article 3.6.1.1.1 μ = Poisson's ratio I = moment of inertia (in.4) J = St. Venant's torsional inertia (in.4) g = distribution factor e = correction factor de = horizontal distance from the centerline of the exterior web of exterior beam at deck level to the interior edge of curb or traffic barrier (feet) b = width of beam (in.) Nb = number of beams, stringers, or girders		

Table 3-1 Distribution of Live Loads for a Superstructure Consisting of Concrete Beams Used in Multi-Beam Decks (AASHTO, 2012)

3.2 Skew Bridge Behavior

Alternate load paths and different load distributions are two complications that arise when designing a bridge with a skew angle (Coletti et al., 2011). Depending on the transverse stiffness of the bridge, some of the load travels transversely to the obtuse corners of the skewed bridge abutments, due to the shorter path, rather than traveling along the longitudinal girders (see Figure 3-1), which reduces the longitudinal bending moments and increases the shear in the obtuse corners (Precast/Prestressed Concrete Institute, 2003).

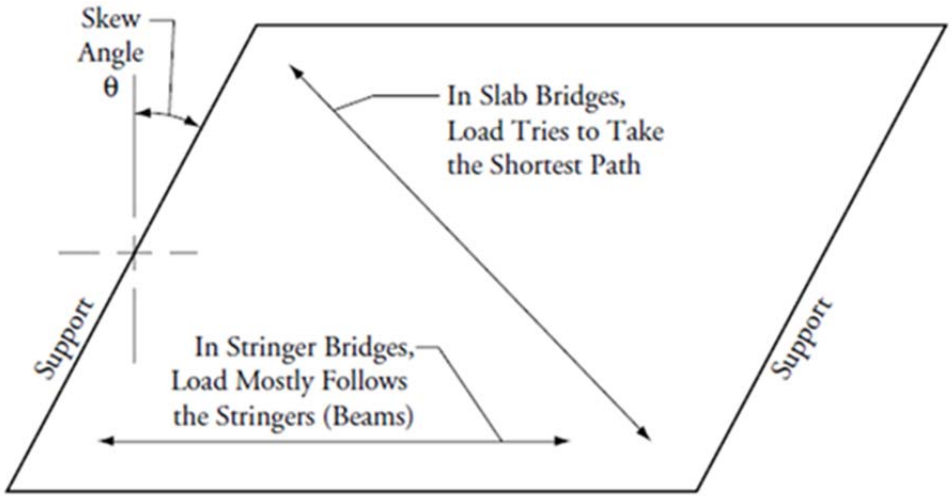

Figure 3-1 Load Path on a Skewed Bridge (Precast/Prestressed Concrete Institute, 2003)

The increased reactions at the obtuse corners of the bridge lead to a corresponding decrease in the reactions at the acute corners of the bridge, which can then lead to the uplift of the acute corners in extreme situations (Oregon Department of Transportation, 2004). These increased reactions in the obtuse corners also lead to an increase in the shear in the exterior beams near the obtuse corners and can produce transverse shear in the structure (Oregon Department of Transportation, 2004). In addition to increasing the shear on the exterior beams of a bridge, skew angles greater than 20˚ affect the bending moment applied to a bridge

(Precast/Prestressed Concrete Institute, 2003). Menassa et al. (2007) showed that as the skew angle increases, the maximum longitudinal bending moment decreases but is offset by an increase in the maximum transverse moment. Corresponding with the decrease in the maximum longitudinal bending moment, the maximum live-load deflection also decreases.

Pertaining to these findings, the AASHTO LRFD Bridge Design Specifications (2012) include corrections for longitudinal bending moments and support shear of the obtuse corner. Article 4.6.2.2.2e states that the bending moment in the longitudinal beams can be reduced based on the skew angle as long as the difference in skew angles of adjacent supports does not exceed 10° (see Table 3-2) (AASHTO, 2012). Additionally, Article 4.6.2.2.3c conservatively applies a correction factor for the shear force at the obtuse corner to all of the beams. However, this correction may not be conservative with respect to uplift at the acute corners and additional investigation should be done to determine the uplift on skewed structures (see Table 3-2) (AASHTO, 2012). See Figure 3-2 for how these equations behave with respect to the skew angle.

Load Distribution Factor Description	Correction Factor	Range of Applicability
Reduction for Moment in Longitudinal Beams	$1.05 - 0.25 * \tan\theta \leq 1.0$	$0^0 \leq \theta \leq 60^0$ If $\theta > 60^0$ use $\theta = 60^0$
Correction for Support Shear of the Obtuse Corner	$1.0 + \frac{12.0 * L}{90 * d} * \sqrt{\tan\theta}$	$0^0 \leq \theta \leq 60^0$ $20 \leq L \leq 120$ $17 \leq d \leq 60$ $35 \leq b \leq 60$ $5 \leq N_b \leq 20$
Where: θ = skew angle (degrees) L = span of beam (feet) d = depth of beam or stringer (inch) b = width of beam (inch) N_b = number of beams, stringers, or girders		

Table 3-2 Corrections for Load Distribution Factors for Concrete Box Beams Used in Multi-Beam Bridges on Skewed Supports (AASHTO, 2012)

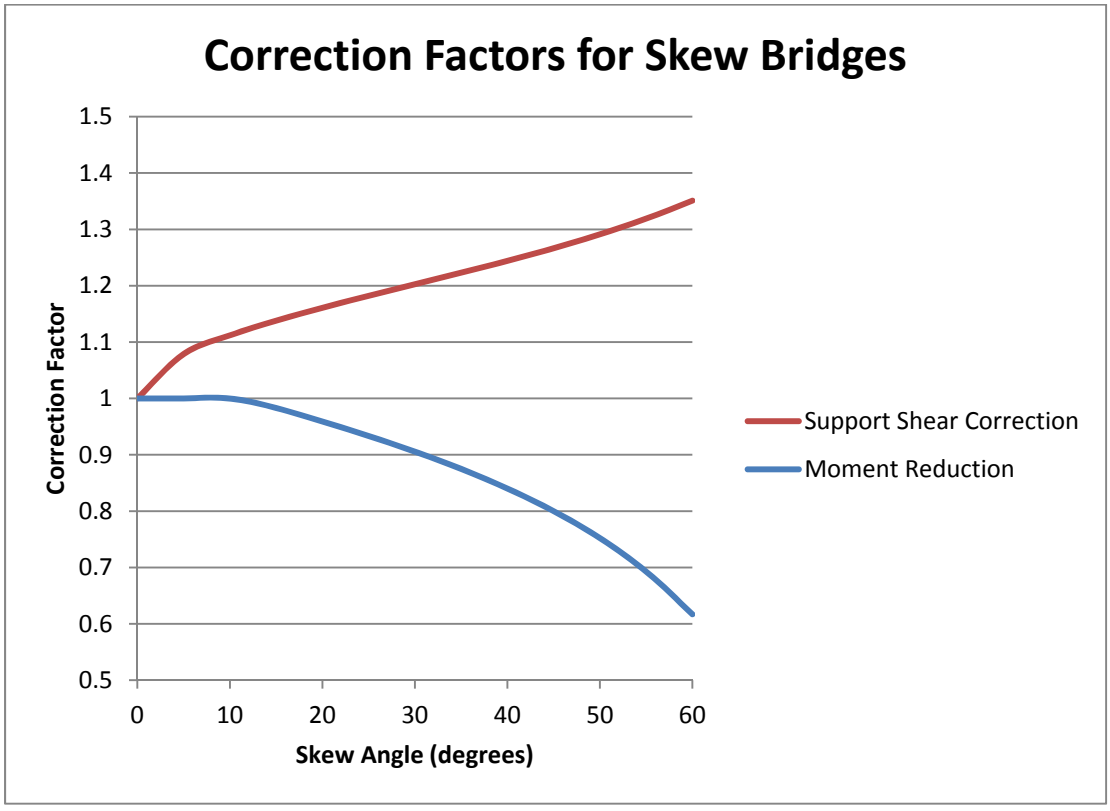

Figure 3-2: Corrections for Load Distribution Factors for Concrete Box Beams Used in Multi-Beam Bridges on Skewed Supports Based on L = 40 ft. and d = 20 in.

Coletti et. al. (2011) showed that the torsional loads and deflections produced depend on the orientation of the diaphragms or transverse supports. For example, when the transverse supports are placed parallel to the skew, they connect longitudinally proportionate points along the beams which undergo consistent vertical deflections and thus can cause some lateral bending. When the transverse supports are placed normal to the beams, however, they connect points on adjacent beams that are undergoing different vertical deflections and thus inducing some torsional loads in the beams.

Skewed bridges undergo differential thermal expansion unlike non-skewed bridges because of their geometry and because their precast-concrete slabs are at least partially affixed to the bridge's abutments. The geometry causes the thermal movement of a skewed bridge to be asymmetrical, with the movement centered on a line between the acute corners of the skewed bridge, as shown in Figure 3-3 (Coletti et al., 2011). Thermal contraction and concrete shrinkage produce similar effects (Precast/Prestressed Concrete Institute, 2003).

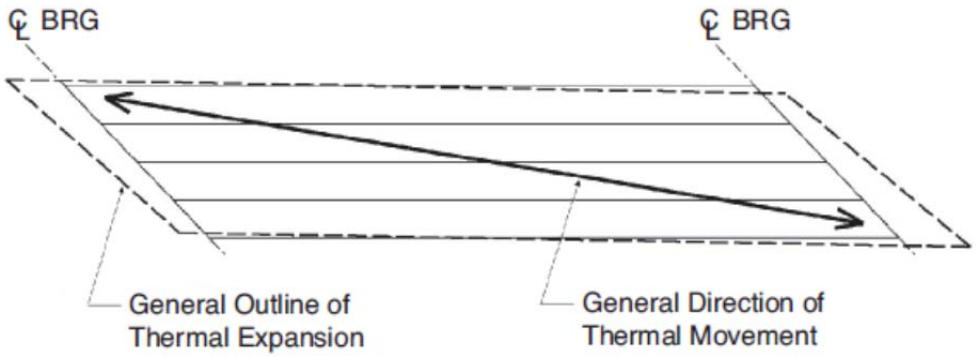

Figure 3-3: General Effect of Thermal Expansion on a Skewed Bridge (CL BRG = Centerline Bearing) (Coletti et al., 2011)

3.3 Post-Tensioning Behavior

The utility of post-tensioning as a tool for crack prevention has been questioned because of the relatively low force some states' bridge design standards assign (about 30 kips) and the minimal amount of post-tensioning provided (two or three strands). Additionally, the small compression force (15 psi near the post-tensioning and 0 psi further from the post-tensioning) is not consistently applied to the shear keys and is miniscule compared to the compressive force suggested to be provided at key points along the bridge, including the ends (Sharpe, 2007). AASHTO LRFD specifications (2012) recommend a transverse post-tensioning stress of at least 0.25 ksi to sufficiently connect adjacent girders and suggests that post-tensioning is more effective than a structural overlay. However, the article fails to provide a depth over which the stress should be applied, which may account for the variation in states' practices (AASHTO, 2012; Russell, 2011). Despite the variation in states' practices, transverse post-tensioning does help the bridge to behave as a monolithic structure and specifically contributes to the shear friction between beams.

Discussed in section 11.6 of the American Concrete Institute (ACI) Building Code Requirements for Structural Concrete ACI 318-11 (2011), shear friction should be applied where it is appropriate to consider shear transfer across a given plane, such as to an existing or potential crack, an interface between dissimilar materials, or an interface between two concretes cast at different times. Steel reinforcement is usually placed across an area where engineers anticipate that the concrete will crack. The steel reinforcement increases the normal force to the crack and acts as a clamp around the crack by creating friction to resist the shear (Badwan & Liang, 2007). The combination of transverse post-tensioning and shear keys on some adjacent precast-concrete multi-beam bridges contributes to the shear friction produced between adjacent beams and

causes the beams to perform as a monolithic plate structure. This configuration, especially after a crack has occurred, helps ensure that stress is distributed among all of the adjacent beams and decreases the possibility that a single beam in the slab bridge will carry the entire applied load.

Chapter 4: Policy Research – Survey of State Practices for Transversely Post-Tensioned Bridges

4.1 Survey Methodology

The research team consulted each state's department of transportation Web site (see Appendix A) and the associated structures' departments and bridge standards for the survey of state practices for constructing adjacent precast-concrete multi-beam bridges. Once the data was obtained and compiled, it was compared with the bridge design standards used in Maryland. Fewer than half of the states have adjacent precast-concrete multi-beam bridge standards on their Web sites, and, of those that do, not all have explicit standards for the following critical design elements: post-tensioning force, transverse tendon specifications, and skew particulars. Twenty states listed applicable specifications for adjacent precast-concrete multi-beam bridges posted online, and seventeen states had some reference to skew limitations for this type of bridge. These standards have all been published within the last decade.

4.2 Beam Types and Span Lengths

A few types of beams are used for adjacent precast-concrete multi-beam bridges with different allowable span lengths. Box beams are the most common beam type, but both voided and solid slabs are used by different states. Maximum span lengths range from 50 feet to greater than 100 feet, although the most common span lengths are between 20 and 80 feet (Russell, 2011).

4.3 Transverse Post-Tensioning Tendons

Post-tensioning specifications need to be fully detailed because of the complexities of building transversely post-tensioned adjacent precast-concrete multi-beam bridges. To be useful for the purposes of this survey, standards should include information about the type, diameter, force, number, and location of transverse tendons. Most of the states surveyed included this information.

4.3.1 Type

States typically use unbonded strands, consisting of six high-tensile strength steel wires wrapped helically around a central wire or unbonded high-strength steel threaded tie rods (bars) (Corven & Moreton, 2004). A few states use multi-strands, bonded strands, or bonded tie rods (Russell, 2011).

4.3.2 Diameter

Diameters of transverse tendons have a relatively large range. States that use strands typically require either a 0.5 or 0.6 inch diameter. Tie rods are required to have a diameter of anywhere between 0.5 and 1.375 inches.

4.3.3 Force

States' standards included a large range of transverse post-tensioning force requirements. The majority of states use 30 kips, but the standards range from 20 kips to 120 kips.

4.3.4 Number and Location

As with the other transverse tendon specifications, the number and location of the tendons varies from state to state. States require from one to ten transverse post-tensioning tendons with the most common requirement ranging between two and four tendons. The tendons can be arranged in a variety of ways, including a regular discretization of the bridge span (e.g., locating tendons at the midspan, third points, quarter points, etc.) or specified distances (e.g., eleven feet apart). Figure 4-1 shows common ways to locate tendons; these location methods depend on the number of tendons being used.

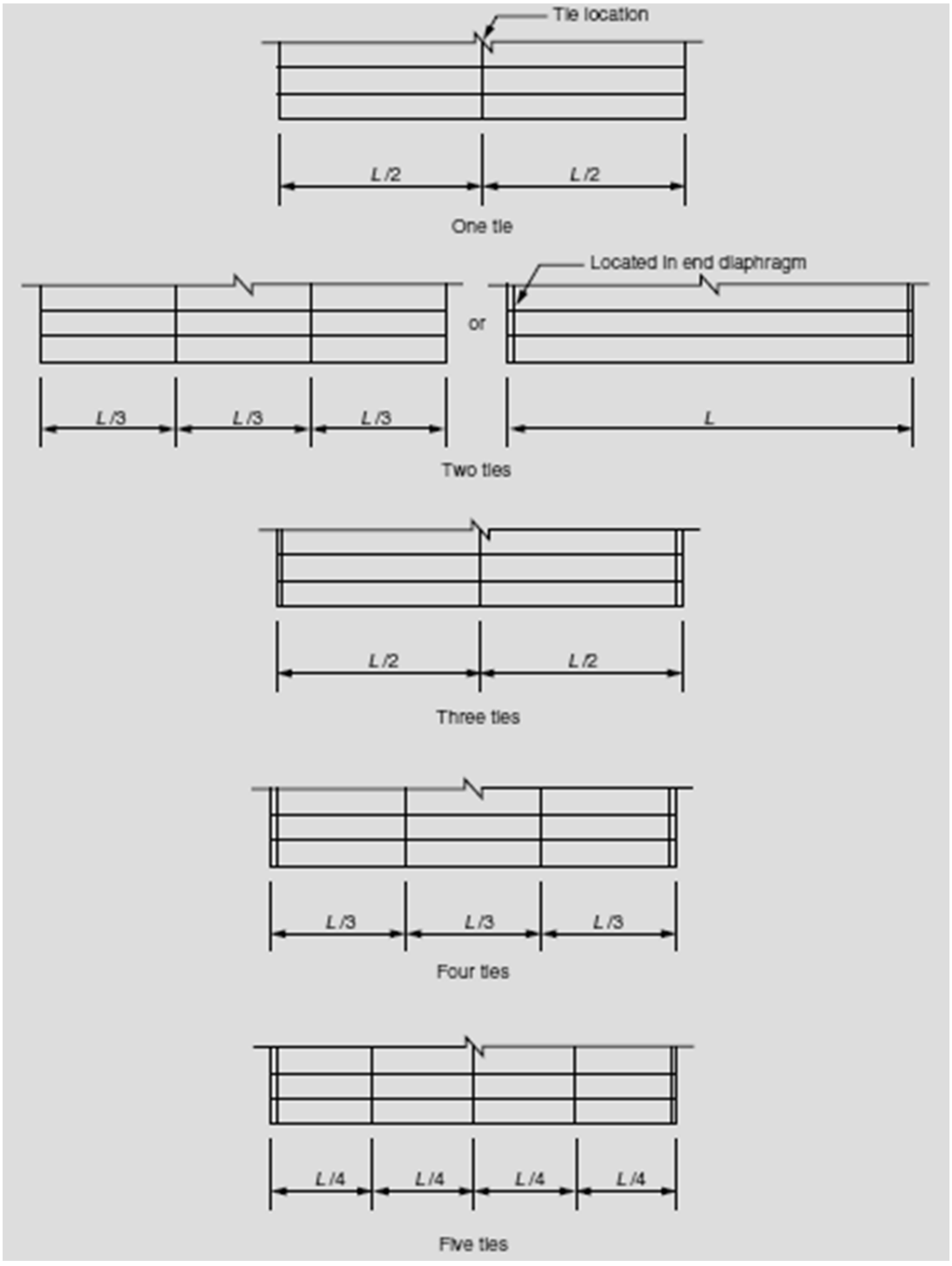

Figure 4-1 Common Transverse Post-Tensioning Tendon Locations Based on the Number of Ties (Note: L = Length of Span) (Russell, 2011)

4.4 Skew Specifications

In addition to specifying the requirements for the transverse post-tensioning, some states' standards also included limitations for skewed bridges. The skew angle often determines both the transverse tendon orientation as well as whether the adjacent precast-concrete multi-beam bridge is permitted to be constructed.

4.4.1 Tendon Orientation

The transverse tendons transfer applied loads to the connected concrete beams in different ways depending on their orientation. The tendons can either remain normal to the beams and staggered throughout the cross-section of a skewed bridge or they can be placed parallel to the bridge's skew angle. A staggered orientation is often easier to install but it connects the beams at different relative distances along the beams. Though more difficult to install, tendons with a skewed orientation connect the beams at their same relative points thus making the skew bridge behave more similarly to a normal bridge. Figure 4-2 shows the possible transverse tendon orientations and the corresponding possible diaphragm construction possibilities for box beams or voided slabs.

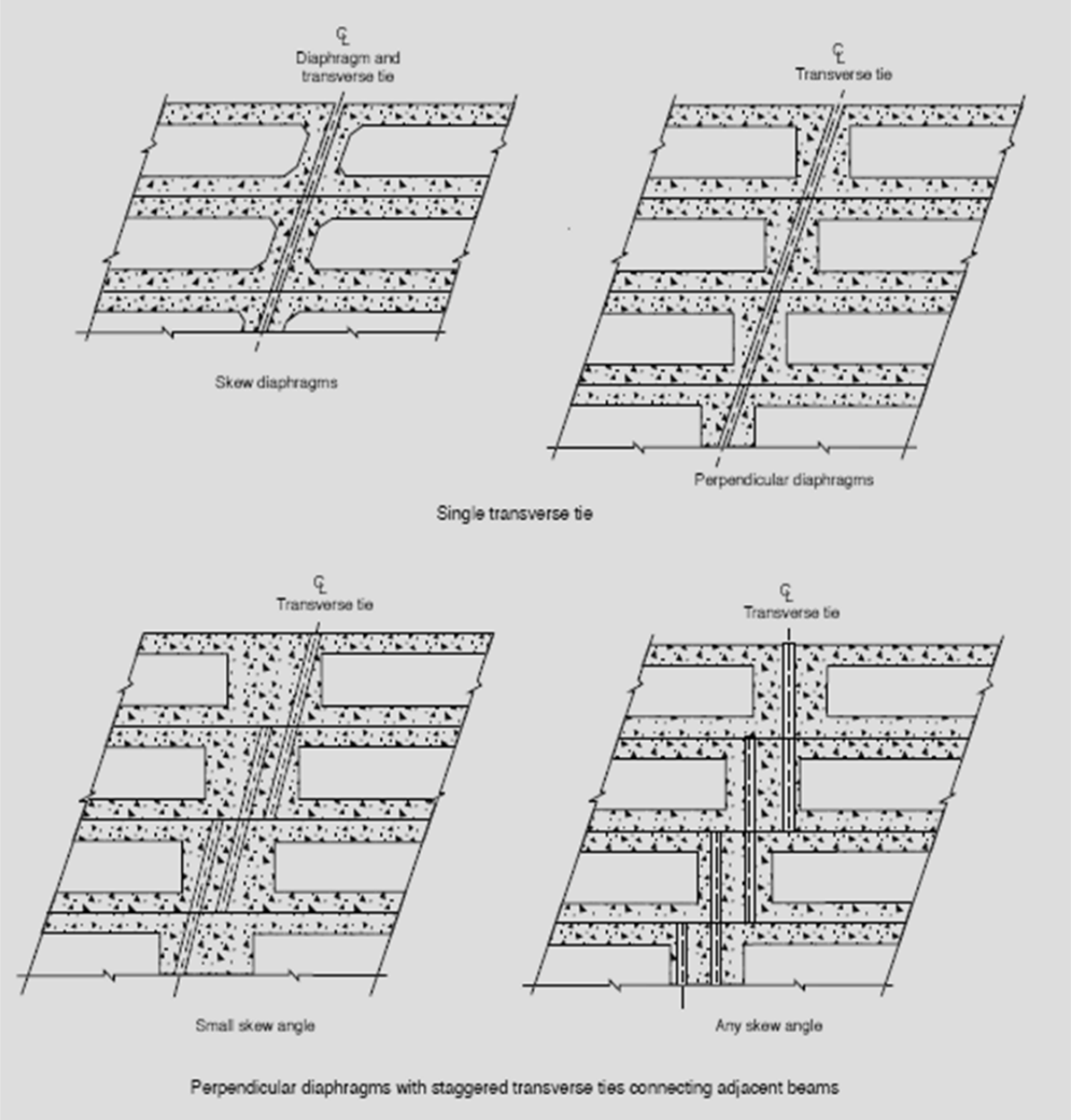

Figure 4-2 Transverse Tendon Orientation and Diaphragm Construction Options (Russell, 2011)

4.4.2 Orientation Parameters

Both the skew angle and the span length affect the transverse tendon orientation practices and whether the bridge is constructed. Most states recommend that the transverse tendons be built parallel to the skew when the skew angle is less than 20-30°. Some states recommended

placing the transverse tendons normal to the beams and staggered at skew angles greater than 20-30°, while some restrict the maximum allowable skew angle to 30°. Again, there is a wide variation in different states' practices as confirmed by a similar survey's findings, as shown in Figure 4-3. A summary of the skew specifications survey is shown in Table 4-1.

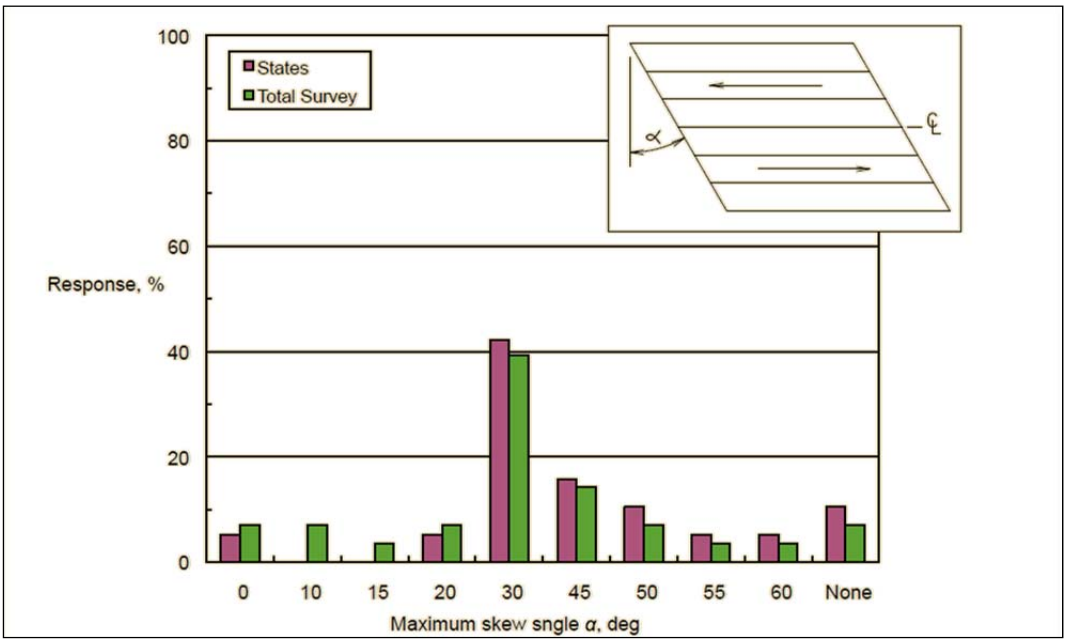

Figure 4-3 Alternate Survey Results for Maximum Skew Angle Specification (Russell, 2011)

Skew	Placement of Transverse Ties	
	Parallel to Skew	Normal and Staggered
$\leq 20^0$	3	0
$\leq 30^0$	6	1
	Do Not Build	Normal and Staggered
$> 20^0$	0	3
$> 30^0$	8	3
$> 45^0$	2	0

Table 4-1 Summary of 17 States' Transverse Post-Tensioning Specifications for Skewed Adjacent Precast Prestressed Concrete Multi-Beam Bridges

4.5 Full Survey Results

The full survey results are shown in Tables 4-2 and 4-3.

State	Beam Type (BB = Box Beam; SS = Solid Slab; VS = Voided Slab)	Span (ft)	Transverse Ties					Year
			Type	Diameter (in)	Force (kips)	Location	Number	
AZ	BB, VS	< 50	Tie rod	1.5	30	Midspan	1	2007
	BB, VS	50 - 75	Tie rod	1.5	30	Third Points	2	
	BB, VS	> 75	Tie rod	1.5	30	Quarter Points, Midspan	3	
CT	BI & BI Mod. BB, VS	≤ 50	Strand		30	Ends, Midspan	3	2003
	BI & BI Mod. BB, VS	> 50	Strand		30	Ends, Third Points	4	
	BII BB, VS	≤ 75	Strand		30	Ends, Third Points	4	
	BII BB, VS	> 75	Strand		30	Ends, Quarter Points	4	
	BIII BB, VS	≤ 75	Strand		30	Ends	2	
	BIII BB, VS	> 75	Strand		30	Ends, Quarter Points	4	
	BIV & BIV Mod. BB, VS	ALL	Strand		30	Ends, Quarter Points, Midspan	5	
DC	BB, VS		Strand or Tie rod	0.5 - 1.375				2009
IN	BB		Tie rod	1	20			2011
KY	BB	≤ 50	Tie rod	1	20	Midspan	1	2008
	BB	> 50	Tie rod	1	20	Third Points	2	
MA	BB	≤ 50	Strand	0.6	44	Ends, Midspan	3	2009
	BB	> 50	Strand	0.6	44	Ends, Quarter Points, Midspan	5	
MI	BB	≤ 50			120	Ends, 2 at Center of Span (11 ft. apart)	4	2011
	BB	50 - 62			120	Ends, Quarter Points, Midspan	5	
	BB	62 - 100			120	Ends, Quarter Points, 2 at Center of Span (11 ft.	6	

						apart)		
	BB	> 100			120	Ends, All Fifth Points	7	
NY	BB, SS, VS	≤ 50	3 Strands	0.5	28	Ends, Midspan	3	2011
	BB, SS, VS	> 50	3 Strands	0.5	28	Ends, Quarter Points, Midspan	5	
NC	BB, VS		Strand	0.6	44			2012
OH	BB	≤ 50	Tie rod	1		Midspan	1	2011
	BB	50 - 75	Tie rod	1		Third Points	2	
	BB	> 75	Tie rod	1		Quarter Points, Midspan	3	
PA	BB	≤ 45				Ends	2	2011
	BB	45 - 55				4 ft. from Ends	2	
	BB	55 - 77				16 ft. from Ends	2	
	BB	> 77				16 ft. from Ends, Midspan	3	
OR	BB, SS		Tie rod	7/8				2011
RI	VS	58	Strand	0.6	44	Ends, Midspan	3	2010
	BB	≤ 50	Strand	0.6	44	Ends, Midspan	3	
	BB	> 50	Strand	0.6	44	Ends, Quarter Points, Midspan	5	
	BB	≤ 50	Strand	0.6	44	Ends, Midspan (2 stacked for depth > 33 in.)	6	
	BB	> 50	Strand	0.6	44	Ends, L/4 (2 stacked for depth > 33 in.)	10	
SC	VS		Strand or Tie rod	0.5	30			2007
	VS	30, 40, 50, 60	Tie rod	1.25		Third Points	2	2010
	VS	70	Tie rod	1.25		Quarter Points, Midspan	3	
TX	SS	40, 50	Strand	0.5				2012
	BB	max: 60-100	Strand	0.5				
VT	BB, VS	≤ 50	Strand	0.6	30			2011

	BB	50 - 90	Strand	0.6	30			2010
WA	BB, VS, SS		Strand	0.6		Ends, Midspan	3	2012
WV	BB	20 - 94	Strand	0.6	80			2004
WI	BB	≤ 24	Strand	0.6	86.7	Ends, Quarter Points, Midspan	5	2012
	BB, VS	24 - 92	Strand	0.6	86.7	Ends, Quarter Points, Midspan	5	
WY		≤ 40	Strand	0.6				2008
		40 - 80	Strand	0.6		Midspan	1	
		> 80	Strand	0.6		Third Points	2	

Table 4-2 States' Transverse Post-Tensioning Specifications for Single Span Precast Prestressed Concrete Beam Bridges

State	Skew	Placement of transverse reinforcement
AZ	$\leq 20^0$	Parallel to abutments and piers
	$> 20^0$	Normal to girders and staggered
CT	$\leq 30^0$	Parallel to abutments and piers
	$> 30^0$	Normal to girders and staggered
DC	$\leq 30^0$	Parallel to abutments at ends, normal to girders at midspan
	$> 30^0$	Do not build
IN	$\leq 25^0$	Parallel to abutments and piers
	$> 25^0$	Normal to girders and staggered
KY	$\leq 10^0$	Parallel to abutments and piers
	$> 10^0$	Normal to girders and staggered
NY	$\leq 50^0$	Parallel to abutments and piers
	$> 50^0$	Do not build
OH	$\leq 4^0$	Parallel to abutment (4 ft. wide beams)
	$\leq 5^0$	Parallel to abutment (3 ft. wide beams)
	4^0 - 30^0	Normal to girders and staggered (4 ft. wide beams)
	5^0 - 30^0	Normal to girders and staggered (3 ft. wide beams)
	$> 30^0$	Do not build
PA	$> 20^0$	Do not build if span > 131ft
	$> 30^0$	Do not build if span > 88ft
	$> 45^0$	Do not build
OR	$> 30^0$	Do not build if precast box
	$> 45^0$	Do not build if precast slab
RI	$> 30^0$	Do not build unless authorized by engineer
SC	$\leq 30^0$	Consider as straight bridge
TX	$> 30^0$	Do not build
VT	$> 30^0$	Fill the clipped void with foam filler prior to the overlay placement or using the overlay concrete to fill the void
	$> 45^0$	Do not build
WA	$\leq 30^0$	Parallel to abutments and piers
	$> 45^0$	Do not build
WV	$\leq 25^0$	Parallel to abutments and piers
	$> 25^0$	Normal to girders and staggered
WI	$\leq 30^0$	Parallel to abutments and piers
	$> 30^0$	Not recommended, Normal to girders and staggered if built
WY	$\leq 20^0$	Parallel to abutments and piers
	$> 20^0$	Normal to girders and staggered

Table 4-3 States' Transverse Post-Tensioning Specifications for Skewed Precast Prestressed Concrete Beam Bridges Based on Skew Angle

Chapter 5: Field Testing Research

5.1 Test Bridge Description

5.1.1 Summary of Test Bridge

The SHA requested that the BEST Center at the University of Maryland test one of five transversely post-tensioned adjacent concrete slab bridges constructed within the past five years that were found to have cracks on their top surfaces. The goal was to determine the cause or causes of the cracks and to propose revisions and/or additions to the Maryland Bridge Standards. The test bridge selected was Structure No. 10381XO, a transversely post-tensioned prestressed concrete slab panel bridge built in 2007 and located in Knoxville, MD, on MD Route 180. The bridge spans a tributary of the Potomac River. It is a two-lane simply-supported single-span bridge with a 22'-3.125" span and a 31.4° skew angle. The superstructure consists of eight adjacent 4'-0" x 1'-3" x 23'-4.125" prestressed concrete beams and a typical 5" minimum thick composite concrete deck. A 2'-0" x 3'-11" concrete barrier parapet is located on each exterior slab along the entire length of the bridge.

5.1.2 Bridge Specifications

The eight concrete slabs were precast and prestressed to have a minimum 28-day strength of f'_c = 7,000 psi and a minimum compressive strength of f'_{ci} = 5,800 psi at the transfer of prestress. The pretensioning steel strands were Grade 270 0.5" diameter 7-wire bright low relaxation strands pretensioned to 31,000 lbs. All of the reinforcing steel used was Grade 60. Each end of the slab is supported by two 1" thick elastomeric bearing pads with a design load of 36 kips.

The slabs were transversely post-tensioned using four 1” diameter tie rods tensioned to 80 kips. The tie rods were staggered and placed normal to the beams in 2.5” diameter holes precast in the slabs. Two tie rods were placed at approximately the third-points of the bridge 7’ apart, each integrating five beams (one integrating beams one through five; the other integrating beams four through eight). Two more tie rods were placed 7’ from the third-point tie rods towards the acute corners of the bridge, each integrating three beams (one integrating beams one through three; the other integrating beams six through eight). See Figure 5-1 for a schematic of the post-tensioning placement.

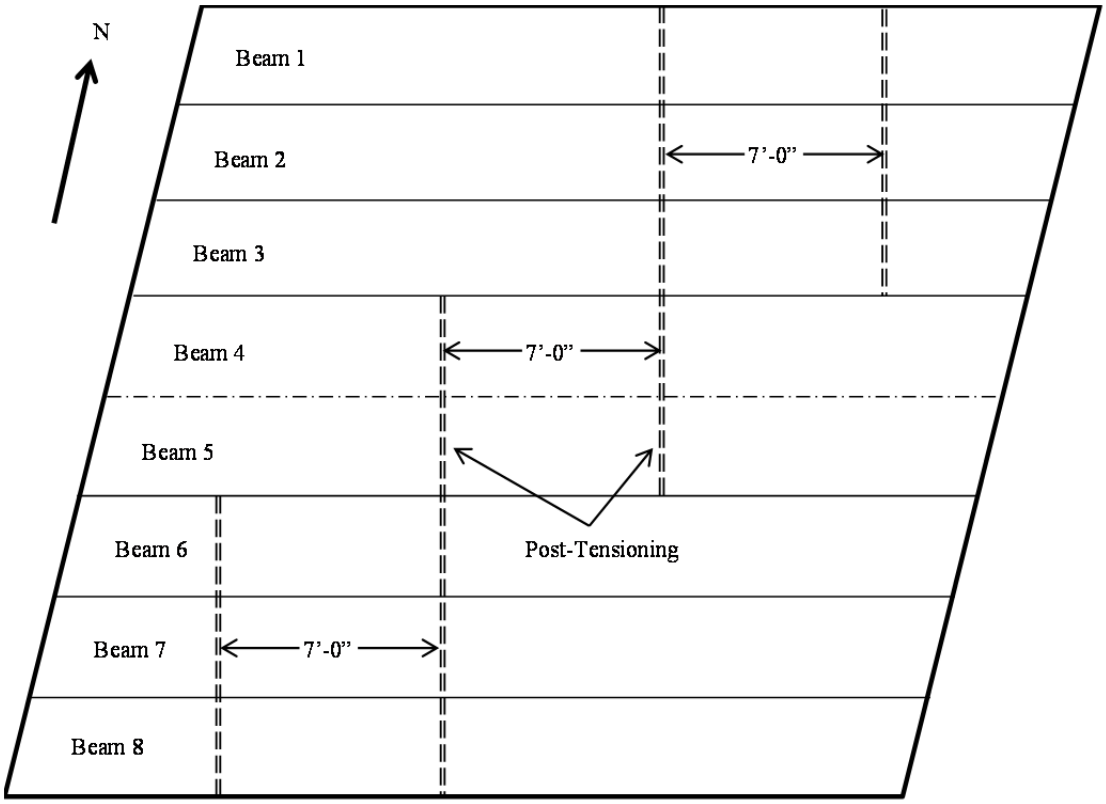

Figure 5-1 Locations of the Post-Tensioning Tie-Rods on the Knoxville, MD, Bridge

The tie-rod bolt recesses were then grouted using nonshrink grout while the post-tensioning remained unbonded to the surrounding slabs. The slabs were then connected longitudinally with partial-depth (7.25”) shear keys using nonshrink grout.

5.1.3 Reasons for Construction and Testing

The previous bridge at this crossing was an 18'-0" single-span concrete girder bridge built in 1910. The bridge's age and traffic conditions at the site necessitated its replacement. Private properties as well as the shape and depth of the Potomac tributary restricted available replacement options. A transversely post-tensioned adjacent concrete slab bridge with a skew angle of 31.4^0 was constructed to minimize traffic disruption and to fit the constraints of the bridge's location. Within four years of being built, longitudinal cracking was found on the top surface of the concrete overlay of the new bridge, which led to SHA's request to determine the cause or causes of the cracking.

5.1.4 Bridge Photos and Plans

The longitudinal cracking on the top surface of the Knoxville, MD, are circled in yellow in Figures 5-2 through 5-5. There is a clear pattern: the cracks begin perpendicular to the abutment, travel up to two feet, then reorient to travel parallel to the bridge beams and follow the shear keys between the slabs. Figures 5-6 and 5-7 show that no leakage occurred on the underside of the bridge, which means that the longitudinal reflective cracks on the top surface probably were not yet sufficiently deep to affect the steel reinforcement and post-tensioning in the bridge. All of the relevant Knoxville, MD, bridge plan sheets pertaining to the major structural elements of the bridge superstructure are included in Appendix B.

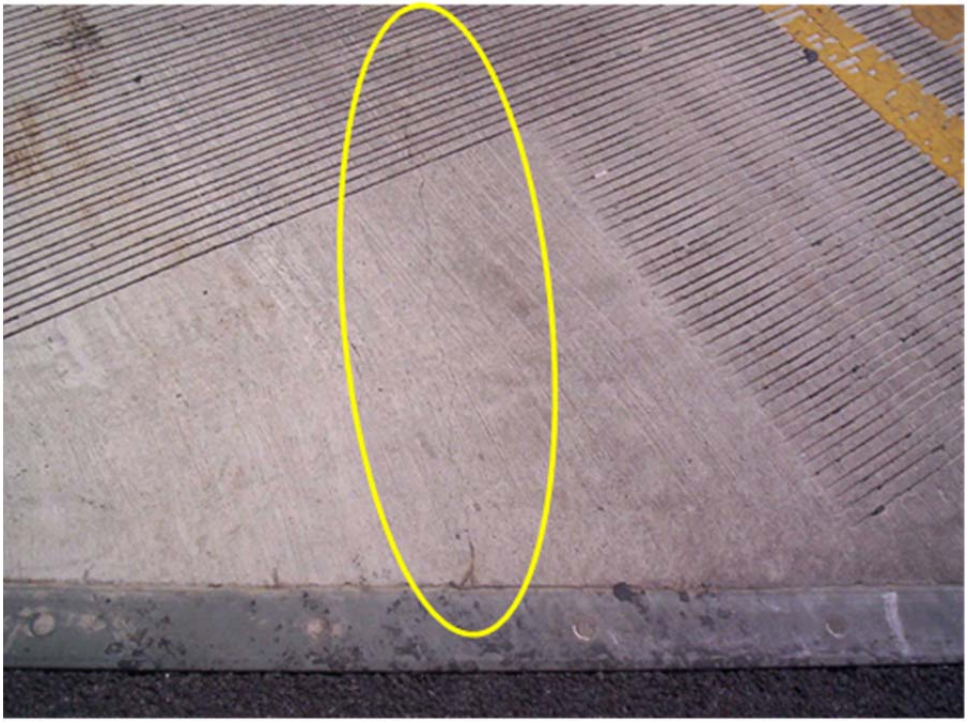

Figure 5-2 Longitudinal Crack on the Top Surface of the Knoxville, MD, Bridge

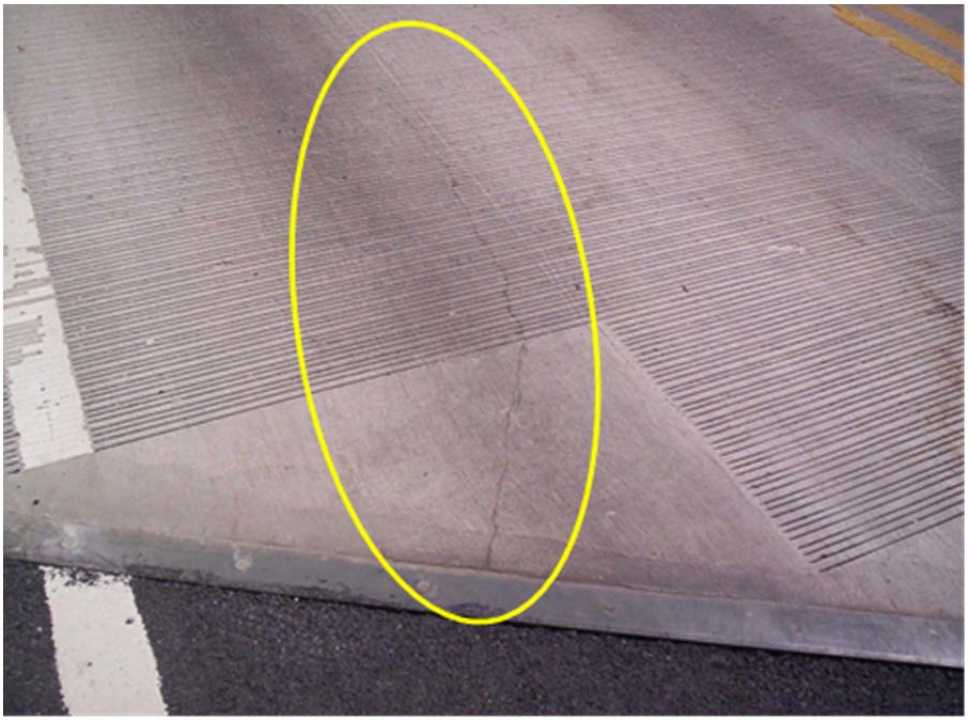

Figure 5-3 Longitudinal Crack on the Top Surface of the Knoxville, MD, Bridge

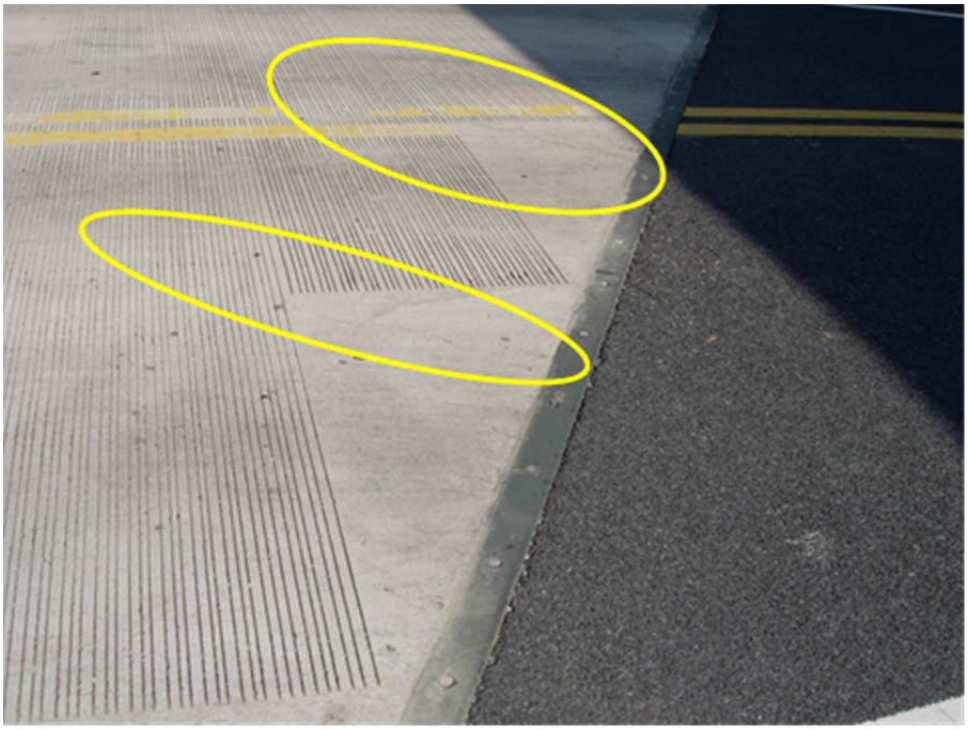

Figure 5-4 Longitudinal Cracks on the Top Surface of the Knoxville, MD, Bridge

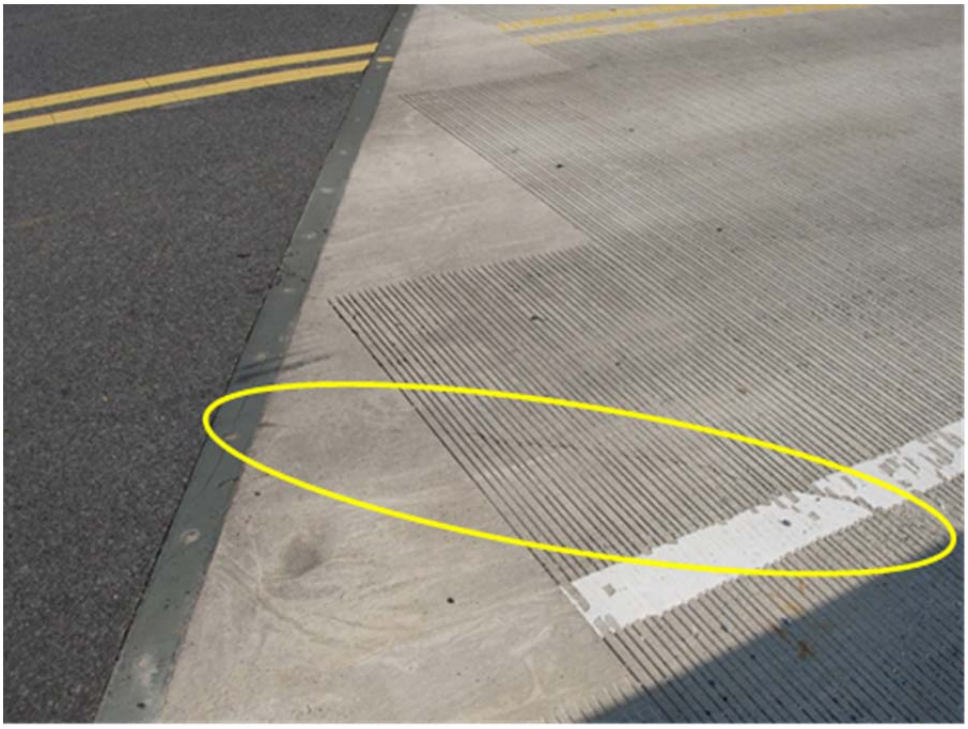

Figure 5-5 Longitudinal Crack on the Top Surface of the Knoxville, MD, Bridge

Figure 5-6 View of the Bottom Surface and the East Abutment of the Knoxville, MD, Bridge

Figure 5-7 View of the Bottom Surface and West Abutment of the Knoxville, MD, Bridge

5.2 Instrumentation Plan

5.2.1 Summary of Instrumentation Plan

An instrumentation and testing plan was formulated to measure the short-term live-load strains on the bottom and top surfaces of the bridge as a test vehicle drove over the bridge. Eight Bridge Diagnostic, Inc. (BDI) strain transducers (strain gauges/sensors) measured the live-load strains. The sensors were placed at approximately the same locations on the top and bottom surfaces of the bridge and with the same orientations to determine the strains near the cracks. A Campbell Scientific data acquisition instrument coordinated with a software program on a laptop computer to obtain the strain data from the sensors.

5.2.2 Strain Gauge Locations

Three criteria formed the basis for selecting the strain gauge locations: (1) the locations necessary to characterize the bridge behavior; (2) the locations of the longitudinal cracks in the bridge; and (3) the ease of accessing similar points on the underside of the bridge. Sensor placement was determined by the cracks on the top surface of the bridge that had an accessible area on the bottom surface of the bridge. One BDI sensor was placed on the top surface of the bridge parallel to the abutment across a crack near where the abutment supported the beams (No. 1644) with a corresponding sensor on the bottom surface of the beams (No. 3213). Two more BDI sensors were placed on the top surface of the bridge, one normal to the beams across another longitudinal crack (No. 1643) and one close by but parallel to the beams (No. 1641), with two more sensors placed approximately in the corresponding positions on the underside of the bridge (Nos. 3214 and 3215, respectively). The last two BDI sensors were placed on the underside of the bridge, one normal and across beams six and seven and the other parallel to the

beams on beam 3. A gauge location schematic and photos of the strain gauges on the bridge are shown in Figures 5-8 to 5-10.

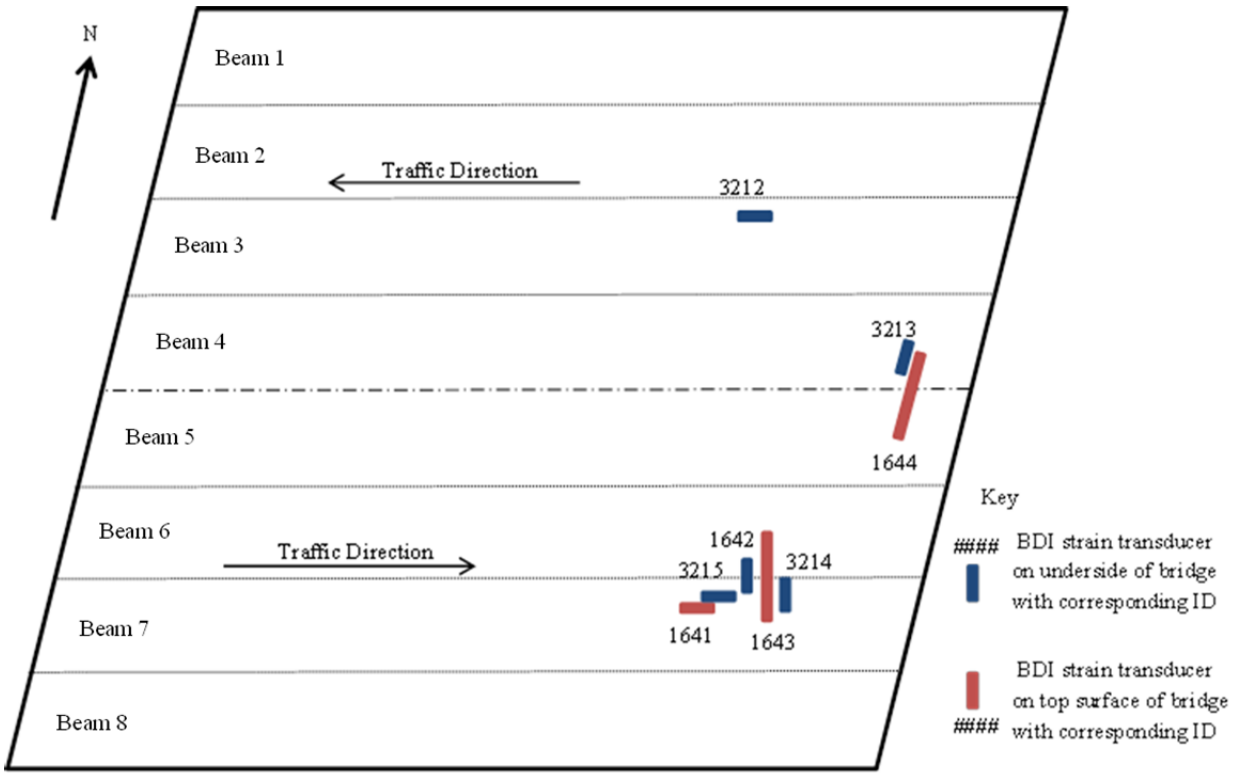

Figure 5-8 Strain Gauge Locations on the Knoxville, MD, Bridge

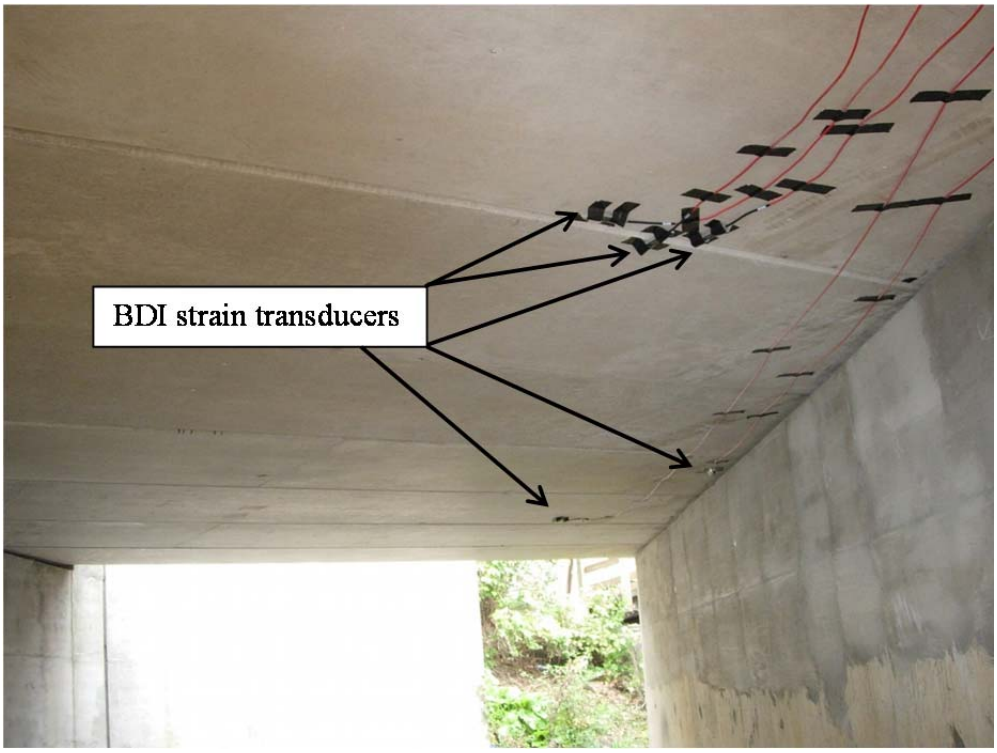

Figure 5-9 Location of BDI Sensors on the Bottom Surface of the Knoxville, MD, Bridge

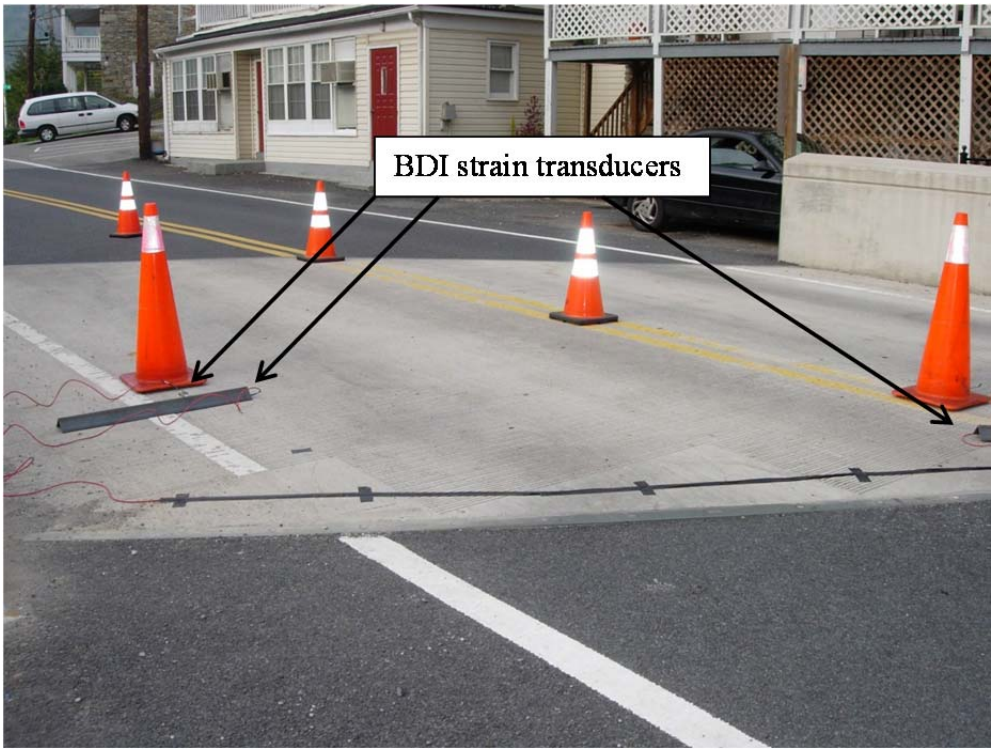

Figure 5-10 Location of BDI Sensors on the Top Surface of the Knoxville, MD, Bridge

5.2.3 Instrumentation Set-up

The instrumentation set-up for the live-load test had multiple components. Eight prefabricated BDI sensors were connected to the Campbell Scientific CR5000 data logger. The CR5000 was powered by a small generator and connected to a laptop computer which ran the PC9000 software. The connections from the sensors to the data logger were correctly made on the same day as the field test and checked using a multi-meter during preliminary test runs. The data was recorded to the CR5000 and transferred using the PC9000 to the computer. A schematic of the data acquisition network and a photo of in operation are shown in Figures 5-11 and 5-12; further descriptions of each component of the system are provided in the following section.

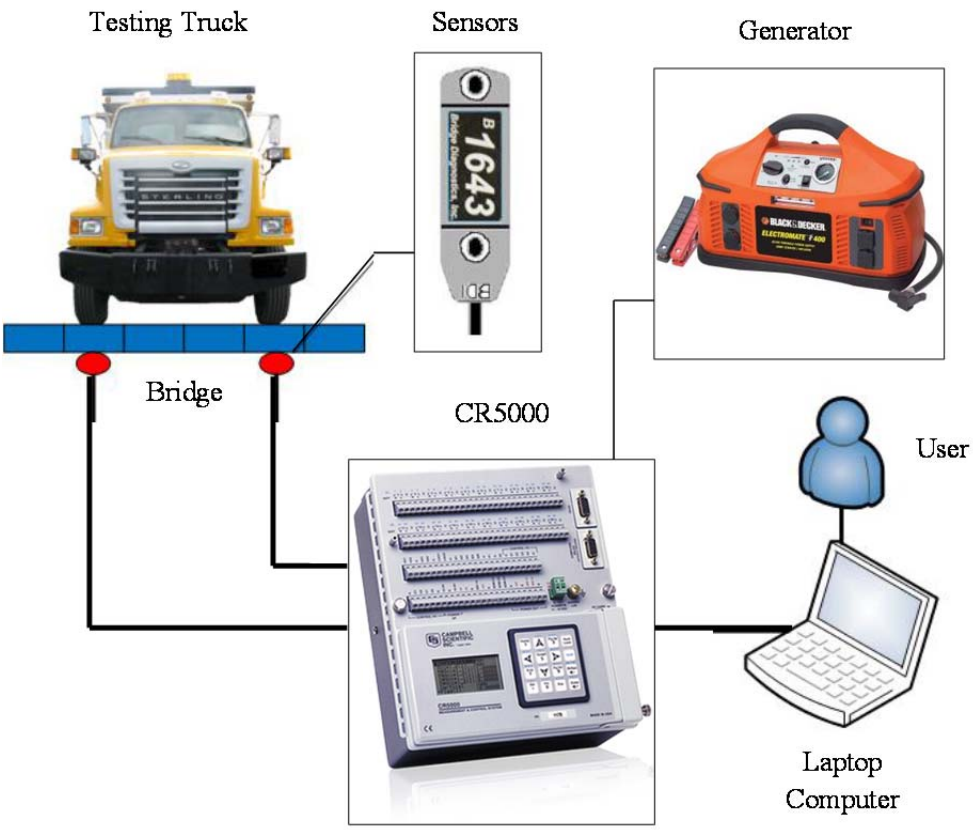

Figure 5-11 Data Acquisition Network (Jeong, 2009)

Figure 5-12 Data Acquisition System Monitoring the Strain Gauges During the Live Load Test

5.3 Data Acquisition Network

5.3.1 Strain Gauge Description, Resistance, Strain, and Installation

Simple strain gauges operate because the resistance of a foil strain gauge is directly proportional to its deformation (the amount of strain it is undergoing). When a load is applied to a structure, the attached strain gauges undergo a length deformation that changes the electrical resistance of the strain gauge. This resistance can then be used to calculate the amount of strain in the gauge and therefore the amount of strain on the structure at the point where the gauge is located. A circuit arrangement known as the Wheatstone bridge is used to detect these small changes in resistance. This data – the changes in resistance, the corresponding deformation calculation, and the strain calculation – is recorded and can be used for further analysis or corrections. A visual representation of this process is represented by Figures 5-13 and 5-14.

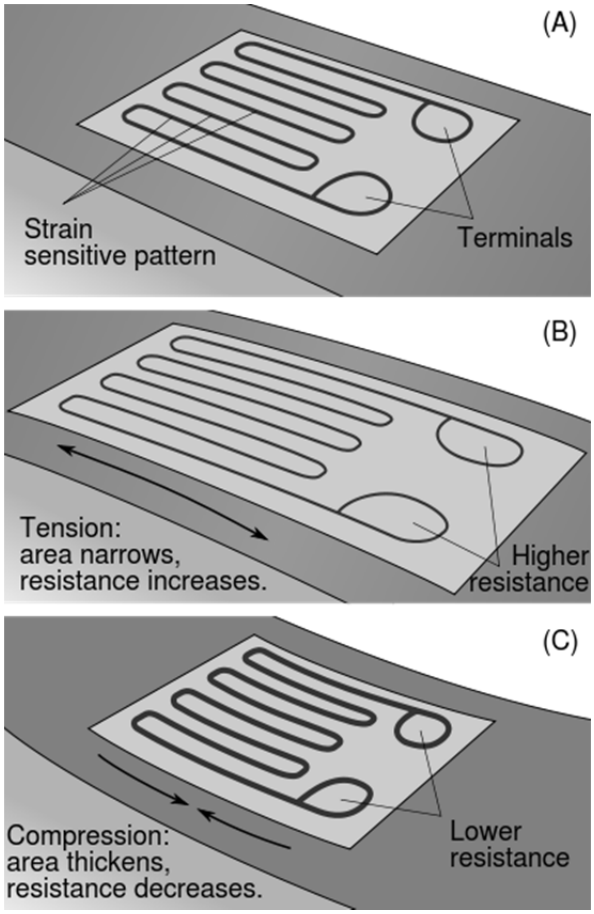

Figure 5-13 Strain Gauge Operation Concept

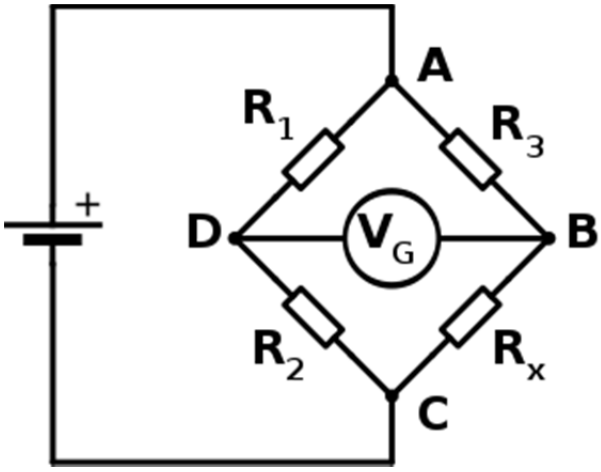

Figure 5-14 Wheatstone Bridge Circuit Used to Measure an Unknown Electrical Resistance

Because of their durability, ease of installation and use, reusability, and ability to be placed over cracks, BDI strain transducers were chosen over other common strain gauges. BDI strain transducers are highly accurate, prefabricated, pre-wired, rugged, weather-resistant, water-proof, reusable strain gauges made using a full Wheatstone bridge circuit with four active 350Ω foil gauge resistors and are compatible with most data acquisition instruments. They are often used to measure strain in civil structures because they have a quick installation time (less than five minutes in some circumstances) and can be attached to a wide range of materials with a variety of attachment methods. The strain transducers have an effective gauge length of 3", but aluminum extensions can be attached to increase their effective gauge length in 3" increments up to 2' in order to calculate average strain over greater distances. They have a strain range of ±2000 με with a sensitivity of 500 με/mV/V and an accuracy of less than ±1% (Bridge Diagnostics, Inc.). See Figures 5-15 to 5-17 for the BDI strain transducer dimensions and photos of the strain gauges installed on the bridge.

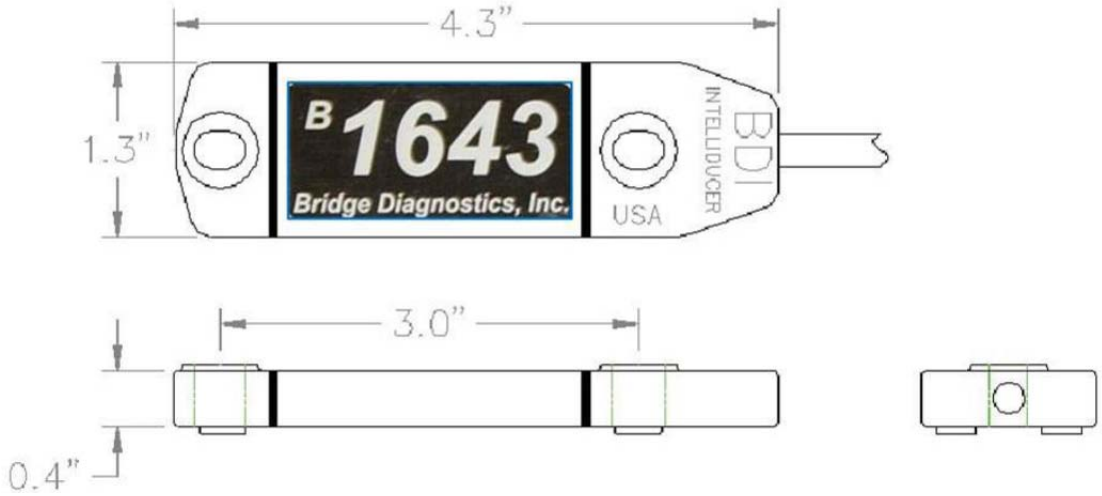

Figure 5-15 Bridge Diagnostics, Inc. (BDI) Strain Transducer Dimensions (Jeong, 2009)

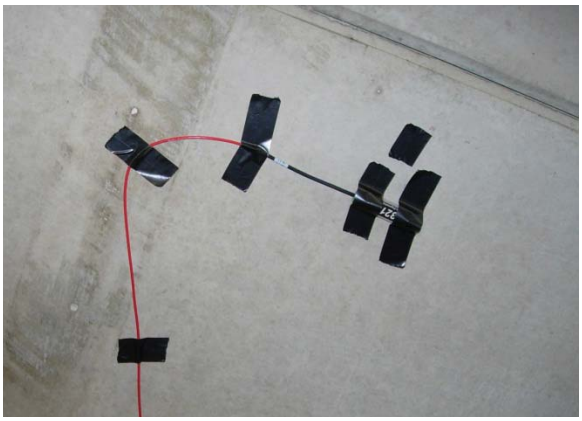

Figure 5-16 A BDI Strain Transducer Installed on the Bottom Surface of the Knoxville, MD, Bridge

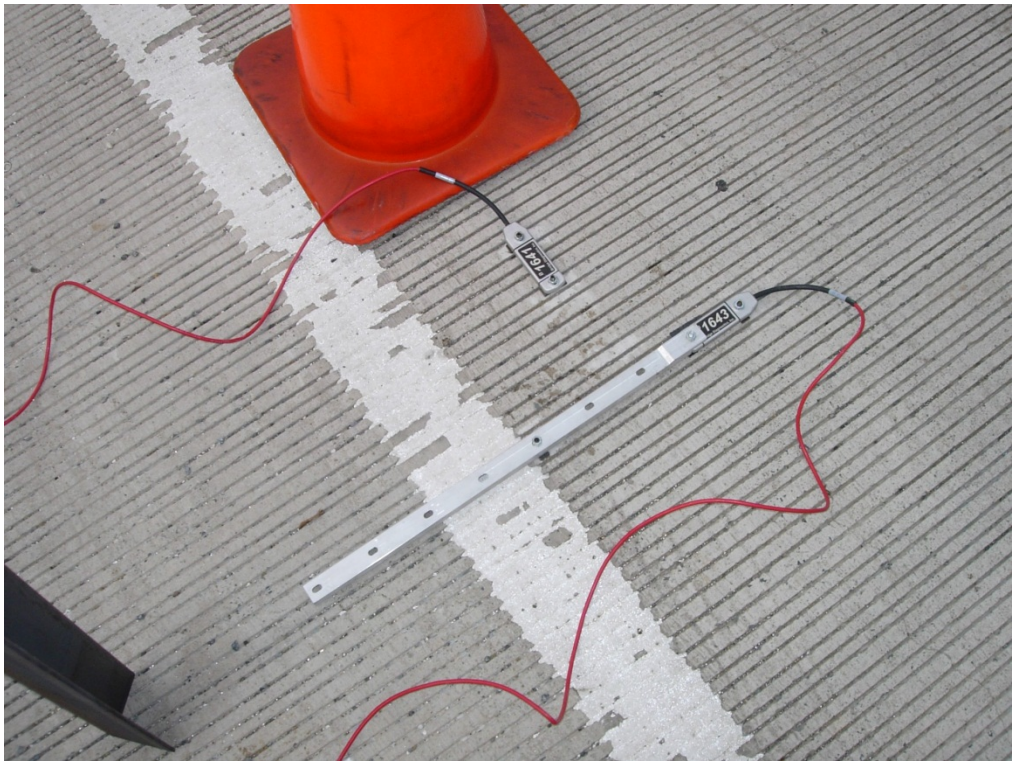

Figure 5-17 Two BDI Strain Transducers Installed on the Top Surface of the Bridge (BDI No. 1643 with an Extension Bar, BDI No. 1641 without an Extension Bar)

5.3.2 Campbell Scientific CR5000 Data Logger

For the live-load field testing, the Campbell Scientific CR5000 Measurement and Control System was used to record the data obtained from the BDI strain transducers. The CR5000 is a

rugged, high-performance data acquisition system that can be used as an excitation source for sensors and can record data at a maximum rate of 5000 Hz (5000 measurements per second). It has twenty differential individually configured inputs that can be used for a variety of different sensor types, including strain gauges. See Figure 5-18 for a photo of the CR5000.

Figure 5-18 Campbell Scientific CR5000 Data Logger

5.3.3 Dell Laptop with PC9000 Software

The code required to operate the CR5000 using the PC9000 software was downloaded onto a laptop running a Windows operating system. The software provides the user with various functionalities including, but not limited to, writing and compiling the required programming code, downloading it to the CR5000, confirming the CR5000's status, monitoring real-time data and the response of the attached sensors, graphing, and retrieving the data stored on the CR5000.

The PC9000 software provides most of the communication functions between a computer and the CR5000.

5.4 Field Testing Procedure

5.4.1 Installation and Setup

The University of Maryland research team installed eight BDI sensors on the testing bridge October 10-11, 2011. The research team decided upon, marked, and installed the sensors on the underside of the bridge October 10. The research team installed sensors on the top surface of the bridge October 11. The sensors were mounted on the bridge, connected to the data logger, and tested to confirm the proper connections on October 11, as well. SHA provided the live-load test vehicle and traffic control during the testing.

5.4.2 Test Vehicle

The pre-weighted test vehicle was a two-axle dump truck provided by SHA and weighed 26,420 pounds. It weighed 5,200 pounds in each front wheel and 8,010 pounds in each rear tandem. The driver was instructed to drive across the bridge a total of eight times (four times in each direction) at varying speeds to obtain live-load strain data for the bridge. See Figures 5-19 and 5-20 for photos of the test vehicle.

Figure 5-19 Test Vehicle Provided by SHA Traveling Westbound across Knoxville, MD, Bridge

Figure 5-20 Test Vehicle Provided by SHA Traveling Westbound across Knoxville, MD, Bridge

5.4.3 Live Load Test

The test vehicle performed eight runs across the bridge for the live-load test. The test vehicle traveled eastbound on odd-numbered runs along beams five, six, and seven (see Figure 5-8), and westbound on even-numbered runs along beams two, three, and four. Runs one, two, seven, and eight were made with the test vehicle driving approximately one mph. Runs three and four were made with the test vehicle traveling at approximately five mph, and runs five and six were made with the test vehicle traveling at approximately 20 mph. Runs three through six were made to confirm that strain data obtained was consistent for a low range of varying speeds. The CR5000 collected the strain data at a rate of 2 Hz (two samples per second).

The PC9000 program retrieved the raw data from the CR5000. Those data included both the resistance values of the BDI strain transducers as well as the calculation using a gauge factor for each sensor to determine the strain. The strain data obtained were then plotted on graphs for a simple comparison and confirmation that the strain data were consistent and reliable among the multiple runs. Portions of the data for specific sensors were taken, further analyzed, and plotted using corrections for initial values and sensor drift. Most of the data included two peaks, corresponding to when the test truck's front axle and rear axle traveled near each BDI sensor. Any temperature effects were disregarded because of the short duration of each test run made by the testing truck (less than 30 seconds each time). The final results of the data are described in the following section.

5.5 Field Testing Results

5.5.1 Maximum Strain

Some of the maximum strain data that resulted from the field test of the Knoxville bridge are listed in Table 5-1. A maximum strain for each sensor and for each direction of the test truck's runs is listed. The positive strain values indicate tensile strain; the negative strain values indicate compressive strain. The large strain values recorded by BDI sensor No. 1642 resulted from this sensor being placed transversely across two beams on the bottom surface of the bridge thus being affected by both the strain in each beam as well as any possible differential displacement of the beams. Though not all of the BDI sensors recorded significant strains because of their locations, the maximums are listed here for comparative purposes.

BDI Identification Number	microstrain	Run Number
1641	-0.5	8
	-5.85	1
1642	67.84	1
	-12.73	2
1643	1.01	2
	-5.25	1
1644	0.72	7
	-1.46	2
3212	3.14	2
	-0.37	1
3213	1.47	2
	-1.35	1
3214	-0.15	2
	-1.03	1
3215	4.06	1
	0.76	2

Table 5-1 Some Maximum Strain Data Results Obtained from the Field Test

5.5.2 Strain Curves

The strain data was also plotted to view significant similarities or differences. The strain data from BDI sensor Nos. 1641 and 3215 (see Figure 5-8) is shown in Figure 5-21. The data from the two runs in the same direction show similar shapes and similar magnitudes. As expected, the difference between the runs indicates the tension and compression the bottom and top of the bridge experienced during the live-load testing.

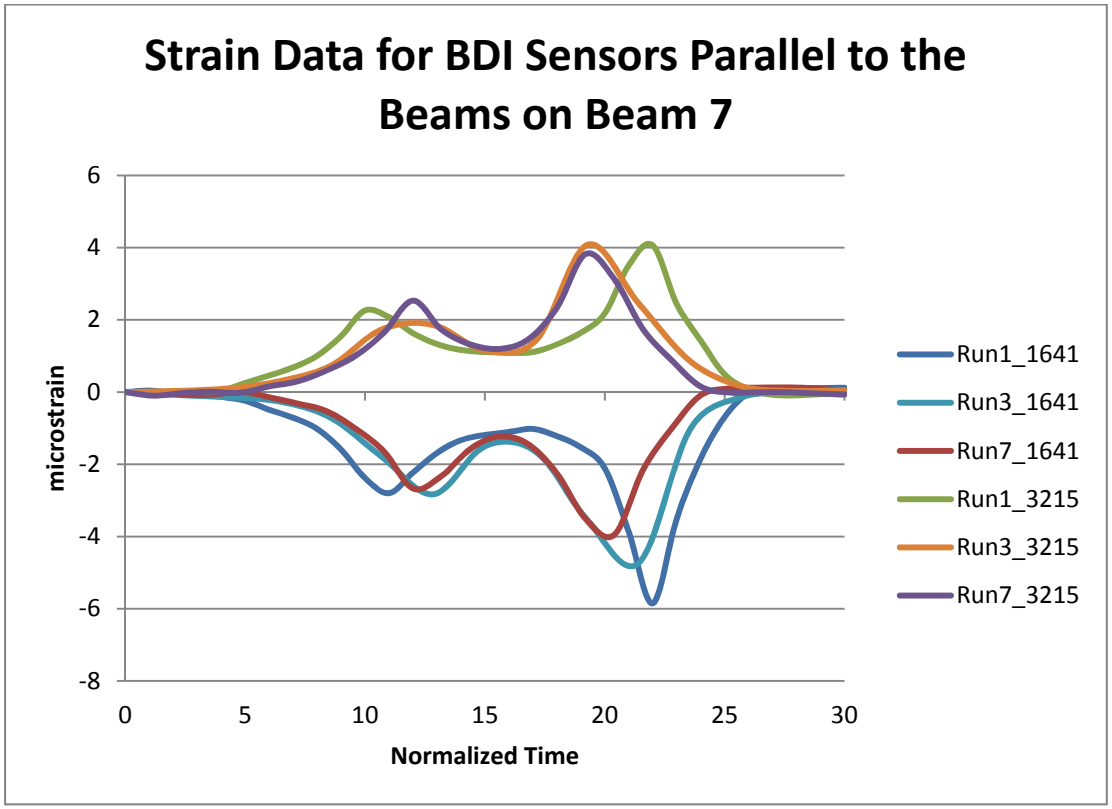

Figure 5-21 Strain Data for BDI Sensor Nos. 1641 and 3215 from Runs One, Three, and Seven

The strain data from BDI sensor Nos. 1643 and 3214 located perpendicular to the beams on the top and bottom of beam seven, respectively, for the eastbound runs is shown in Figure 5-22. As can be seen, the data from the runs in the same direction show similar shapes with all of the magnitudes in the same direction. However, there are some discrepancies in the magnitude

of some of the records, notably by the same sensor (BDI No. 1643). This may be explained by its location on the top surface of the bridge across a crack and very close to where the test truck made its run. It is important to note the absence of a return to the initial strain value in the data from both runs and the lack of some data from run seven (removed because of an obvious error, caused by the truck contacting a portion of the sensor's protective cover). Taking these matters into consideration, the data is not nearly as conflicting as it may first seem and seems in more agreement with the data from run 3.

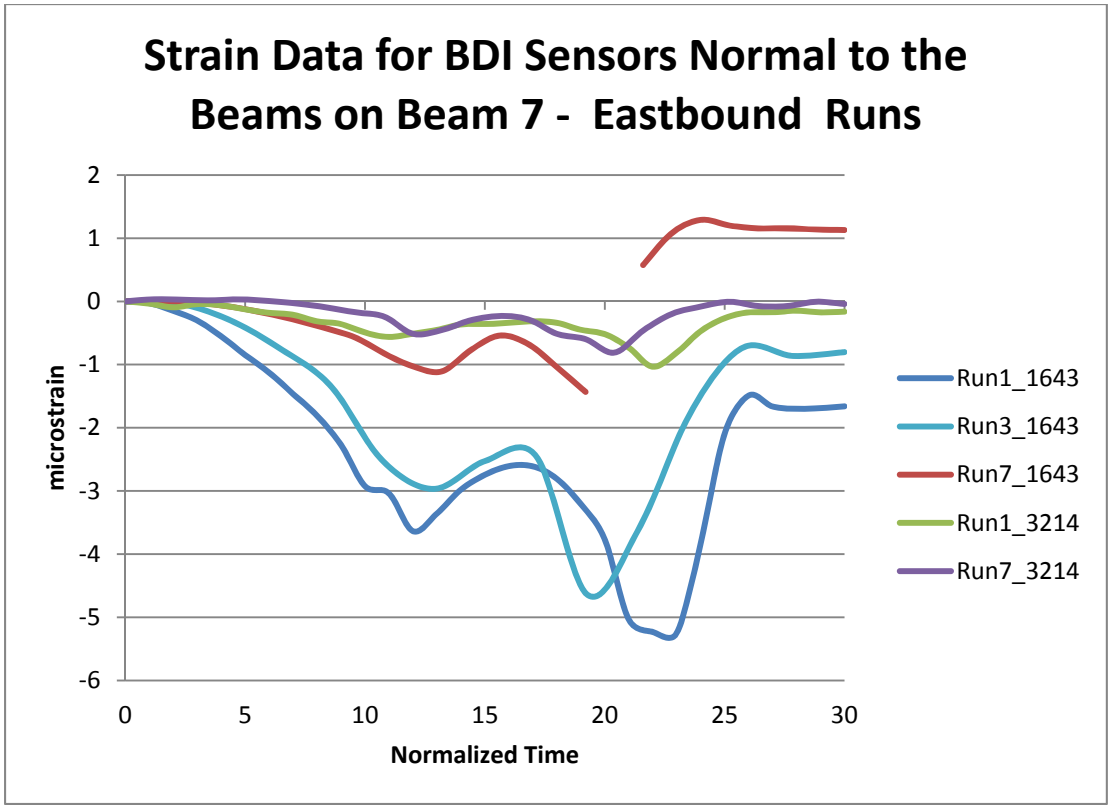

Figure 5-22 Strain Data for BDI Sensor Nos. 1643 and 3214 from Runs One, Three, and Seven

The strain data from BDI sensor Nos. 1643 and 3214 located perpendicular to the beams on the top and bottom of beam seven, respectively, for the westbound runs is shown in Figure 5-23. As can be seen, the data from the runs in the same direction show similar shapes for each sensor. However BDI sensor No. 1643 shows some discrepancies in the magnitude of some of

the data. This may be due to its location on the top surface of the bridge across a crack. Although the strain gauge on the top surface of the bridge (BDI No. 1643) recorded compression in the transverse direction when the test truck made the eastbound runs, it recorded tension in the transverse direction when the test truck made the westbound runs. This may indicate that the live loads are contributing to the cracks in the concrete overlay.

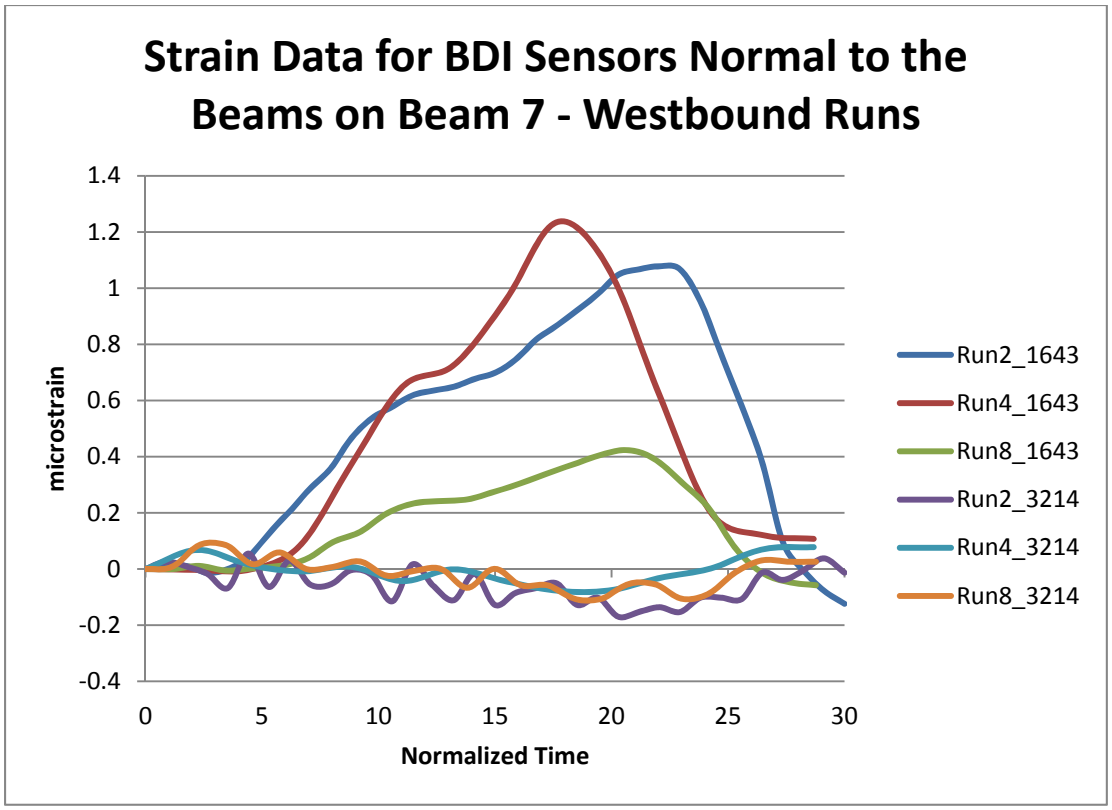

Figure 5-23 Strain Data for BDI Sensor Nos. 1643 and 3214 from Runs Two, Four, and Eight

The strain data from BDI sensor Nos. 1644 and 3213, which are located parallel to the abutment on the top and bottom of beam four, respectively, is shown in Figure 5-24. The data from these runs in the same direction show similar shapes and similar magnitudes that are in the same direction as expected.

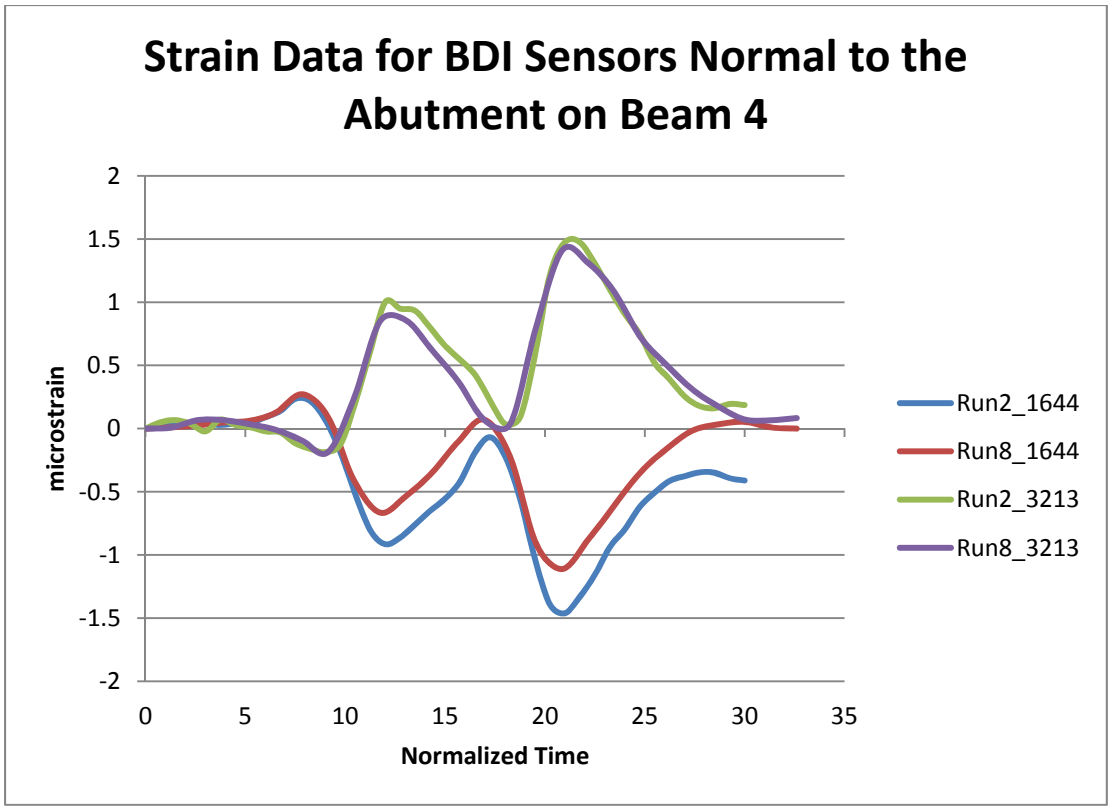

Figure 5-24 Strain Data for BDI Sensor Nos. 1644 and 3213 from Runs Two and Eight

Chapter 6: Theoretical Evaluation and Analysis of Field Testing

6.1 Summary of the FEA Model and Results for the Knoxville, MD, Bridge

This research team used the field test results to create and refine a FEA model of the Knoxville, MD, bridge in order to identify causes of the longitudinal cracking on the bridge's deck (see Figure 6-1). Although other analysis methods such as grillage analysis have been used, FEA has proven to be both robust and accurate for refined analyses. Using FEA, researchers can detect detailed forces and stress and strain distributions in complicated structures while having the flexibility to analyze specific material characteristics (Jeong, 2009). In order to create an accurate model, the strain data from the FEA model was compared to the strain data from the field test and then the model was refined until results were sufficiently close to the field data. ANSYS version 10.0 was used to create this model. The model details are described in the following section.

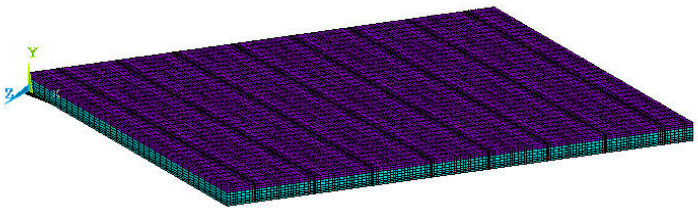

Figure 6-1 FEA Model of the Knoxville, MD, Bridge

6.2 FEA Model Description

6.2.1 Sections and Elements

Four main sections composed the FEA model of the bridge: The precast, prestressed solid concrete slabs, the prestressing strands, the transverse post-tensioning, and the concrete

overlay (see Figures 6-2 to 6-5). A necessary simplification of the model was to exclude a modeled shear key because of its complex construction and minimal contribution to the overall model. The concrete in the precast-concrete beams and the concrete overlay were modeled using solid brick elements (Solid 45), and the pretensioning strands in the precast-concrete beams and the post-tensioning tie rods were modeled using link elements (Link 8). Both the solid brick and the link elements have three degrees of freedom (translation) at each node. There were 46,080 solid brick elements and 3,520 link elements for a total of 49,600 elements.

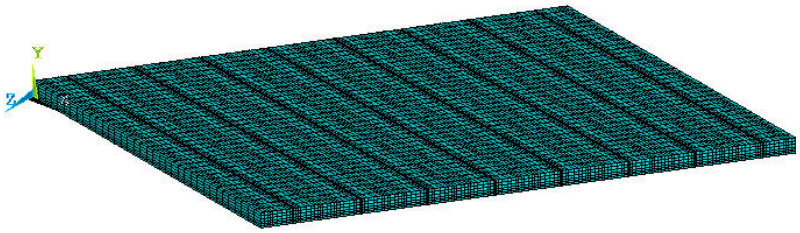

Figure 6-2 FEA Model Concrete Slabs/Beams

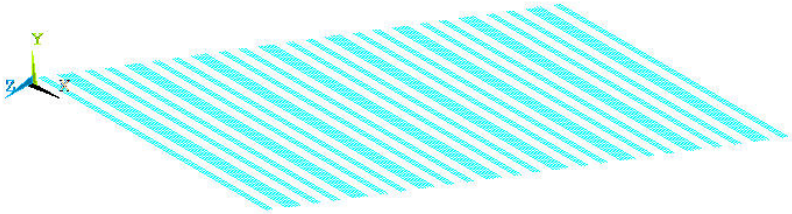

Figure 6-3 FEA Model Prestressing Strands

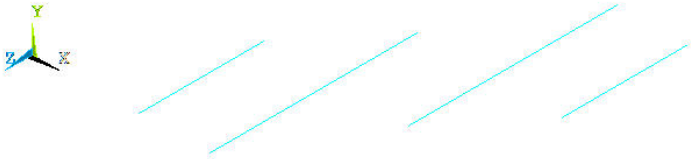

Figure 6-4 FEA Model Post-Tensioning Rods

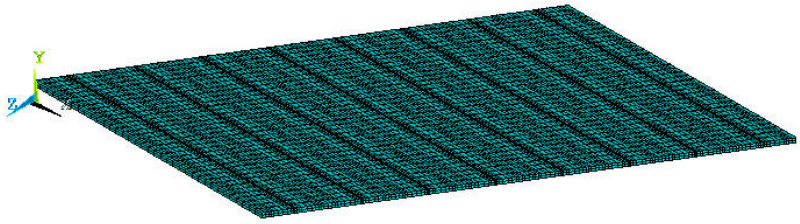

Figure 6-5 FEA Model Concrete Deck

6.2.2 Material Properties and Tensioning Force

Construction plans were the source of the material properties for the model and are listed in Table 4-1. The isotropic reinforcing steel in the concrete overlay was not included because of its negligible effect on the stiffness of the structure. The modulus of elasticity (stiffness) of the cast-in-place concrete for the concrete overlay and the precast-concrete for the concrete beam were adjusted to further refine the model. The prestressing and post-tensioning forces prescribed by the bridge plans were applied to the respective steel modeled elements.

Material	Section	Properties
Concrete	Precast-Concrete Beam	f'_c = 7000 psi E = 5224136 psi
Cast-in-Place Concrete	Concrete Overlay	f'_c = 4000 psi E = 3604997 psi
Prestressing Steel	Precast-Concrete Beam	E = 28592160 psi A = 0.19625 $in.^2$ P = 31,000 lbs
Post-Tensioning Steel	Post-Tensioning Tie Rod	E = 30043540 psi A = 0.7854 $in.^2$ P = 80,000 lbs

Table 6-1 Material Properties of FEA Model of the Knoxville, MD, Bridge

6.2.3 Geometry

ANSYS offers two modeling choices: solid modeling and direct generation. Solid modeling consists of establishing the boundaries of the model and setting some element specifications allows ANSYS to generate all of the nodes and elements. Direct generation allows the user to have more control over the process by requiring the user to define the geometry, numbering, size, and connectivity of all the elements (Jeong, 2009). The research team used direct generation for these FEA models.

6.2.4 Loading and Boundary Conditions

The loads and boundary conditions applied to the model were made as similar as possible to the field test. The test truck load was applied as four groups of point loads corresponding to the wheel loads and defined as 5,200 pounds for the front wheel loads and 8,010 pounds for the rear wheels loads. A time-history analysis was used comparing the FEA model with the field test results under the modeled load (truck) traveling in a path that corresponded with eastbound runs on beams six and seven in the field. The model bridge was defined as simply-supported even though this bridge was partially fixed to the abutments which may have some impact on the results (Menassa et al., 2007).

6.2.5 Iterations for Strain Data Comparisons

The strain data from the model was taken at approximately the same locations the BDI strain transducers were placed in the field test. The model data were then compared with the field test strain data. The field test results were used to further refine the model to create as accurate a representation of the bridge as possible. When the shape of the model strain data did not

correspond with the shape obtained from the field test, the boundary conditions or structural geometry of the finite element model were refined; when the shapes of the model and field test results were similar but the magnitudes were different, some of the members' stiffness (i.e. material properties) were refined (Jeong, 2009).

6.3 FEA Model Strain Comparison with Field Test Results

6.3.1 FEA Model and Field Test Results Comparison Introduction

The final model strain results are compared with the field test data in the following sections. It is important to note that a perfectly representative model was difficult to obtain for three reasons: simplifications were required to create the FEA model; cracks on the Knoxville, MD, bridge were not modeled; and the non-linear strain response with load positioning (Jeong, 2009).

The model was refined based on data from BDI strain transducers Nos. 3215 and 1641 because of the sensors' consistent, significant results from the field test. As the FEA model iteration results grew closer to the field test results, further comparisons were made with the data from the other strain transducers. After a model was created that correlated well with the main BDI strain gauges that were considered, the rest of the field test strain data was compared with the strain data obtained from similar locations on the FEA model. Recall that positive strain values indicate tensile strain while the negative strain values indicate compressive strain.

6.3.2 BDI Strain Gauge Sensors Placed Parallel to the Precast-Concrete Slabs

The FEA model results correspond closely to the field test results. As expected, the model results for the strain gauges placed parallel to the slabs and on the bottom and top surfaces

of beam seven are similar to the field test data (see Figures 6-6 and 6-7). The data show logical strain directions (tensile on the bottom surface and compressive on the top) and similar trends and maximum values of strain. The bottom surface underwent approximately four microstrain longitudinally and the top surface underwent approximately six microstrain longitudinally. The results for the sensor placed parallel to the slabs on the bottom surface of beam three do not correspond as well with the field test results because of the minimal amount of strain that beam three underwent due to the loading on the opposite side of the bridge. However, the model result does show a similar trend and only differs by approximately 0.3 microstrain (see Figure 6-8). When the corresponding point on the opposite side of the bridge was examined in the model and compared with the data obtained from field runs two and eight (the testing truck traveled westbound on beams two and three), both the trends and the maximum peaks (three microstrain longitudinally in tension) match well, confirming that the FEA model is a reasonably accurate model for the Knoxville, MD, bridge (see Figure 6-9).

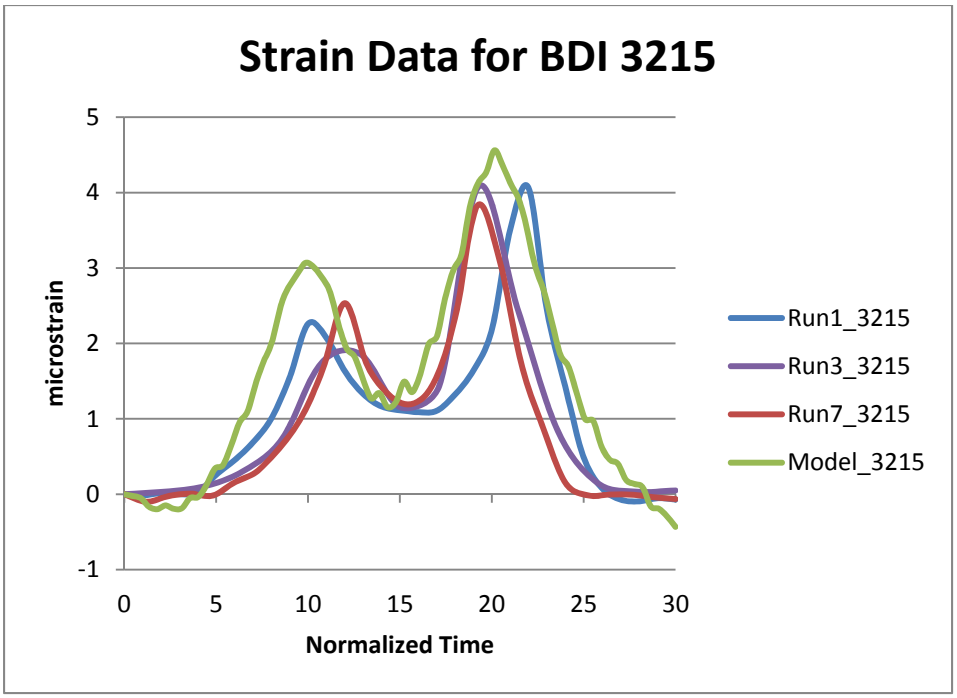

Figure 6-6 BDI Strain Transducer No. 3215 - Placed Parallel to the Slabs on the Bottom Surface of Beam Seven

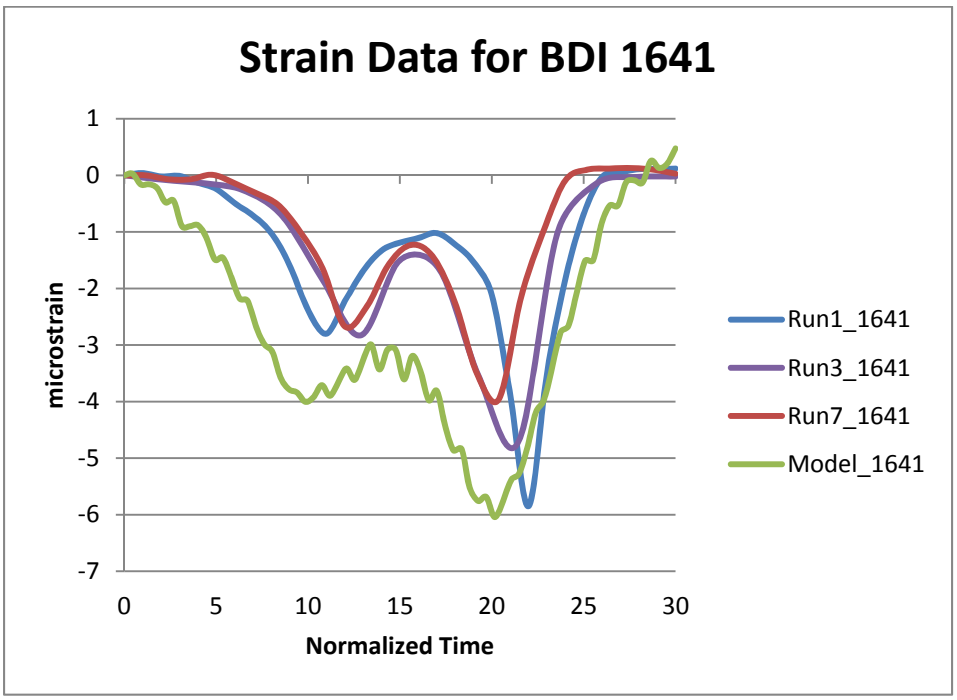

Figure 6-7 BDI Strain Transducer No. 1641 - Placed Parallel to the Slabs on the Top Surface of Beam Seven

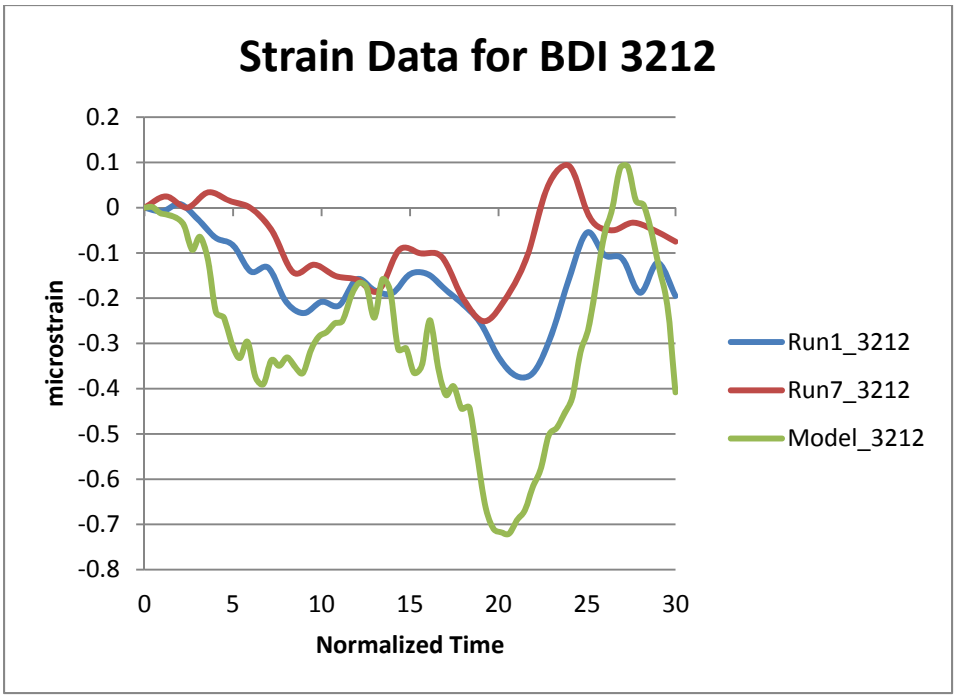

Figure 6-8 BDI Strain Transducer No. 3212 - Placed Parallel to the Slabs on the Bottom Surface of Beam Three

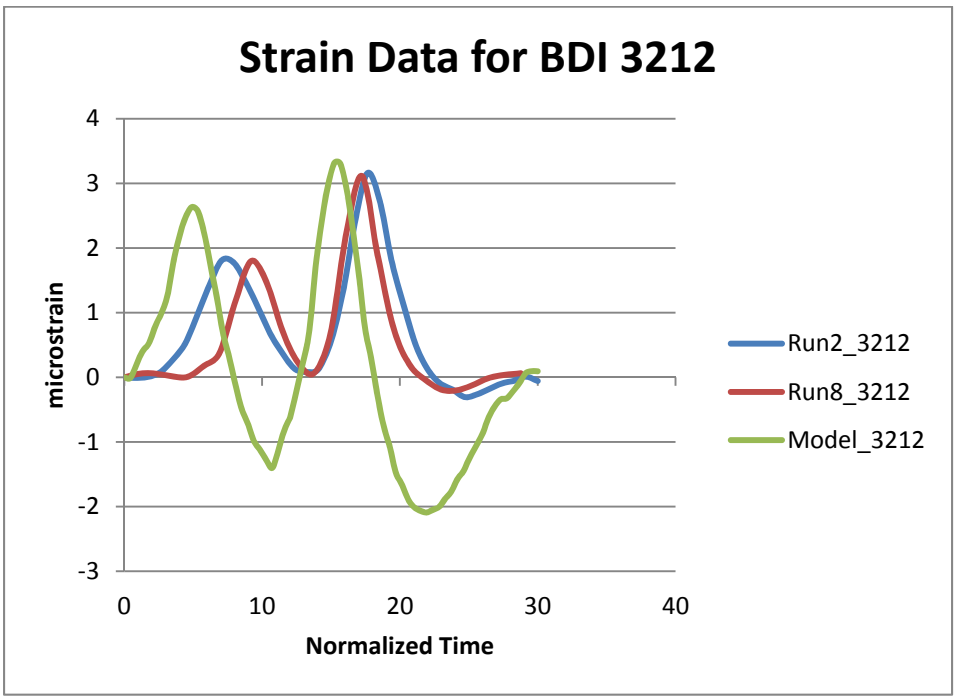

Figure 6-9 Field Test Data Based on BDI Strain Transducer #3212 - Placed Parallel to the Slabs on the Bottom Surface of Beam Three Near the East Side of the Knoxville, MD, Bridge; Model Data Based on an Equivalent Position on Beam Six Near the West Side of the Knoxville, MD, Bridge

6.3.3 BDI Strain Gauge Sensors Placed Normal to the Precast-Concrete Slabs

Field test strain data obtained from the strain transducers placed normal to the precast-concrete slabs were then compared with the FEA model results. The model results for the strain gauge placed on the bottom surface of beam two (BDI No. 3214) matched well with the field test data, with both a similar trend and peak, with a maximum value of about one microstrain transversely in compression (see Figure 6-10). The model results for BDI No. 1643 which was placed on beams six and seven across a crack between the slabs did not correspond well with the field test results (see Figure 6-11). This poor fit may be because the strain gauge in the field calculated strain across the two beams whereas the model included only one node on beam seven that could be analyzed for strain. Additionally, the model did not include cracking or the consequences of it because of insufficient data about the cracks in the test bridge.

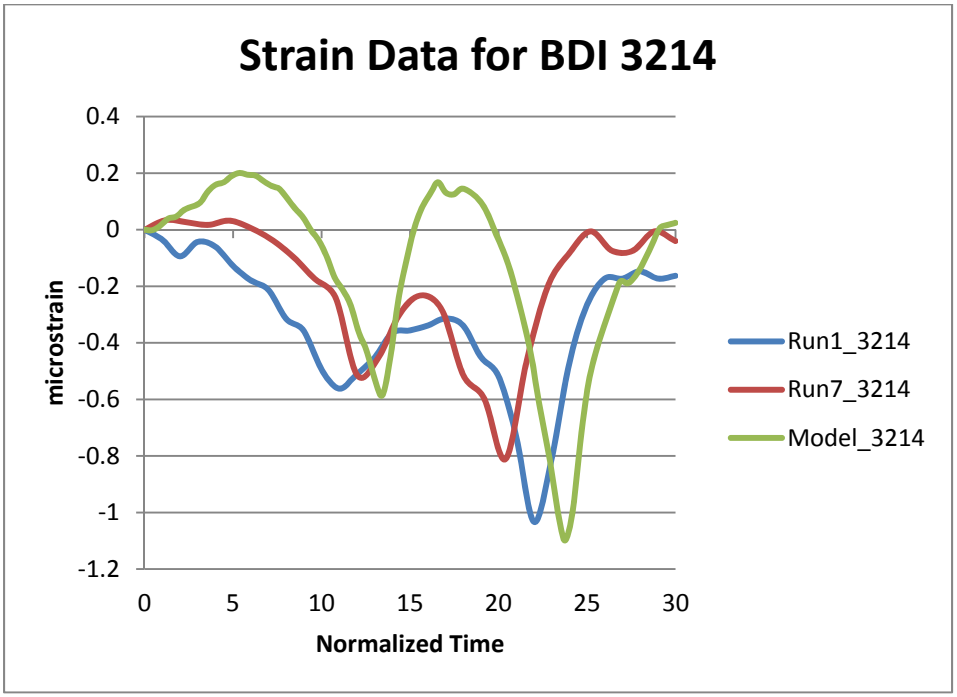

Figure 6-10 BDI Strain Transducer No. 3214 - Placed Normal to the Slabs on the Bottom Surface of Beam Two

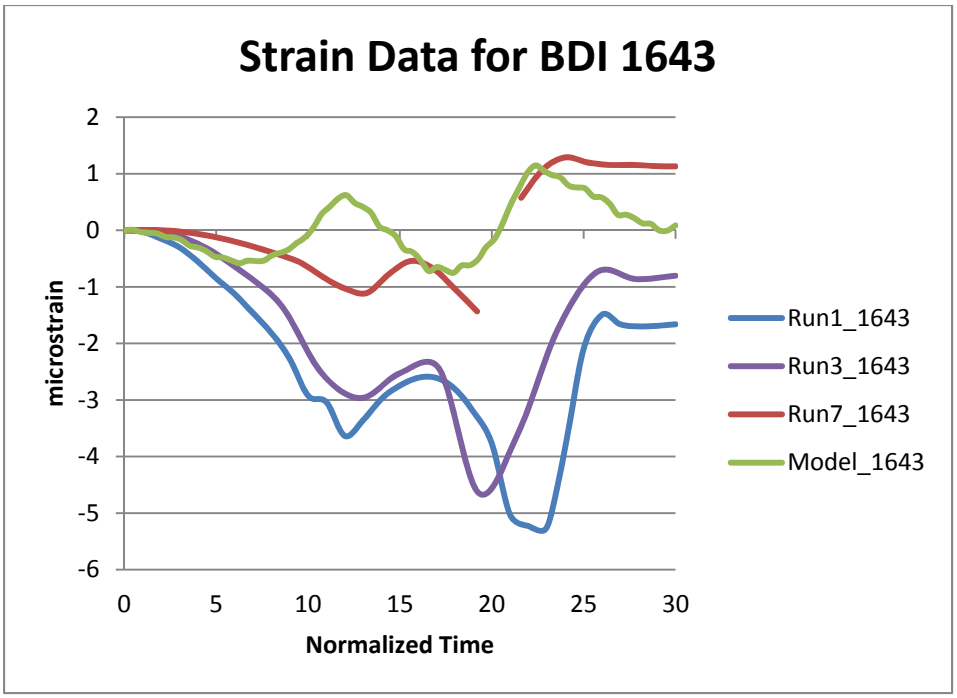

Figure 6-11 BDI Strain Transducer No. 1643 - Placed Normal to the Slabs on the Top Surface across a Crack between Beams Six and 7; Model Data Based on an Approximately Equivalent Position on Beam Seven

6.3.4 BDI Strain Gauge Sensors Placed Parallel to the Abutment

The model results were also compared to the strain data obtained by the strain gauges placed parallel to the abutment (BDI Nos. 3213 and 1644). However, this comparison was difficult because of the orientation of the field strain gauges and the model's capability to examine only the longitudinal and transverse strains at specific points. The longitudinal and transverse strains from the model were mathematically combined to form an approximate composite strain that was then compared to field data. The individual and composite strains are shown in the following figures. The model results for the sensor on the bottom surface of beam four for the eastbound loading case accorded well with the field data; each had a peak near 1.4 microstrain in compression (see Figure 6-12). There seems to be a major discrepancy when the corresponding point on the opposite mirrored side of the bridge was compared with the data

obtained from runs two and eight (when the testing truck was traveling westbound on beams two and three). The trends and magnitudes in the calculated composite strain were approximately equal, but where the field data indicates tensile strain, the model undergoes compressive strain (see Figure 6-13). However, the transverse strain from the model shows the closest fit to the field data. When the model results for the sensor on the top surface of the bridge are compared with the field data, further discrepancies are apparent. For both the eastbound and westbound cases, the calculated composite strain data trends are similar, but the magnitudes are significantly different (see Figures 6-14 and 6-15). For the eastbound case, the longitudinal strain from the model shows similarities to the field test data; and for the westbound case, the transverse strain from the model shows similarities to the field test data. For the strain gauge on the top surface of the bridge, these discrepancies may be compounded because that sensor was placed across a crack between beams four and five, whereas the strain data in the model could only be calculated from one point on beam five. Significantly, the transverse stress results from the model were closest to the field data and thus were primarily used in the model's stress analyses for both the bridge and the parametric studies.

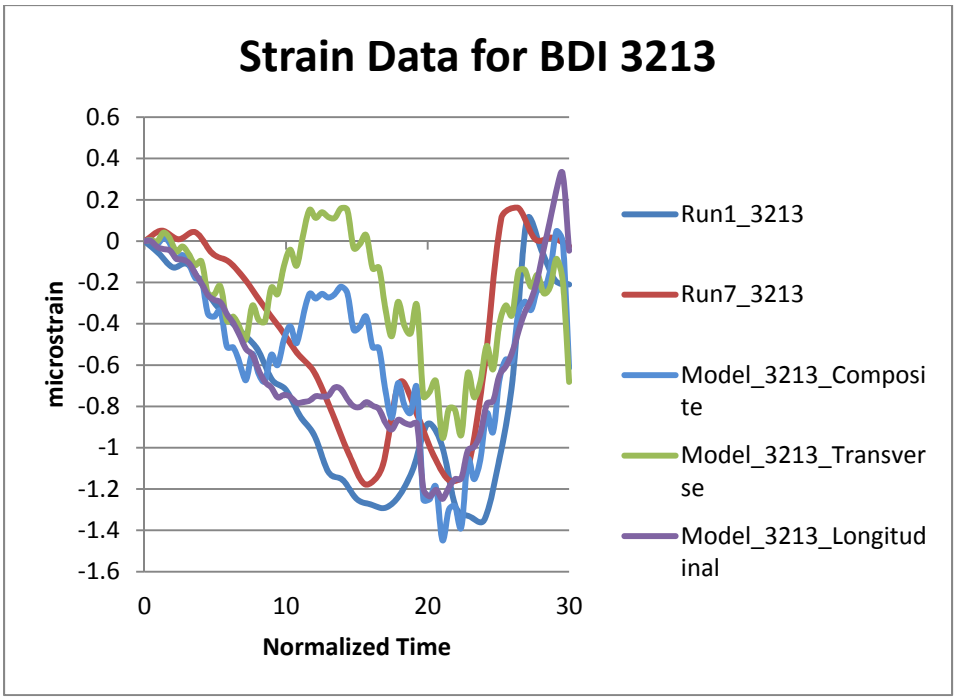

Figure 6-12 BDI Strain Transducer No. 3213 - Placed Parallel to the Abutment on the Bottom Surface of Beam Four

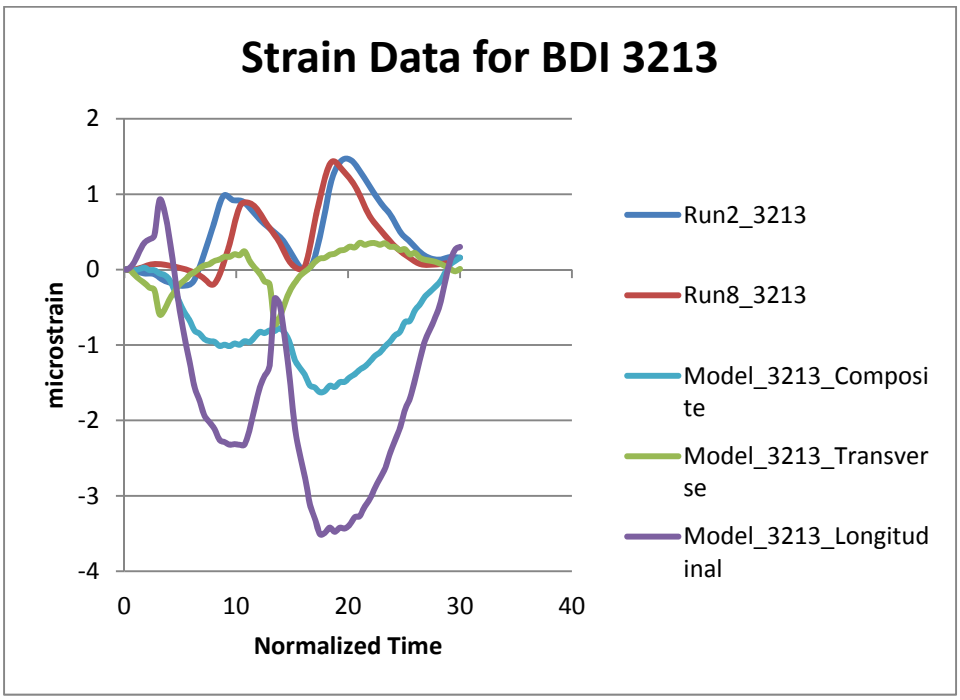

Figure 6-13 Field Test Data Based on BDI Strain Transducer No. 3213 - Placed Parallel to the Abutment on the Bottom Surface of Beam Four Near the East Side of the Bridge; Model Data Based on an Equivalent Position on Beam Five Near the West Side of the Bridge

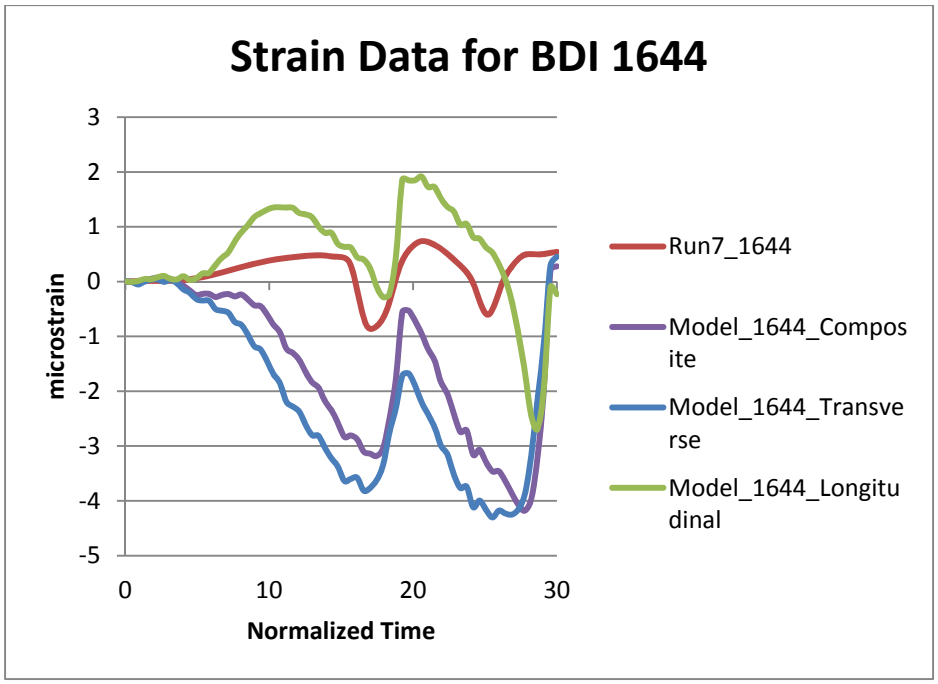

Figure 6-14 BDI Strain Transducer No. 1644 - Placed Parallel to the Abutment on the Top Surface across a Crack between Beams Four and Five; Model Data Based on an Approximately Equivalent Position on Beam 5

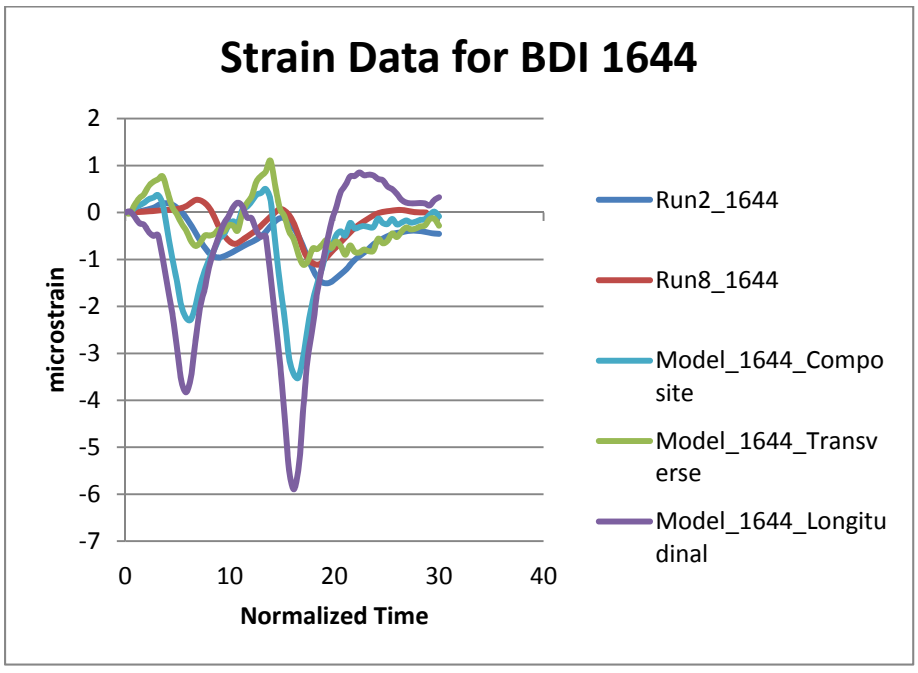

Figure 6-15 Field Test Data Based on BDI Strain Transducer No. 1644 - Placed Parallel to the Abutment on the Top Surface across a Crack between Beams Four and Five Near the East Side of the Bridge; Model Data Based on an Equivalent Position on Beam Four Near the West Side of the Bridge

6.4 FEA Model Stress Distributions

The model was then run with a static H-20 truck loading (a truck applying 8,000 pounds beneath the front axle and 32,000 pounds beneath the rear axle) on beams six and seven. The stress distributions at the slab-deck interface and the top surface were then analyzed to determine the cause of the cracks on the top surface of the concrete overlay. The stress displayed in the following figures has units of pounds per square inch (psi). Generally, the greatest tensile stresses exist near the abutments and on the opposite side of the bridge from the loading (see Figures 6-16 to 6-22). The tensile stresses between the beams (along the shear key) are evident from the transverse, first principal, and second principal stresses.

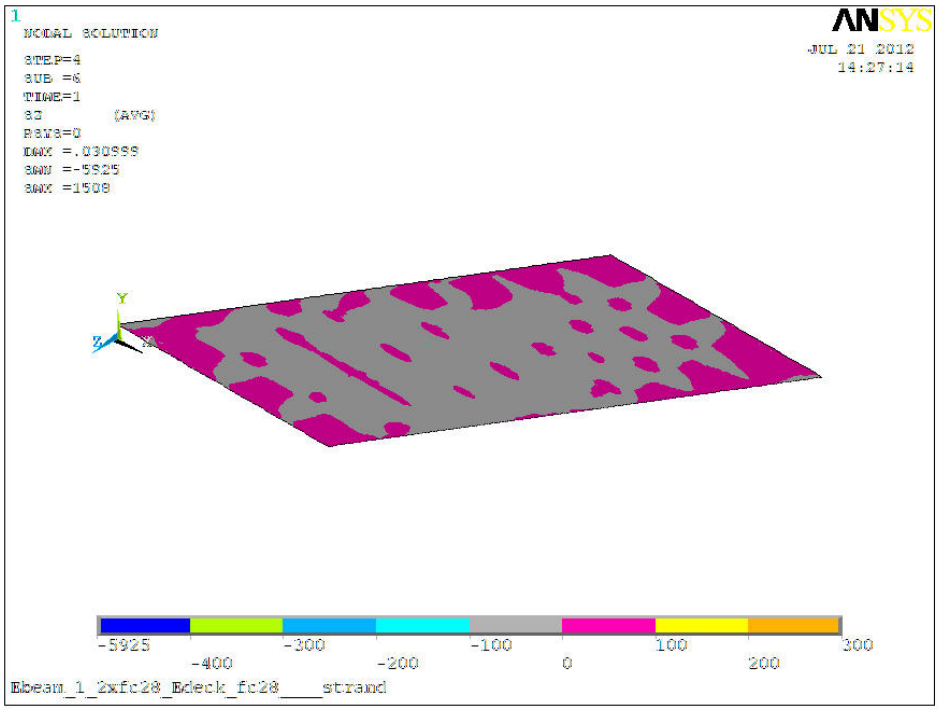

Figure 6-16 Transverse Stress at the Slab-Deck Interface

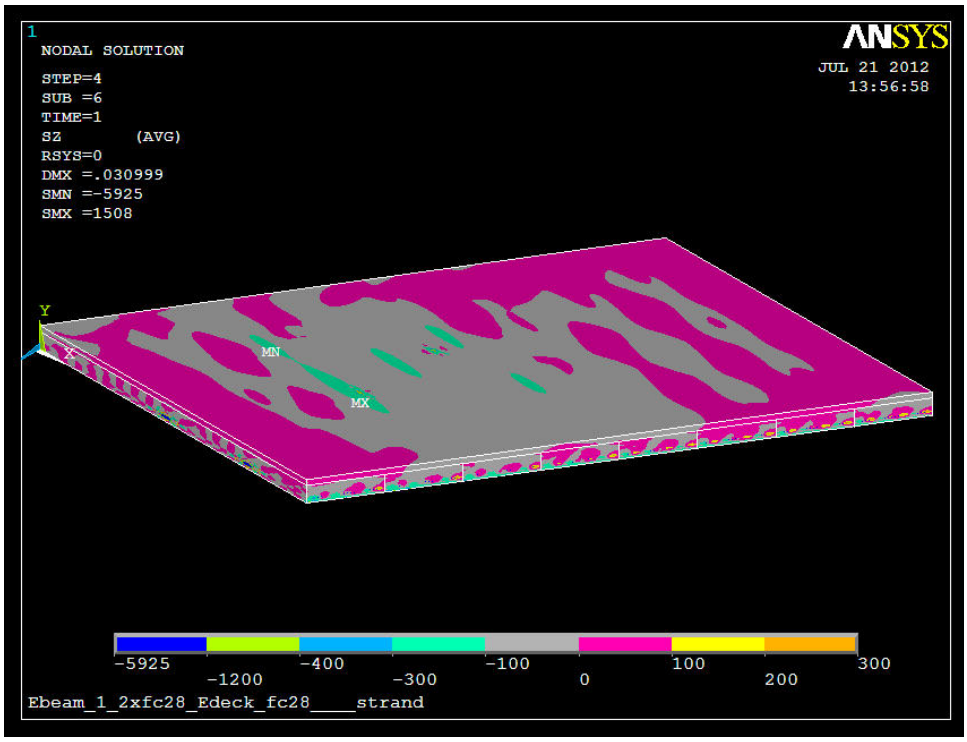

Figure 6-17 Transverse Stress at the Top Surface

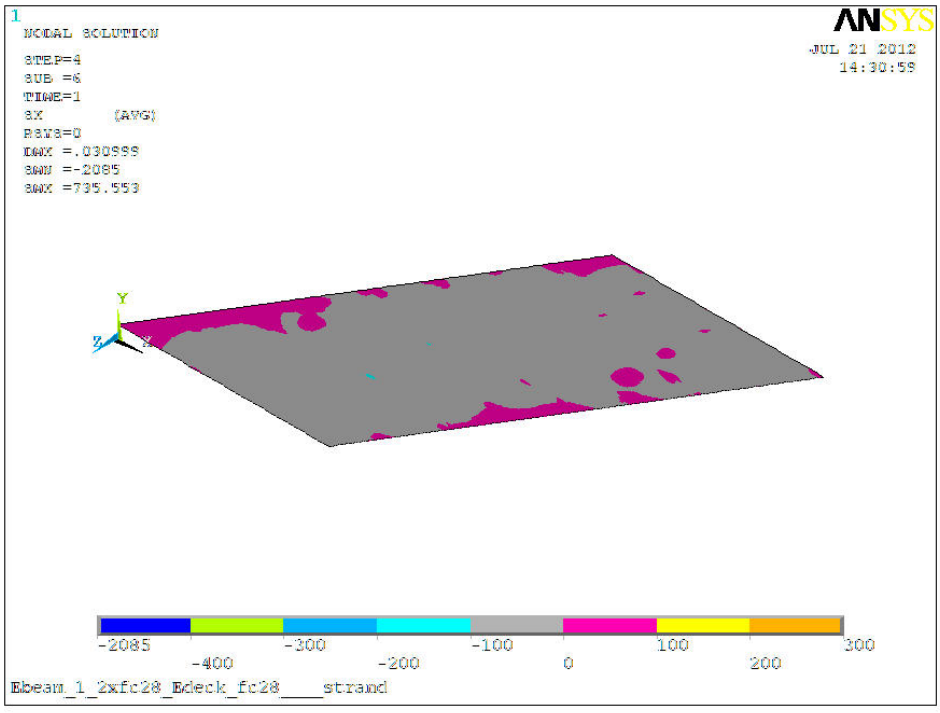

Figure 6-18 Longitudinal Stress at the Slab-Deck Interface

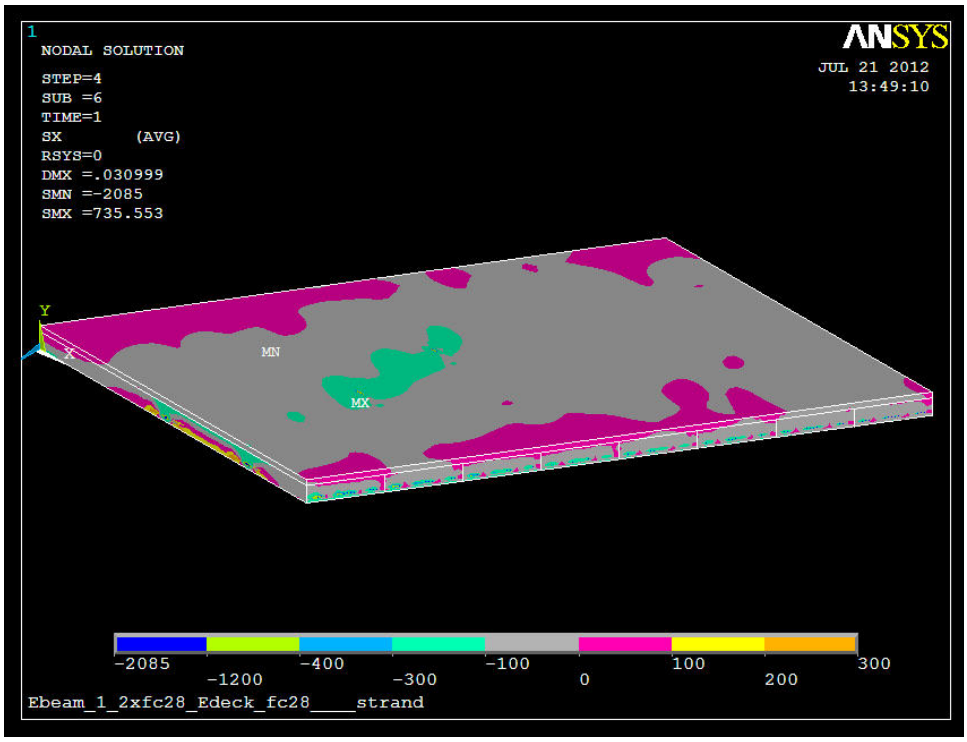

Figure 6-19 Longitudinal Stress at the Top Surface

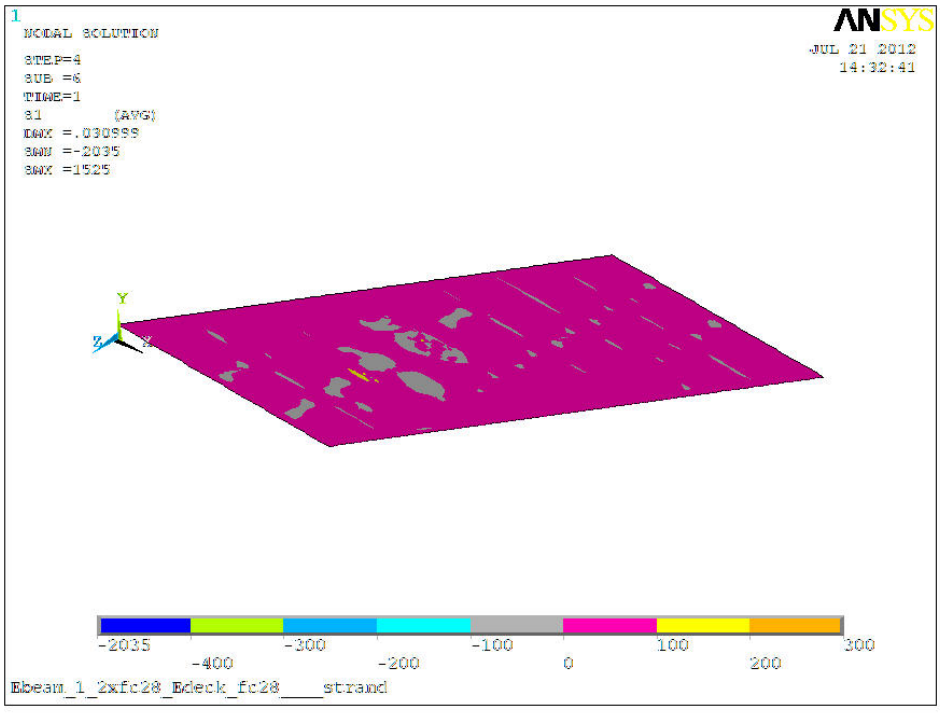

Figure 6-20 First Principal Stress at the Slab-Deck Interface

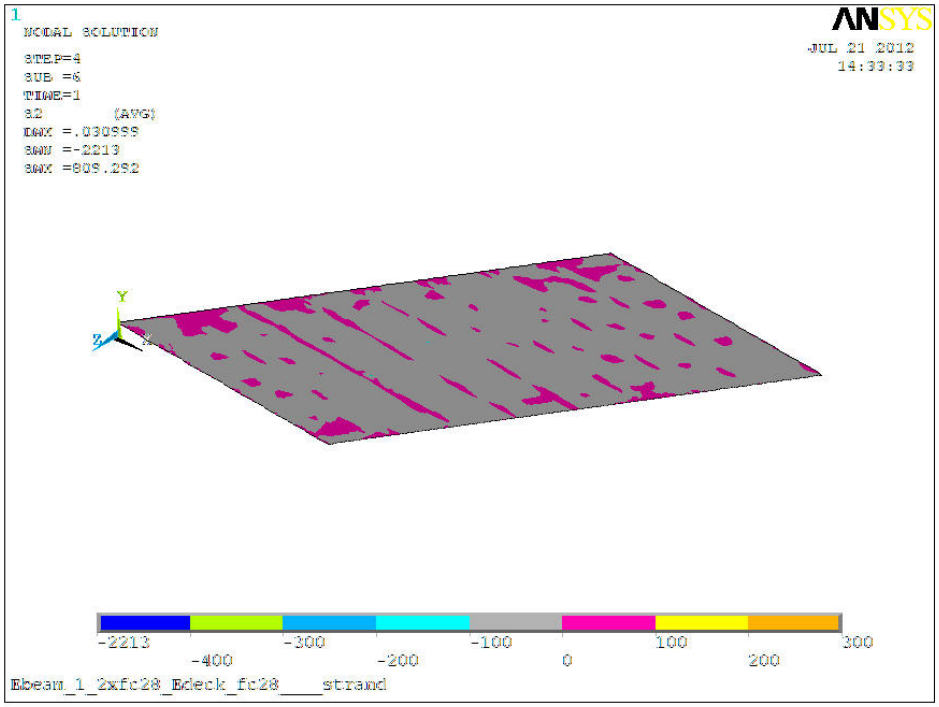

Figure 6-21 Second Principal Stress at the Slab-Deck Interface

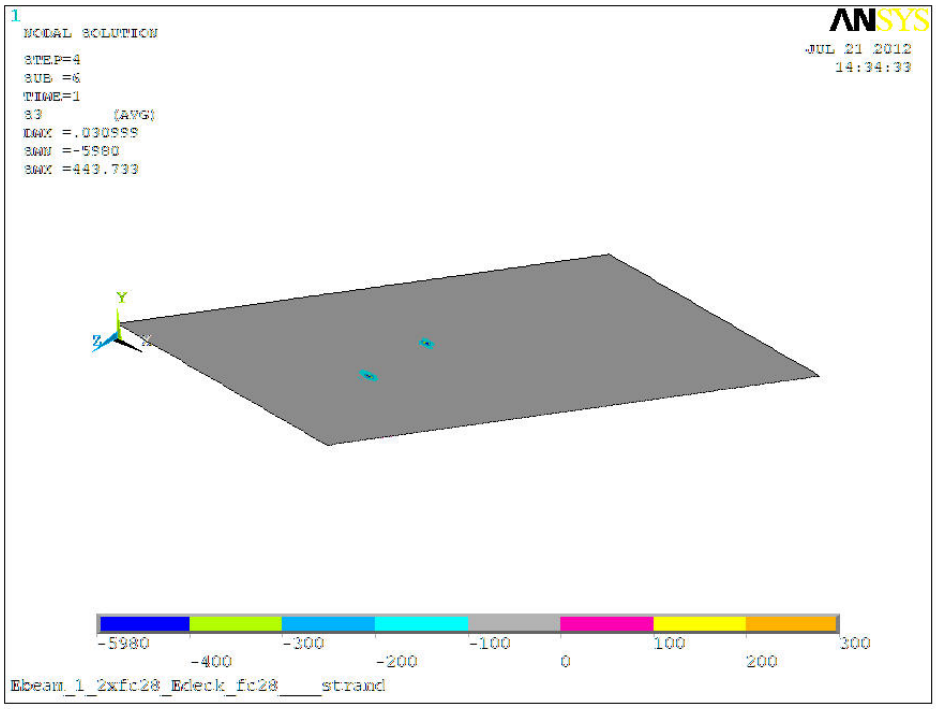

Figure 6-22 Third Principal Stress at the Slab-Deck Interface

Chapter 7: Parametric Study

7.1 Parametric Study Analysis Details

7.1.1 Parametric Study Analysis Assumptions

To obtain a more complete idea of how the skew angle affects transversely post-tensioned adjacent precast-concrete slab bridges, this research team conducted a parametric study with twenty-one different FEA models. Each bridge in the parametric study was designed as a simply supported two-lane bridge, with its 32'-0" width comprised of eight 4'-0" wide adjacent precast prestressed concrete slabs. These bridges were then fitted with a 5" concrete overlay. The transverse tie rod diameters and forces were based on the span length of each bridge model and designed according to the SHA standards. The transverse post-tensioning was designed as an ungrouted system. As with the FEA model described in Chapter 6, an H-20 truck loading was applied to each model. The longitudinal, transverse, first principal, second principal, and third principal stresses were examined for each model. The transverse stress at the slab-deck interface was chosen to be the critical analysis component because this stress predominately contributes to the longitudinal reflective cracking in the concrete overlay observed in the field. The longitudinal stress and the main component of the first principal stress are primarily carried by the concrete slabs which have not shown any structural or serviceability failures. The second and third principal stresses did not show a significant impact on the models used for the parametric study. The full results for the stresses present at the slab-deck interface for the first model as well as the longitudinal and first principal stresses for the remaining models are in Appendix C.

7.1.2 Parametric Study Analysis Procedure

The span length, skew angle, and transverse post-tensioning orientation of transversely post-tensioned adjacent precast-concrete slab bridges were investigated in order to produce the set of recommendations in Chapter 8. Three standard span lengths were considered: 25'-0", 40'-0", and 55'-0". Two skew angles were considered: 15° and 30°. (The behavior of these models changes as a function of both the skew angle and the length-to-width ratio. As the skew angle decreases and the bridge span length increases, the bridges act more similarly to a beam than a plate.) Finally, two orientations for the transverse post-tensioning were considered: parallel to the bridge abutments (skewed tie rods) and normal to the slabs (normal/staggered tie rods); these orientations are referred to as "skewed" or "normal" in the following sections. Additionally, our recommended transverse post-tensioning orientation is always on the left side of the page and other possible transverse post-tensioning orientations are on the right.

7.2 Twenty-Five Foot, Fifteen-Degree Skewed Bridge

Six FEA models were created to determine the best transverse post-tensioning practice for a 25'-0", 15° skewed bridge. In the first analysis, two loading conditions were compared to determine a standard loading condition for the rest of the FEA models in the parametric study. Four possible transverse post-tensioning orientations were considered in the second step of the analysis: four normal and staggered tie rods (connecting three or five beams together) located equidistant from each other; two skewed tie rods located at the third points; two skewed tie rods located 3'-0" from each abutment; and three skewed tie rods located 2'-6" from each abutment and at the midspan.

7.2.1 Loading: One Truck vs. Two Trucks

To determine the load that should be applied to each FEA model, a 25'-0", 15° skewed bridge model was created. A skewed post-tensioning tie rod was placed at each of the third points of the bridge, which is one orientation in accordance with current practice. One H-20 truck loading was applied and was followed in a separate run by two H-20 trucks loading to provide a comparison. As seen in Figure 7-1, there is little difference in the transverse stress at the slab-deck interface, so for the rest of the models only one H-20 truck loading was applied.

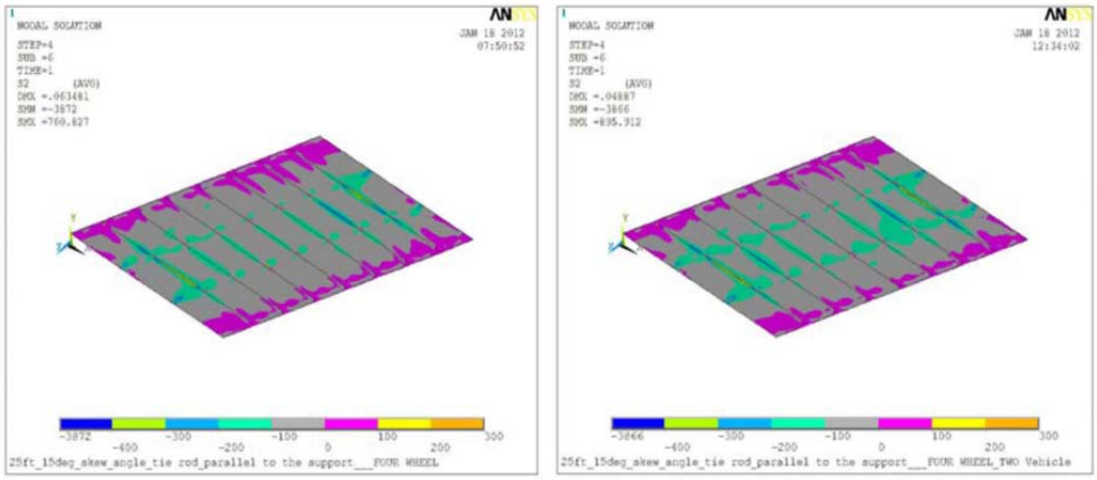

Figure 7-1 Transverse Stress Present at Slab-Deck Interface of a Twenty-Five Foot, Fifteen Degree Skewed Bridge (On the left, one truck loading and third points skewed; on the right, two truck loading and third points skewed.)

The magnitude of the transverse stress in pounds per square inch (psi) is indicated by the color bar below each image; the magnitude increases when moving toward the right. Any negative transverse stress indicates compression while positive transverse stress indicates tension. Because this project is concerned with the longitudinal cracking that is possibly initiated between slabs at the abutments, post-tensioning orientations that result in significant positive transverse stresses (pink/purple, yellow, and orange colors) in those areas are discouraged.

7.2.2 Post-Tensioning Orientation: Third Points Skewed vs. Four Normal and Staggered

As seen in Figure 7-2, using two skewed tie rods located at the third points shows significant improvement over using four tie rods that are normal and staggered (and that connect three or five beams together) located equivalent distances apart on the 25'-0", 15° skewed bridge.

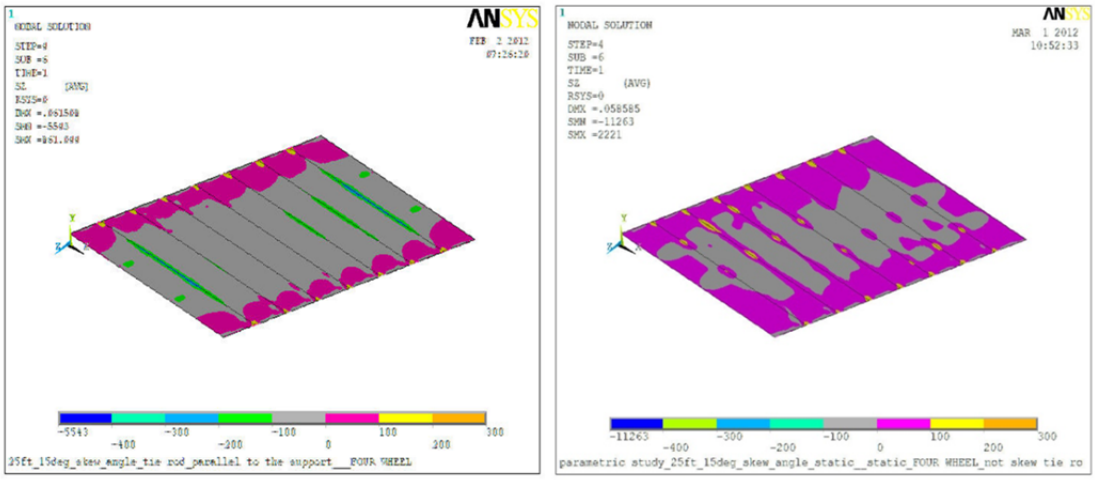

Figure 7-2 Transverse Stress Present at Slab-Deck Interface of a Twenty-Five Foot, Fifteen Degree Skewed Bridge (On the left, third points skewed; on the right, four normal and staggered.)

7.2.3 Post-Tensioning Orientation: Third Points Skewed vs. Ends Skewed

As Figure 7-3 demonstrates, using two skewed tie rods located 3'-0" from each abutment shows some improvement over using two skewed tie rods located at the third points of the 25'-0", 15° skewed bridge; however, this improvement is not significant.

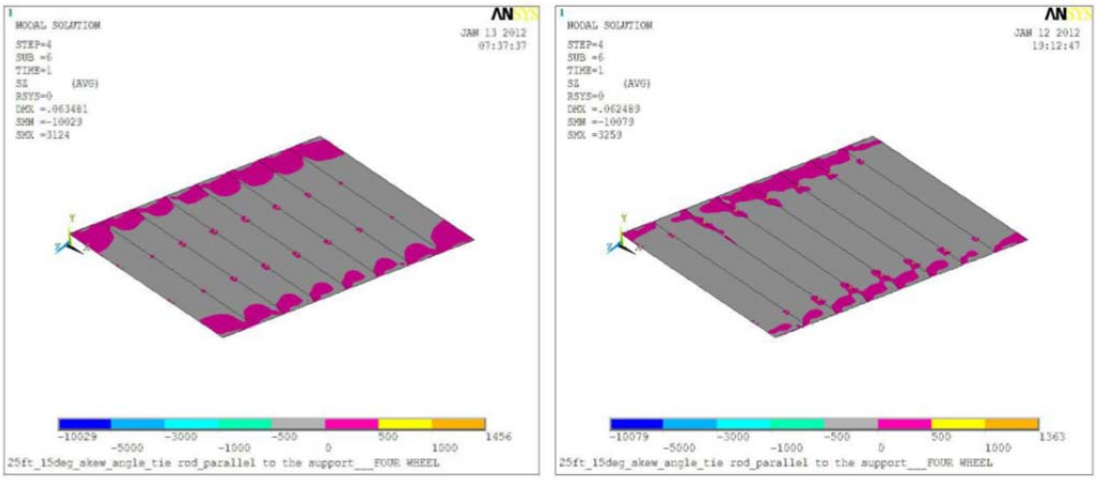

Figure 7-3 Transverse Stress Present at Slab-Deck Interface of a Twenty-Five Foot, Fifteen Degree Skewed Bridge (On the left, third points skewed; on the right, ends skewed.)

7.2.4 Post-Tensioning Orientation: Third Points Skewed vs. Ends and Midspan Skewed

As seen in Figure 7-4, three skewed tie rods located 2'-6" from each abutment and at the midspan shows some improvement over using two skewed tie rods located at the third points of the 25'-0", 15^0 skewed bridge. As with the post-tensioning comparison between third points skewed and ends skewed, the improvement was not significant.

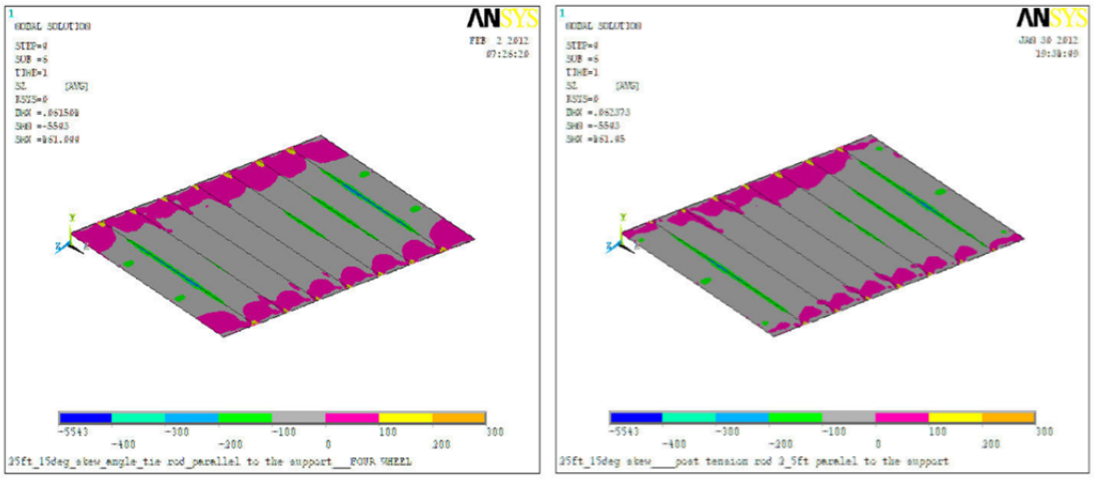

Figure 7-4 Transverse Stress Present at Slab-Deck Interface of a Twenty-Five Foot, Fifteen Degree Skewed Bridge (On the left, third points skewed; on the right, ends and midspan skewed.)

7.3 Twenty-Five Foot, Thirty Degree Skewed Bridge

Two FEA models were created to determine the best transverse post-tensioning practice for a 25'-0", 30° skewed bridge. Two transverse post-tensioning orientations were considered: four normal and staggered tie rods (connecting three or five beams together) located equivalent distances apart on the bridge and two skewed tie rods located at the third points.

7.3.1 Post-Tensioning Orientation: Third Points Skewed vs. Four Normal and Staggered

As Figure 7-5 demonstrates, using two skewed tie rods located at the third points shows significant improvement over using four normal and staggered tie rods located equidistant from each other on the 25'-0", 30° skewed bridge. However, there are significant stresses in both designs.

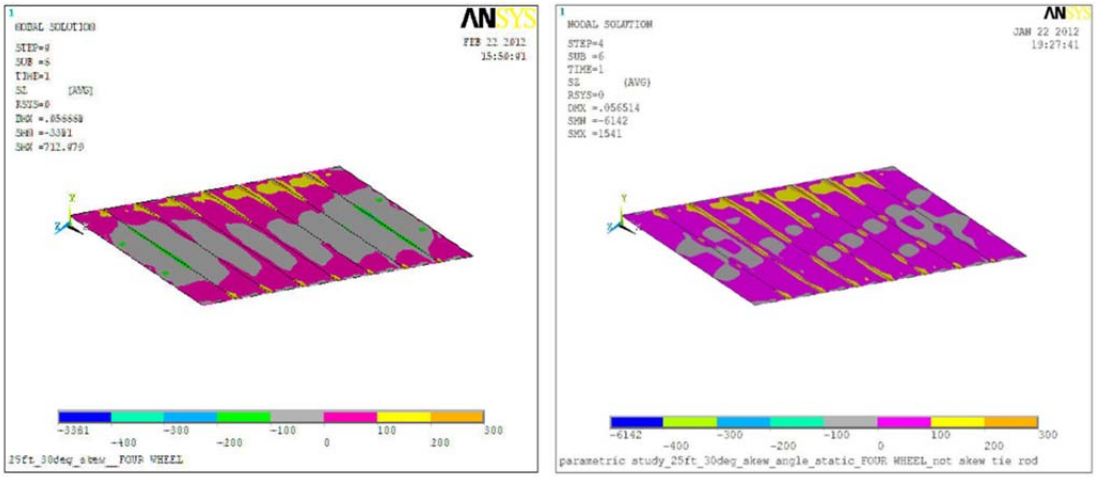

Figure 7-5 Transverse Stress Present at Slab-Deck Interface of a Twenty-Five Foot, Thirty Degree Skewed Bridge (On the left, third points skewed; on the right, four normal and staggered.)

7.4 Forty Foot, Fifteen Degree Skewed Bridge

Five FEA models were created to determine the best transverse post-tensioning practice for a 40'-0", 15° skewed bridge. Five possible transverse post-tensioning orientations were

considered: two normal tie rods (that connect all eight beams together) located at approximately the third points of the bridge, four normal and staggered tie rods (that connect three or five beams together) located equal distances apart, two skewed tie rods located at the third points, three skewed tie rods located 5’-0” from each abutment and at the midspan, and four skewed tie rods located 2’-0” and 14’-0” from each abutment.

7.4.1 Post-Tensioning Orientation: Ends and Midspan Skewed vs. Two Normal

As seen in Figures 7-6 through 7-8, using three skewed tie rods located 5’-0” from each abutment and at the midspan shows significant improvement over using two normal tie rods (that connect all eight beams together) located at approximately the third points of the 40’-0”, 15˚ skewed bridge, four normal and staggered tie rods (that connect three or five beams together) located equal distances apart, and two skewed tie rods located at the third points..

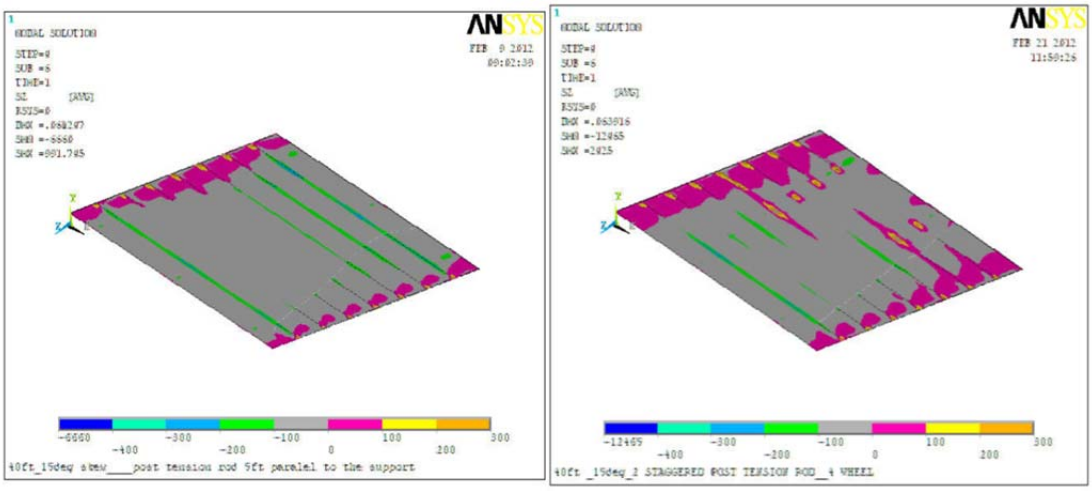

Figure 7-6 Transverse Stress Present at Slab-Deck Interface of a Forty Foot, Fifteen Degree Skewed Bridge (On the left, ends and midspan skewed; on the right, two normal.)

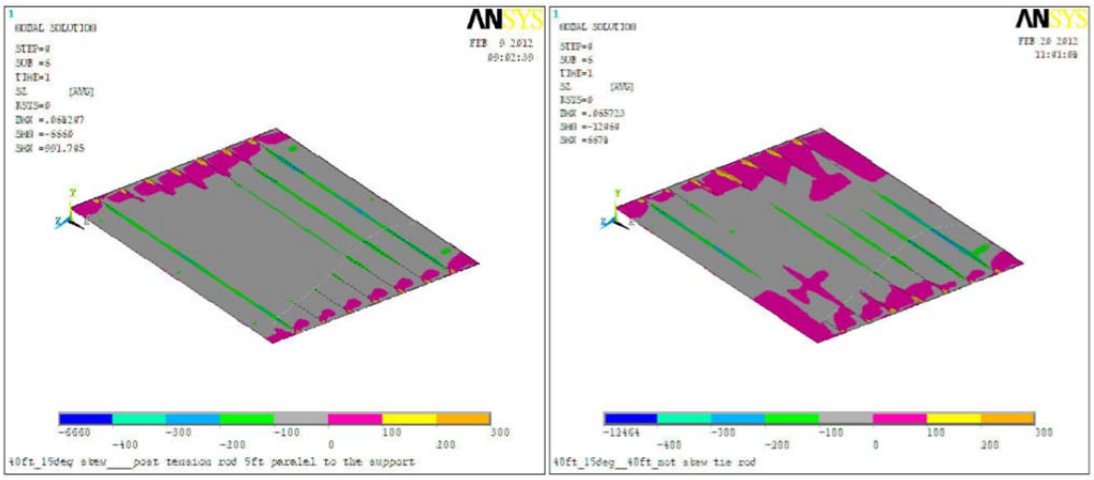

Figure 7-7 Transverse Stress Present at Slab-Deck Interface of a Forty Foot, Fifteen Degree Skewed Bridge (On the left, ends and midspan skewed; on the right, four normal and staggered.)

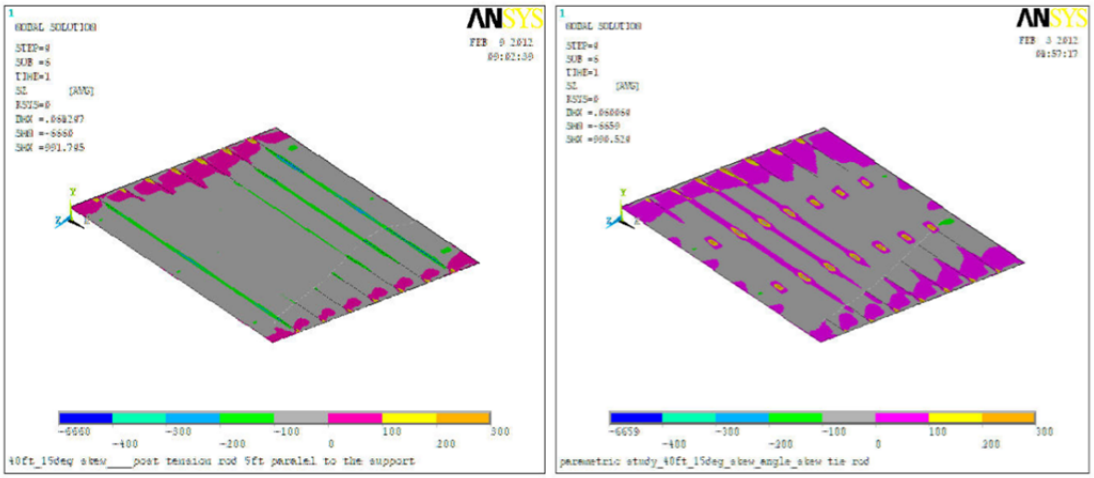

Figure 7-8 Transverse Stress Present at Slab-Deck Interface of a Forty Foot, Fifteen Degree Skewed Bridge (On the left, ends and midspan skewed; on the right, third points skewed.)

7.4.2 Post-Tensioning Orientation: Ends and Midspan Skewed vs. Four Skewed

As Figure 7-9 demonstrates, using four skewed tie rods located 2'-0" and 14'-0" from each abutment shows some improvement over using three skewed tie rods located 5'-0" from each abutment and at the midspan of the 40'-0", 15° skewed bridge, but this improvement is not significant.

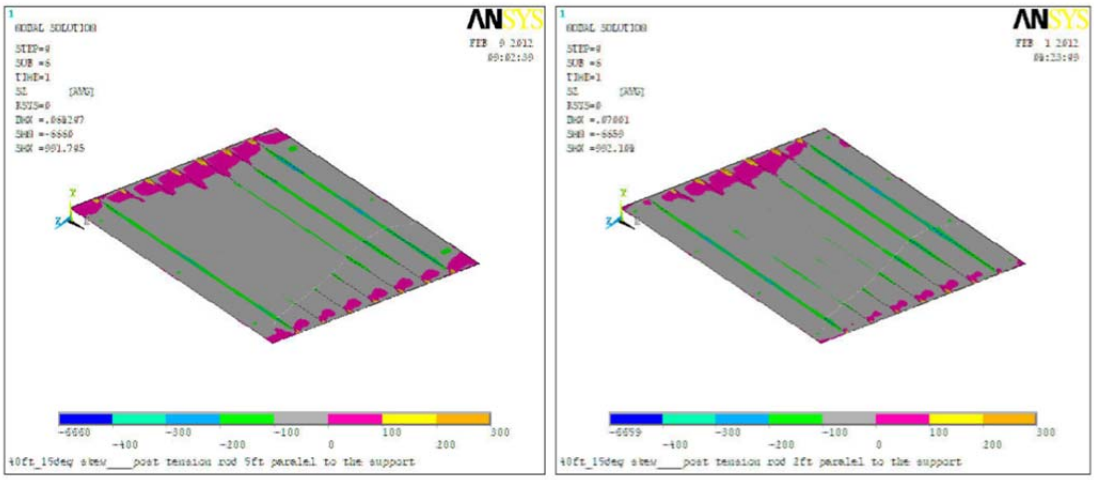

Figure 7-9 Transverse Stress Present at Slab-Deck Interface of a Forty Foot, Fifteen Degree Skewed Bridge (On the left, ends and midspan skewed; on the right, four skewed.)

7.5 Forty Foot, Thirty Degree Skewed Bridge

Four FEA models were created to determine the best transverse post-tensioning practice for a 40'-0", 30° skewed bridge. As in the previous models, the same four possible transverse post-tensioning orientations were considered: two normal tie rods (that connect all eight beams together) located at the third points of the bridge, four normal and staggered tie rods (that connect three or five beams together) located equal distances apart, two skewed tie rods located at the third points, and three skewed tie rods located 5'-0" from each abutment and at the midspan.

7.5.1 Post-Tensioning Orientation: Ends and Midspan Skewed vs. Two Normal

As seen in Figures 7-10 through 7-12, using three skewed tie rods located 5'-0" from each abutment and at the midspan shows some improvement over using two normal tie rods (connecting all eight beams together) located at approximately the third points of the 40'-0", 30° skewed bridge, over four normal and staggered tie rods (that connect three or five beams

together) that are located equal distances of the bridge, and over two tie rods located at the third points of the bridge.

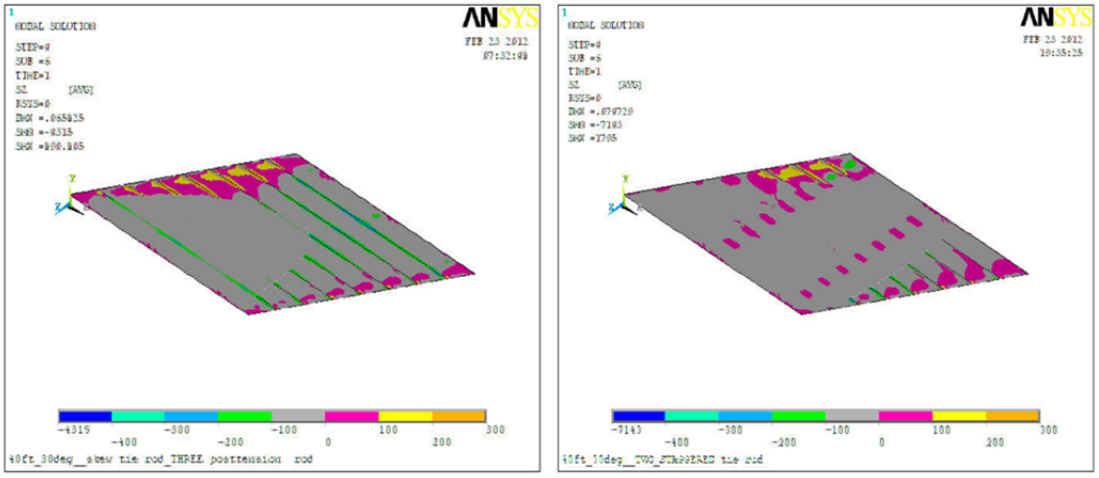

Figure 7-10 Transverse Stress Present at Slab-Deck Interface of a Forty Foot, Thirty Degree Skewed Bridge (On the left, ends and midspan skewed; on the right, two staggered.)

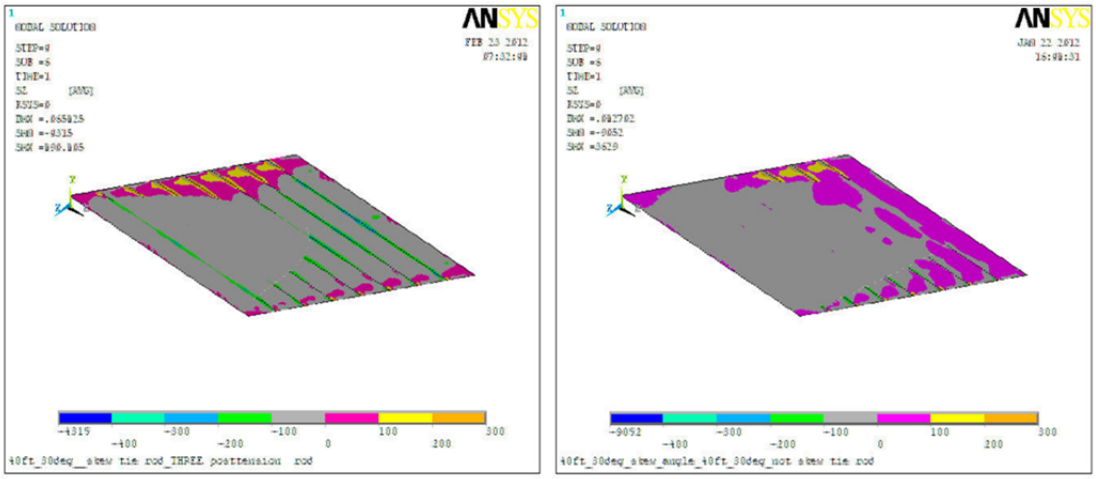

Figure 7-11 Transverse Stress Present at Slab-Deck Interface of a Forty Foot, Thirty Degree Skewed Bridge (On the left, ends and midspan skewed; on the right, four normal and staggered.)

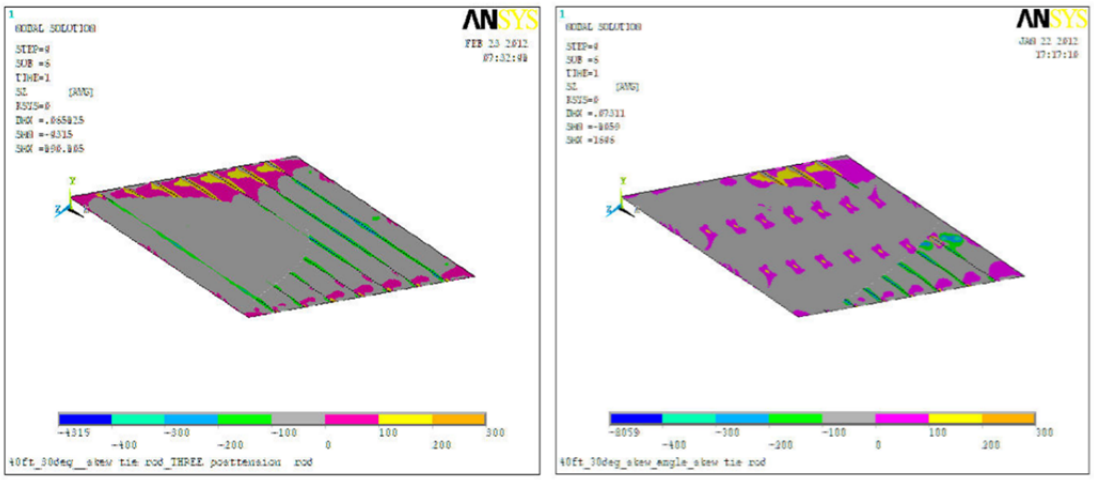

Figure 7-12 Transverse Stress Present at Slab-Deck Interface of a Forty Foot, Thirty Degree Skewed Bridge (On the left, ends and midspan skewed; on the right, third points skewed.)

7.6 Fifty-Five Foot, Fifteen Degree Skewed Bridge

Two FEA models were created to determine the best transverse post-tensioning practice for a 55'-0", 15° skewed bridge. Two possible transverse post-tensioning orientations were considered: two normal tie rods (that connect all eight beams together) located at approximately the third points of the bridge and four skewed tie rods located 5'-0" and 20'-0" from each abutment.

7.6.1 Post-Tensioning Orientation: Four Skewed vs. Two Normal

As Figure 7-13 demonstrates, using four skewed tie rods located 5'-0" and 20'-0" from each abutment shows minimal improvement over using two normal tie rods (that connect all eight beams together) located at approximately the third points of the 55'-0", 15° skewed bridge.

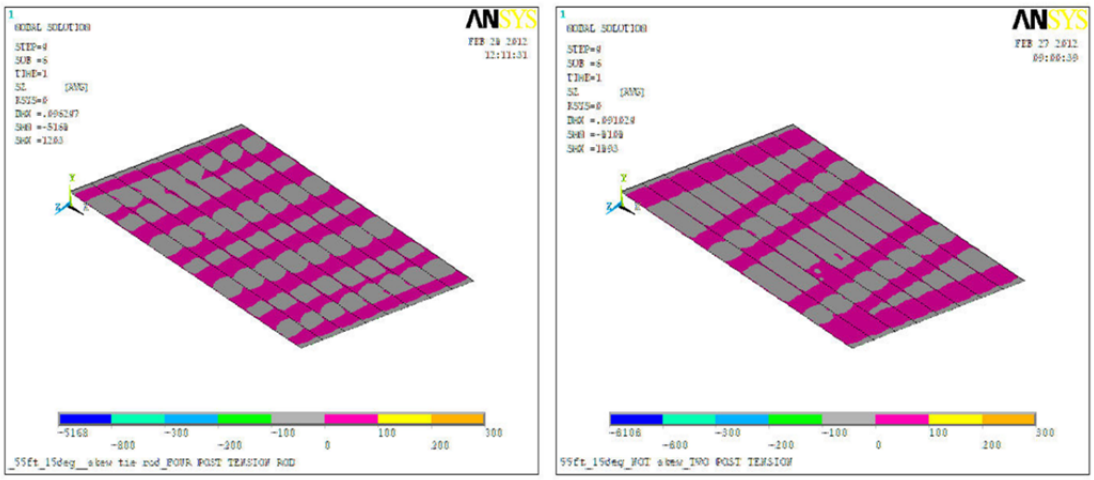

Figure 7-13 Transverse Stress Present at Slab-Deck Interface of a Fifty-Five Foot, Fifteen Degree Skewed Bridge (On the left, four skewed; on the right, two normal.)

7.7 Fifty-Five Foot, Thirty Degree Skewed Bridge

Two FEA models were created to determine the best transverse post-tensioning practice for a 55'-0", 30° skewed bridge. Two possible transverse post-tensioning orientations were considered: two normal tie rods (connecting all eight beams together) located at approximately the third points of the bridge and four skewed tie rods located 5'-0" and 20'-0" from each abutment.

7.7.1 Post-Tensioning Orientation: Four Skewed vs. Two Normal

As can be seen in Figure 7-14, using four skewed tie rods located 5'-0" and 20'-0" from each abutment shows significant improvement over using two normal tie rods (that connect all eight beams together) located at approximately the third points of the 55'-0", 30° skewed bridge.

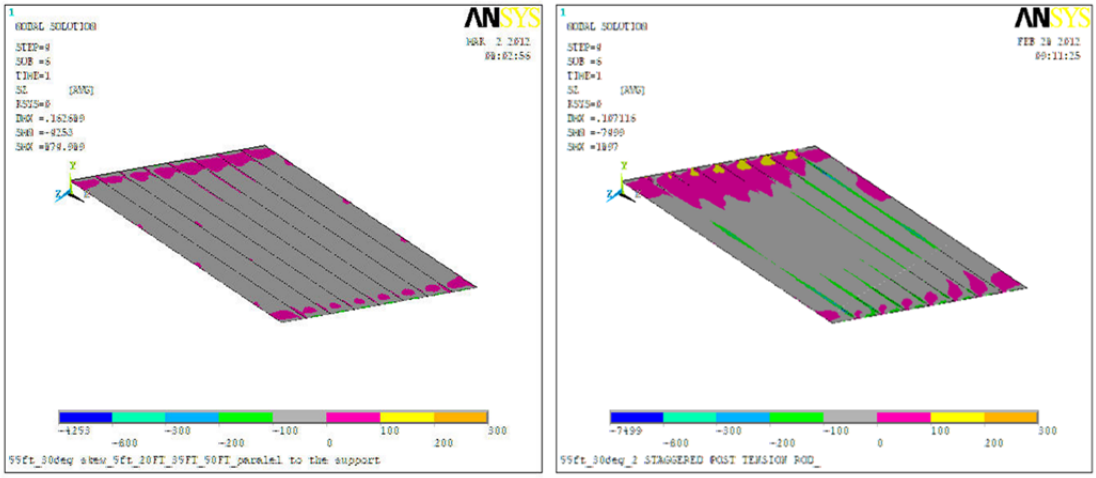

Figure 7-14 Transverse Stress Present at Slab-Deck Interface of a Fifty-Five Foot, Thirty Degree Skewed Bridge (On the left, four skewed; on the right, two normal.)

7.8 SHA Requested Parametric Study Extension

7.8.1 Parametric Study Extension Description

Constructing transverse post-tensioning normal to the beams is easier than constructing it parallel to the skew. Therefore, the SHA requested the parametric study be further extended to compare a combination of transverse post-tensioning orientations. In prior studies, only two orientations for the transverse post-tensioning were considered: parallel to the bridge abutments (skewed tie rods) and normal to the slabs (normal/staggered tie rods). For this extension, a combination of the two orientations was considered: skewed tie rods near the abutments but normal tie rods near the midspan of the bridge. For brevity, this orientation combination will be referred to as "combined" in the descriptions in the following sections. For consistency, our previously recommended transverse post-tensioning orientation is always placed on the left side of the page when in comparison with the alternatives. When three tie rods are used in this combined configuration, only the middle tie rod is normal to the beams; when four tie rods are used in this combined configuration, the two middle tie rods are normal to the beams. Miniature

figures displaying the orientation of the transverse post-tensioning will be inset in the upper right of each of the following stress distribution figures. All other features of these six FEA models are the same as those created in the main parametric study.

7.8.2 Forty Foot, Fifteen Degree Skewed Bridge – Post-Tensioning Orientation: Three Skewed vs. Three Combined

As seen in Figure 7-15, using three skewed tie rods located 5'-0" from each abutment and at the midspan shows minimal improvement over using a combined configuration of two skewed tie rods located 5'-0" from each abutment and one normal tie rod (connecting all eight beams together) located at the midspan of the 40'-0", 15° skewed bridge.

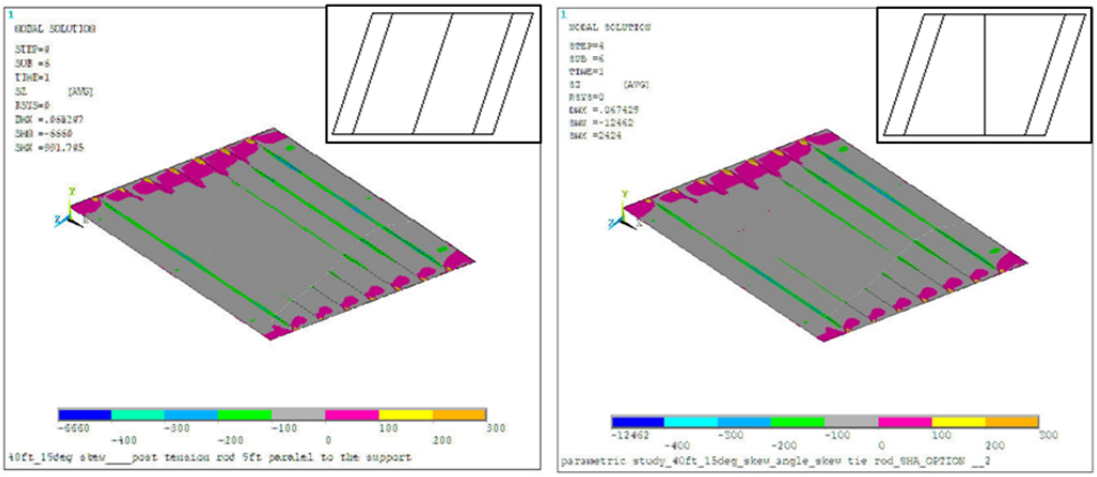

Figure 7-15 Transverse Stress Present at Slab-Deck Interface of a Forty Foot, Fifteen Degree Skewed Bridge (On the left, ends and midspan skewed; on the right, three combined.)

7.8.3 Forty Foot, Thirty Degree Skewed Bridge – Post-Tensioning Orientation: Three Skewed vs. Three Combined

As Figure 7-16 demonstrates, using three skewed tie rods located 5'-0" from each abutment and at the midspan shows minimal improvement over using a combined configuration

of two skewed tie rods located 5’-0” from each abutment and one normal tie rod (that connect all eight beams together) located at the midspan of the 40’-0”, 30˚ skewed bridge. There is, however, a different stress distribution.

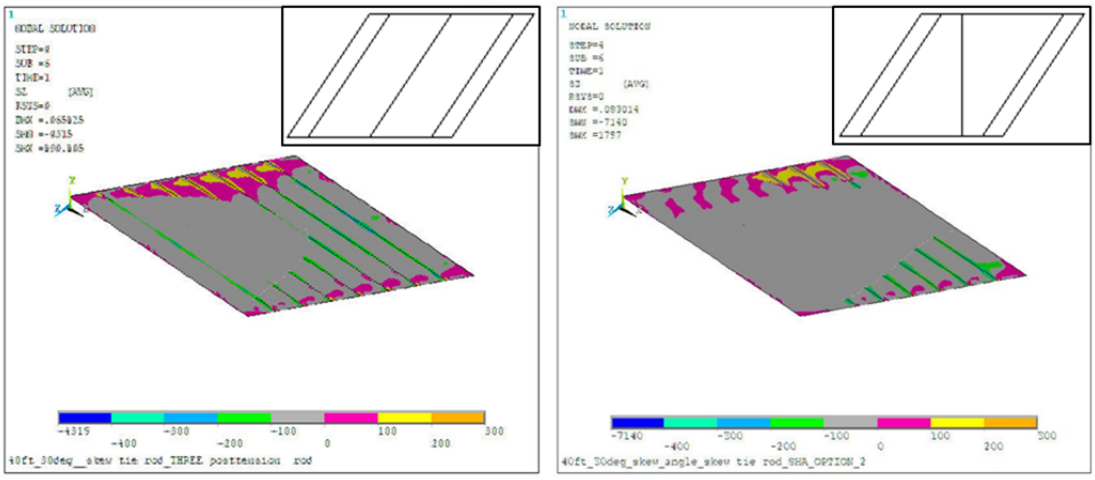

Figure 7-16 Transverse Stress Present at Slab-Deck Interface of a Forty Foot, Thirty Degree Skewed Bridge (On the left, ends and midspan skewed; on the right, three combined.)

7.8.4 Fifty-Five Foot, Fifteen Degree Skewed Bridge – Post-Tensioning Orientation: Four Skewed vs. Three Combined

As seen in Figures 7-17 and 7-18, using four skewed tie rods located 5’-0” and 20’-0” from each abutment shows minimal improvement over both a combined configuration of two skewed tie rods located 5’-0” from each abutment and one normal tie rod (that connect all eight beams together) located at the midspan and a combined configuration of two skewed tie rods located 5’-0” from each abutment and two normal tie rods (that connect all eight beams together) located 20’-0” from each abutment of the bridge of the 55’-0”, 15˚ skewed bridge.

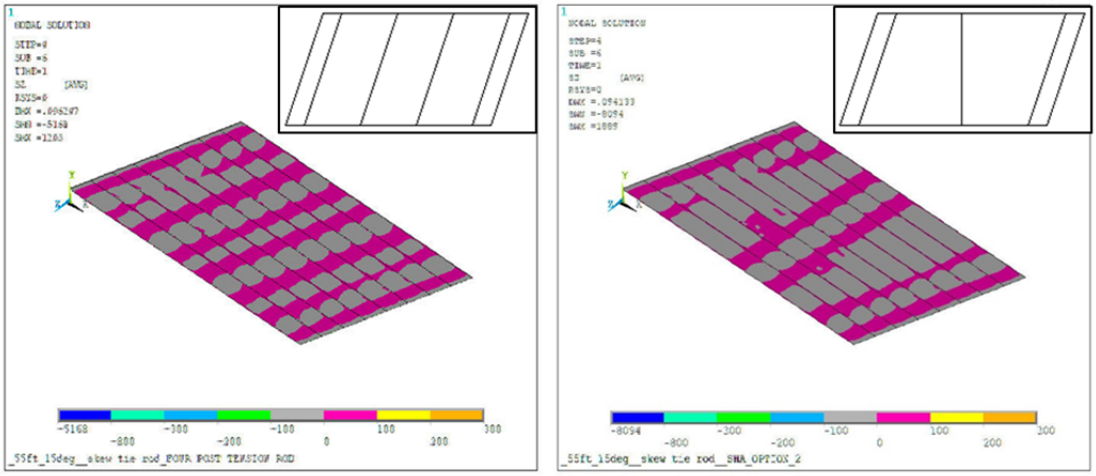

Figure 7-17 Transverse Stress Present at Slab-Deck Interface of a Fifty-Five Foot, Fifteen Degree Skewed Bridge (On the left, four skewed; on the right, three combined.)

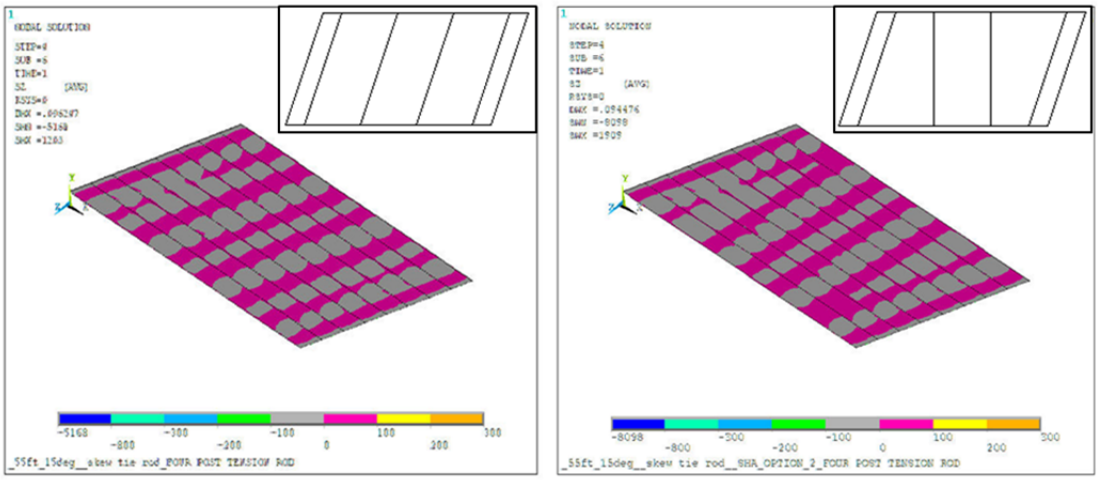

Figure 7-18 Transverse Stress Present at Slab-Deck Interface of a Fifty-Five Foot, Fifteen Degree Skewed Bridge (On the left, four skewed; on the right, four combined.)

7.8.5 Fifty-Five Foot, Thirty Degree Skewed Bridge – Post-Tensioning Orientation: Four Skewed vs. Three Combined

As seen in Figure 7-19, using four skewed tie rods located 5'-0" and 20'-0" from each abutment shows minimal improvement over using a combined configuration of two skewed tie

rods located 5’-0” from each abutment and one normal tie rod (connecting all eight beams together) located 20’-0” located at the midspan of the 55’-0”, 30˚ skewed bridge.

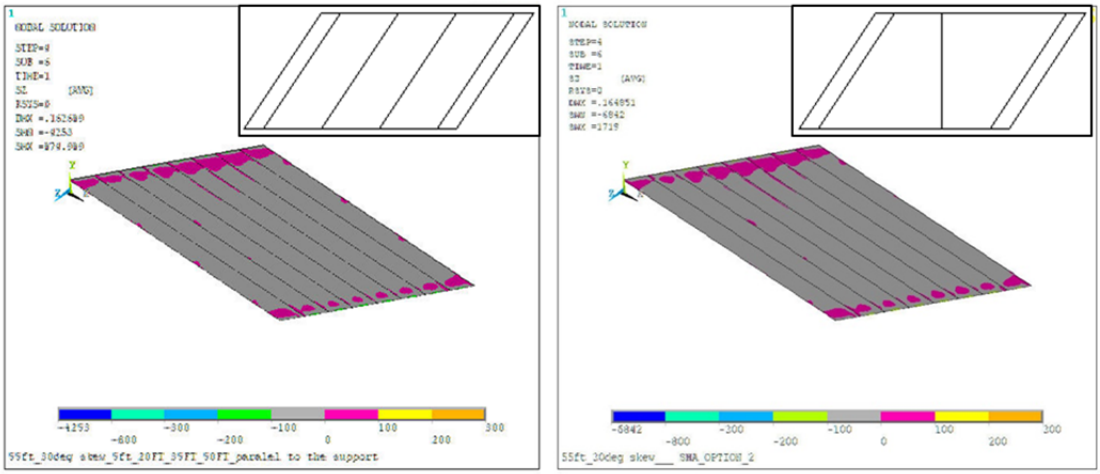

Figure 7-19 Transverse Stress Present at Slab-Deck Interface of a Fifty-Five Foot, Thirty Degree Skewed Bridge (On the left, four skewed; on the right, three combined.)

7.8.6 Fifty-Five Foot, Thirty Degree Skewed Bridge – Post-Tensioning Orientation: Four Skewed vs. Four Combined

As Figure 7-20 demonstrates, using four skewed tie rods located 5’-0” and 20’-0” from each abutment shows minimal improvement over using a combined configuration of two skewed tie rods located 5’-0” from each abutment and two normal tie rods (that connect all eight beams together) located 20’-0” from each abutment of the 55’-0”, 30˚ skewed bridge.

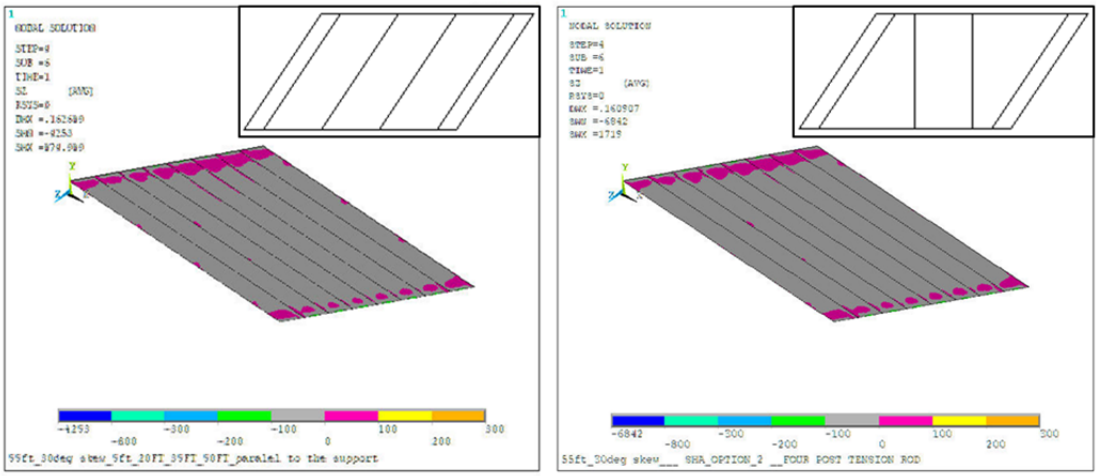

Figure 7-20 Transverse Stress Present at Slab-Deck Interface of a Fifty-Five Foot, Thirty Degree Skewed Bridge (On the left, four skewed; on the right, four combined.)

7.8.7 Loading: Two Axle vs. Three Axle

One FEA model was created to examine loading effects on the longer bridges. An H-20 truck loading had been used for the parametric study for consistency within the study because only two axles (fourteen feet apart) could fit on the twenty-five foot span bridge. A standard HS-20 truck loading (a truck with an 8,000-pound front axle and two 32,000-pound rear axles with at least fourteen feet between each axle) was applied to the 55'-0", 15° skewed bridge model (with a combined transverse post-tensioning configuration using three tie rods) to confirm that there was no difference between the parametric study loading and the normal bridge design loading. As Figure 7-21 demonstrates, there is negligible difference in the transverse stress at the slab-deck interface produced from the H-20 truck loading and the HS-20 truck loading.

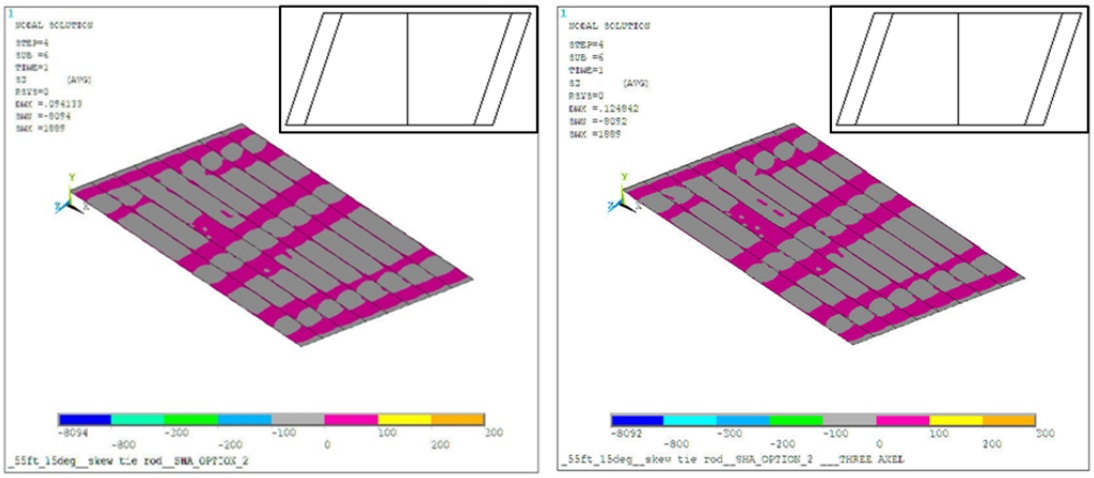

Figure 7-21 Transverse Stress Present at Slab-Deck Interface of a Fifty-Five Foot, Thirty Degree Skewed Bridge (On the left, H-20 (two axle) load; on the right, HS-20 (three axle) load.)

Chapter 8: Summary and Conclusions

8.1 Summary

This study had two main objectives. The first was to determine possible causes of the longitudinal cracking in the concrete overlays of some recently built Maryland bridges. The second was to propose revisions and additions to the current Maryland bridge design code for transversely post-tensioned adjacent precast-concrete slab bridges. First, a survey was performed using the bridge design standards posted on each state's Web site and compared with recently performed surveys also pertaining to the design of this type of bridge. Then, a comprehensive literature review was conducted to gain more complete knowledge of the behavior, design evolution, and construction options of this type of bridge. Next, a field test was completed on a local bridge that displayed cracking, and a FEA model was created of this bridge to perform more extensive analysis of the cracking and to provide a base model for the parametric study. Finally, a parametric study was performed using FEA models. The main conclusion to be drawn from these data is that although the skew angle and the bridge's span have a significant effect on the stress these types of bridge undergo, transverse post-tensioning can be an effective means for reducing the stress.

The following points summarize key findings:

- States share no consensus about best practices for transversely post-tensioning adjacent precast-concrete multi-beam bridges. Some states do not even consider the effects the skew angle has on the stress distribution caused by loads on this type of bridge.

- As a bridge's skew angle increases and the length-to-width ratio of a bridge decreases, the likelihood of reflective cracking occurring greatly increases due to the introduction of alternate load paths.
- The reflective cracking is probably initiated due to thermal strains, but vehicle loads play a large part in crack propagation.
- Transverse post-tensioning placed close to the abutments and oriented parallel to the skew angle is very effective at reducing the transverse stress in this type of bridge.

The conclusions are more fully enumerated in the following section.

8.2 Conclusions

8.2.1 Causes of Cracks in the Knoxville, MD, Bridge

Four likely contributors to the reflective cracking on the top surface of the concrete overlay of the Knoxville, MD, bridge are: temperature effects, grout shrinkage, the large skew angle, and heavy vehicle loads. Frequently, the bond between the shear key and the concrete beams is the weakest point and the cause of failure; this is critical because the bond has a lower strength than either the grout or the concrete (Sharpe, 2007). Reports often indicate that thermal loads cause crack initiation, sometimes even before a bridge is opened to traffic. These thermal loads may have contributed to cracking in this specific case (Badwan & Liang, 2007; Sharpe, 2007). In addition, conventional grout has relatively low shear and tensile strength, (approximately 360 psi and 220 psi, respectively), but tests have recorded failure at as little as 61 psi and 75 psi (longitudinal shear and direct tension, respectively; Sharpe, 2007). The results of the parametric study (Chapter 7) make clear that large skew angles significantly increase the

amount of transverse stress (tension) applied to the shear keys, especially at the abutments. (The Knoxville, MD, bridge, has a skew angel of 31.4°.) The field data and the FEA models indicate the bridge undergoes large strains and stresses significant enough to, at a minimum, propagate the existing cracks.

8.2.2 Parametric Study Results

Based on the results from the twenty-eight FEA models in the parametric study, a few conclusions can be made that are likely to reduce the likelihood of reflective cracking on the top surfaces of precast-concrete multi-beam bridges. The transverse post-tensioning orientation and locations can greatly decrease stresses caused by vehicular loads. Transversely post-tensioning should be done parallel to the supports (i.e., parallel to the skew), especially when near the abutments of a skewed adjacent precast-concrete slab bridge. Transversely post-tensioning that is parallel to the skew instead of normal to the beams decreases the transverse stresses present at the slab-deck interface. All bridges should be built with as small a skew as is practical, but there is significant increase in transverse stress in bridges with skew angles that exceed 30°. Table 8-1 summarizes the preliminary recommendations for the SHA bridge design standards.

Span (feet)	Maximum Skew Angle (degrees)	Number of Transverse Tie Rods	Orientation of Transverse Tie Rods	Location of Transverse Tie Rods
< 30	30	2	Parallel to Skew	Third Points (L/3)
30 – 45	30	3	Parallel to Skew	5’-0” from Supports and Midspan (L/2)
> 45	30	4	Parallel to Skew	5’-0” and 20’-0” from Supports

Table 8-1 Recommended Skew Particulars for Transversely Post-Tensioned Adjacent Precast-Concrete Slab Bridge Standard in Maryland

The research team's findings from the SHA-requested extension to the parametric study show that constructing the transverse post-tensioning tie rods normal to the beams instead of parallel to the skew near the midspan of the bridge has a negligible effect on the resulting transverse stress at the slab-deck interface. As a result, the SHA bridge design standards should provide the following notes: (1) The tie rods closest to the abutment must be constructed parallel to the skew of the bridge; (2) the tie rods near the midspan of the bridge may be constructed normal to the beams as long as the maximum spacing between the ends of adjacent tie rods on both sides of the bridge is less than 25'; and (3) should the bridge width require it, transverse post-tensioning may be staggered (i.e., one tie rod does not have to connect all of the beams across the width of the bridge) as long as the tie-rods are overlapped (i.e. the tie rods originating from each exterior beam should overlap at least one interior beam).

8.3 Future Research

The research team recommends two additional aspects of the construction process be studied in the SHA's attempt to reduce reflective cracking on the top surfaces of bridges. First, full-depth shear key designs should be further investigated in future research because they have been shown to be more effective than partial-depth shear keys at transferring shear force between beams and, as a result, can reduce shear key-related longitudinal cracking by up to 50% (Russell, 2009). Second, investigations into the construction sequence to determine whether grouting the shear keys should occur before transversely post-tensioning the slabs are recommended. When the slabs grouted after post-tensioning, the transverse stress at the slabs' contact points increase and the grout merely acts as a filler. As a result, the grout transfers a minimal amount of shear force and only transfers the compressive stress of any transverse bending moments (Russell, 2009). Grouting before post-tensioning places compressive stress in the grout and across the

interface, both allowing the shear key to transfer more shear force and providing a higher moment capacity while minimizing tensile stresses in the shear key that lead to longitudinal cracking (Russell, 2009). A few states have included a construction sequence detail in their bridge design specifications and reported the construction sequence successfully reduced the amount of cracking in adjacent precast-concrete multi-beam bridges. In order to see reduced cracking, the following three steps should be taken: (1) the transverse tendons should be tensioned to approximately a tenth of the total force; (2) the shear keys should be filled with grout; and (3) the transverse tendons are tensioned to the full post-tensioning force (Massachusetts Department of Transportation, 2009; Rhode Island Department of Transportation, 2010; Russell, 2011; Vermont Agency of Transportation, 2011). Data resulting from investigations into these matters would be helpful in preventing further reflective cracking.

Appendix A: Source Websites for the Survey of State Practices for Transversely Post-Tensioned Bridges

Arizona Department of Transportation (ADOT) (2007). *Bridge Design Guidelines*. August 17, 2011. <http://www.azdot.gov/Highways/bridge/Guidelines/DesignGuidelines/>.

District of Columbia Department of Transportation (DDOT) (2009). *Design and Engineering Manual*. August 17, 2011. <http://ddot.dc.gov/DC/DDOT/Projects+and+Planning/Standards+and+Guidelines/Design+and+Engineering+Manual/DDOT+Design+and+Engineering+Manual+-+April+2009>.

Indiana Department of Transportation (INDOT) (2011). *The Indiana Design Manual*. August 25, 2011. <http://www.in.gov/dot/div/contracts/standards/dm/2011/index.html>.

Kentucky Department of Highways (2008). *Kentucky Standard Drawings*. August 25, 2011. <http://transportation.ky.gov/Highway-Design/Standard%20Drawing%20%20Sepia%20PDFs/Structure-SERIES2008.pdf#bdp004-03>.

Massachusetts Department of Transportation (MassDOT) (2009). *2009 LRFD Bridge Manual*. August 25, 2011. <http://www.mhd.state.ma.us/default.asp?pgid=bridge/bridgemanual_01&sid=about>.

Michigan Department of Transportation (MDOT) (2011). *Bridge Design Guides*. August 25, 2011. <http://mdotwas1.mdot.state.mi.us/public/design/englishbridgeguides/>.

New York State Department of Transportation (NYSDOT) (2011). *Bridge Manual*. August 25, 2011. <https://www.dot.ny.gov/divisions/engineering/structures/manuals/bridge-manual-usc>.

North Carolina Department of Transportation (NCDOT) (2012). *Standard Specifications for Roads and Structures*. February 20, 2012. <http://www.ncdot.gov/doh/preconstruct/ps/specifications/2012draft.pdf>.

Ohio Department of Transportation (ODOT) (2007). *Bridge Design Manual (BDM 2007)*. August 29, 2011. <http://www.dot.state.oh.us/Divisions/Engineering/Structures/standard/Bridges/Pages/BDM2007.aspx>.

Ohio Department of Transportation (ODOT) (2011). *Standard Bridge Drawings*. August 25, 2011. <http://www.dot.state.oh.us/Divisions/Engineering/Structures/standard/Bridges/Pages/StandardBridgeDrawings.aspx>.

Oregon Department of Transportation (ODOT) (2004, rev. April 2011). *Bridge Design and Drafting Manual*. February 20, 2012. <http://www.oregon.gov/ODOT/HWY/BRIDGE/docs/BDDM/apr-2011_finals/section_1-2004_apr2011.pdf>.

Pennsylvania Department of Transportation (2011). *Bridge Standard Drawings*. February 20, 2012. <http://www.dot.state.pa.us/Internet/BQADStandards.nsf/home?OpenFrameset>.

Rhode Island Department of Transportation (RIDOT) (2010). *Bridge Design Standard Details*. August 29, 2011. <http://www.dot.ri.gov/documents/engineering/BlueBook/RIDOT_Bridge_Standards%202010.pdf>.

South Carolina Department of Transportation (SCDOT) (2007). *2007 Standard Specifications for Highway Construction*. February 22, 2012. <http://www.scdot.org/doing/construction_StandardSpec.aspx>.

South Carolina Department of Transportation (SCDOT) (2010). *Bridge Drawings and Details*. February 22, 2012. <http://www.scdot.org/doing/structural_Drawings.aspx>.

State of Connecticut Department of Transportation (ConnDOT) (2003). *Bridge Design Manual*. August 17, 2011. <http://www.ct.gov/dot/lib/dot/documents/dpublications/bridge/bdm.pdf>.

Texas Department of Transportation (TXDOT) (2011). *Bridge Design Manual - LRFD*. February 20, 2012. <http://onlinemanuals.txdot.gov/txdotmanuals/lrf/index.htm>.

Texas Department of Transportation (TXDOT) (2012). *Superstructure Design Information*. February 20, 2012. <http://www.txdot.gov/business/contractors_consultants/bridge/super_design.htm>.

Vermont Agency of Transportation (VTrans) (2010). *Structures Design Manual*. February 20, 2012. <http://www.aot.state.vt.us/progdev/Publications/DocumentsPUBLICATIONS/Structures_Design_Manual.pdf>.

Vermont Agency of Transportation (VTrans) (2011). *2011 Standard Specifications for Construction Book*. February 20, 2012. <http://www.aot.state.vt.us/conadmin/2011StandardSpecs.htm>.

Washington Department of Transportation (WSDOT) (2012). *Bridge Design Manual LRFD*. February 22, 2012. <http://www.wsdot.wa.gov/Publications/Manuals/M23-50.htm>.

West Virginia Division of Highways (WVDOH) (2004). *Bridge Design Manual*. February 22, 2012. <http://www.transportation.wv.gov/highways/engineering/files/WVBDML.pdf>.

Wisconson Department of Transportation (WisDOT) (2012). *LRFD Bridge Manual*. February 22, 2012. <http://on.dot.wi.gov/dtid_bos/extranet/structures/LRFD/LRFDManualIndex.htm>.

Wyoming Department of Transportation (WYDOT) (2008). *Bridge Applications Manual*. February 22, 2012. <http://www.dot.state.wy.us/wydot/engineering_technical_programs/bridge/bridge_applications_manual>.

Appendix B: Knoxville, MD, Test Bridge Plans

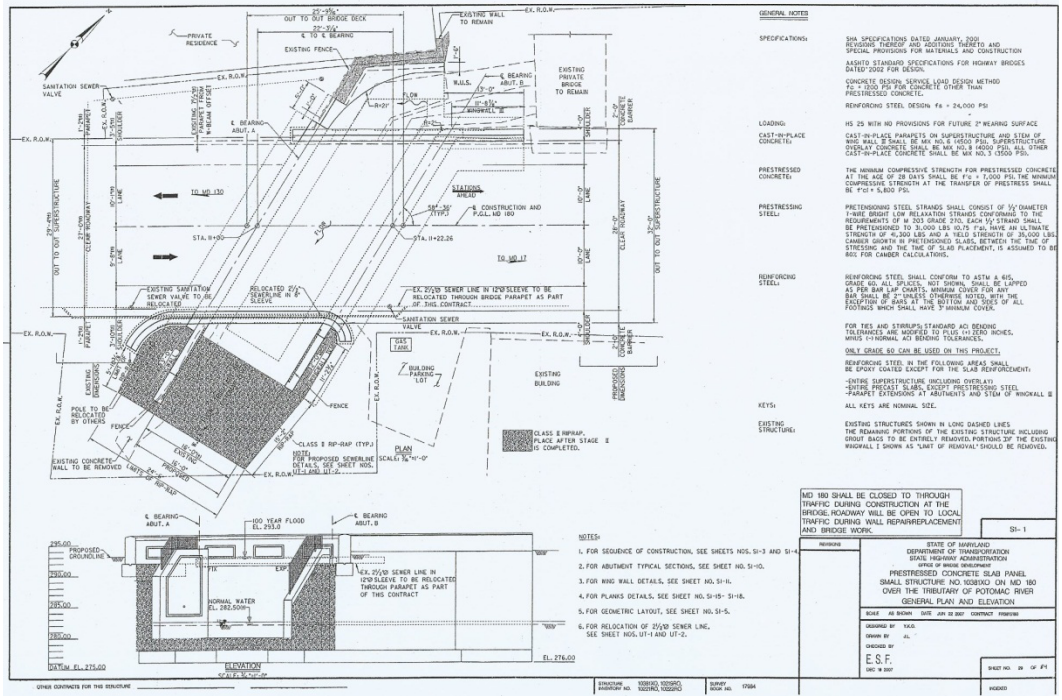

Figure B-1 General Plan and Elevation View of the Knoxville, MD, Bridge

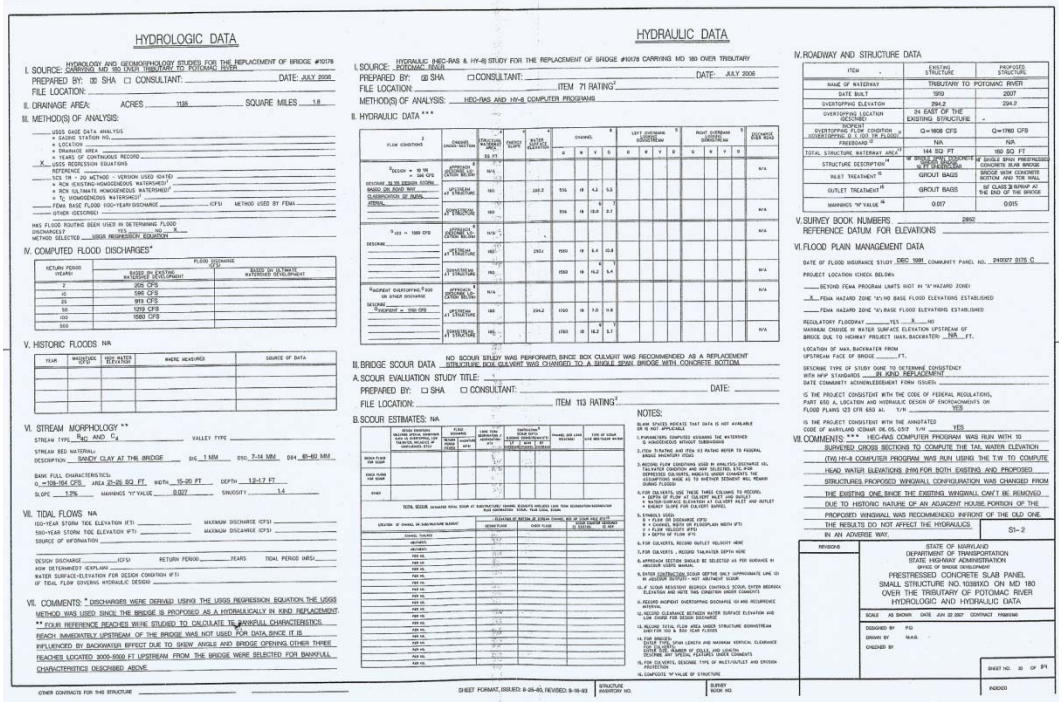

Figure B-2 Information Summary of the Knoxville, MD, Bridge

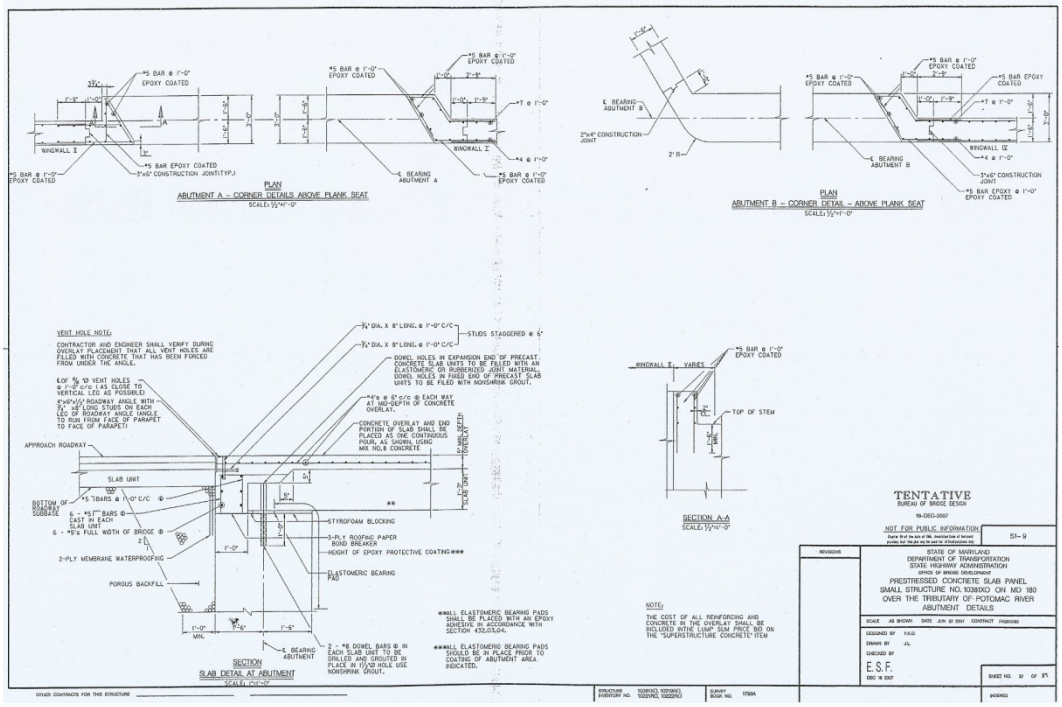

Figure B-3 Abutment and Corner Details of the Knoxville, MD, Bridge

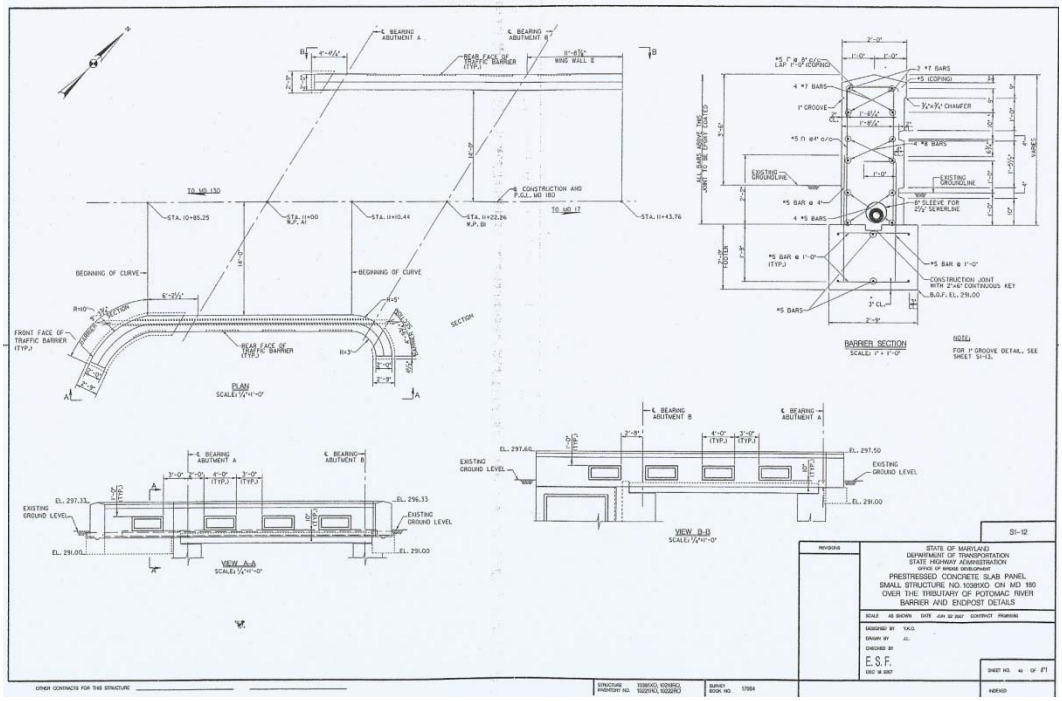

Figure B-4 Parapet Details of the Knoxville, MD, Bridge

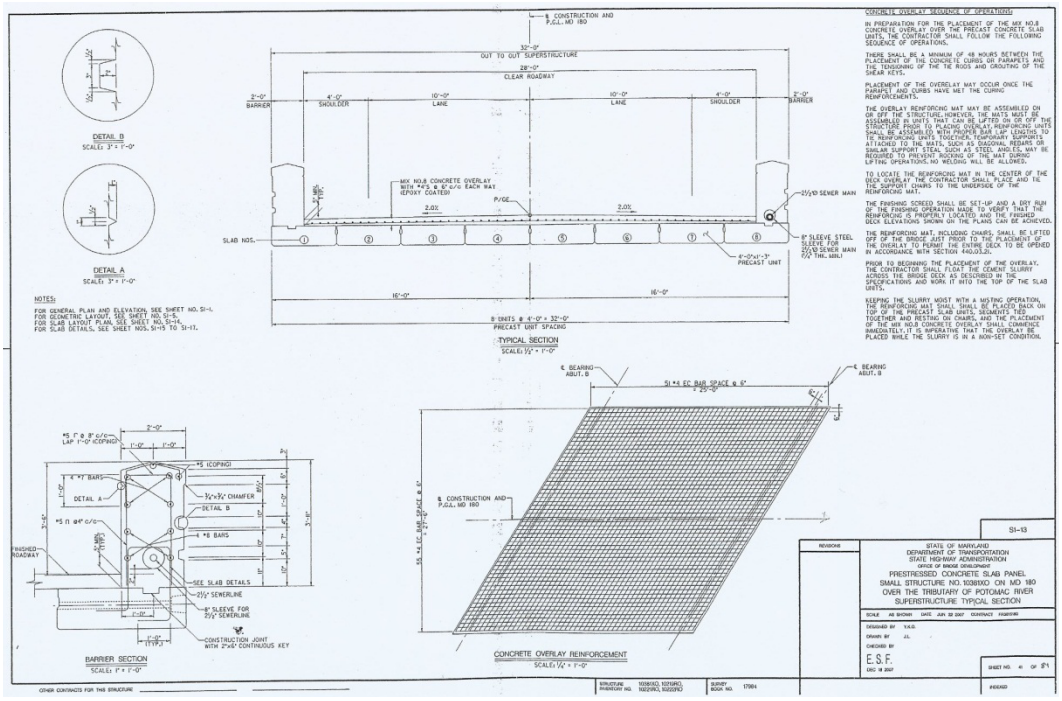

Figure B-5 Knoxville, MD, Bridge Superstructure Typical Section

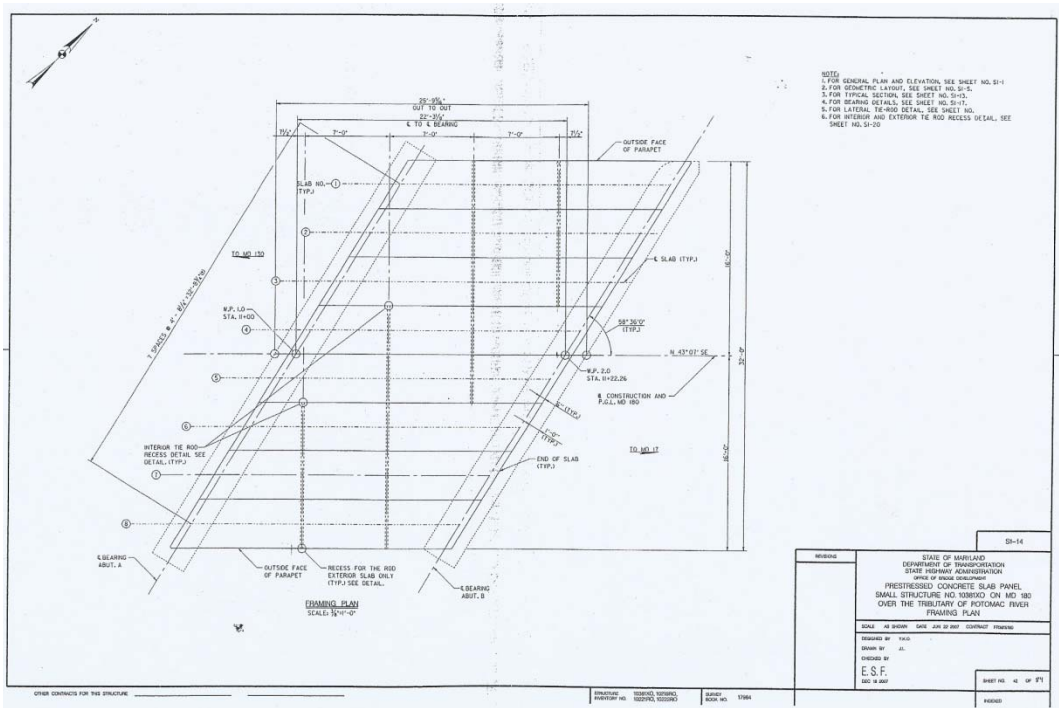

Figure B-6 Knoxville, MD, Bridge Framing Plan

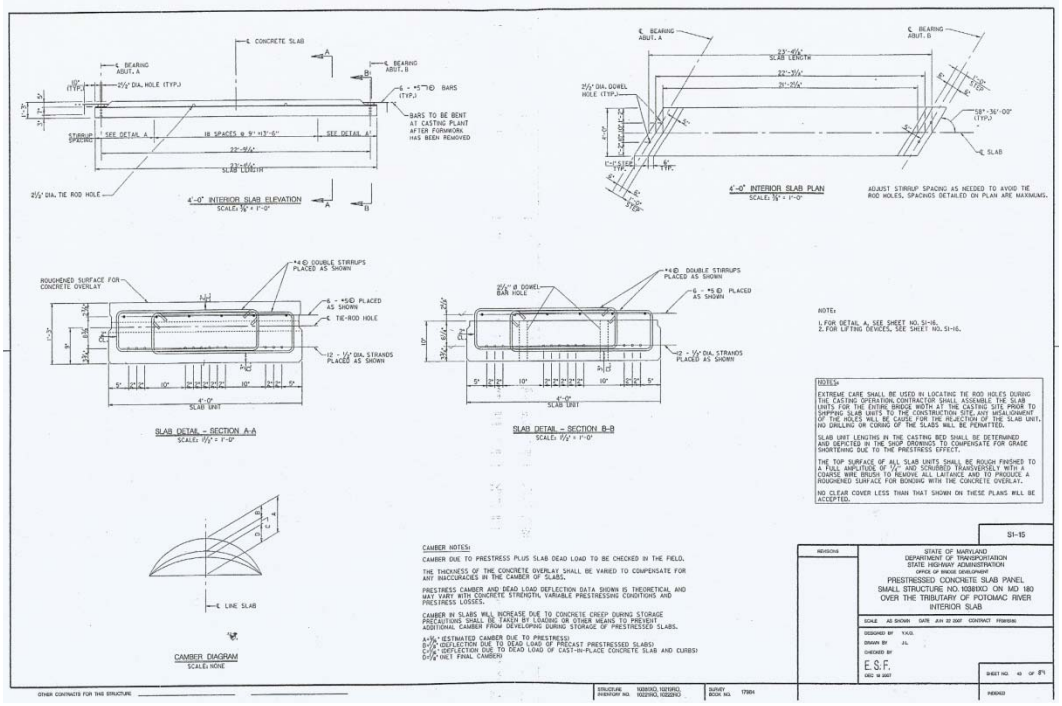

Figure B-7 Slab Details of the Knoxville, MD, Bridge

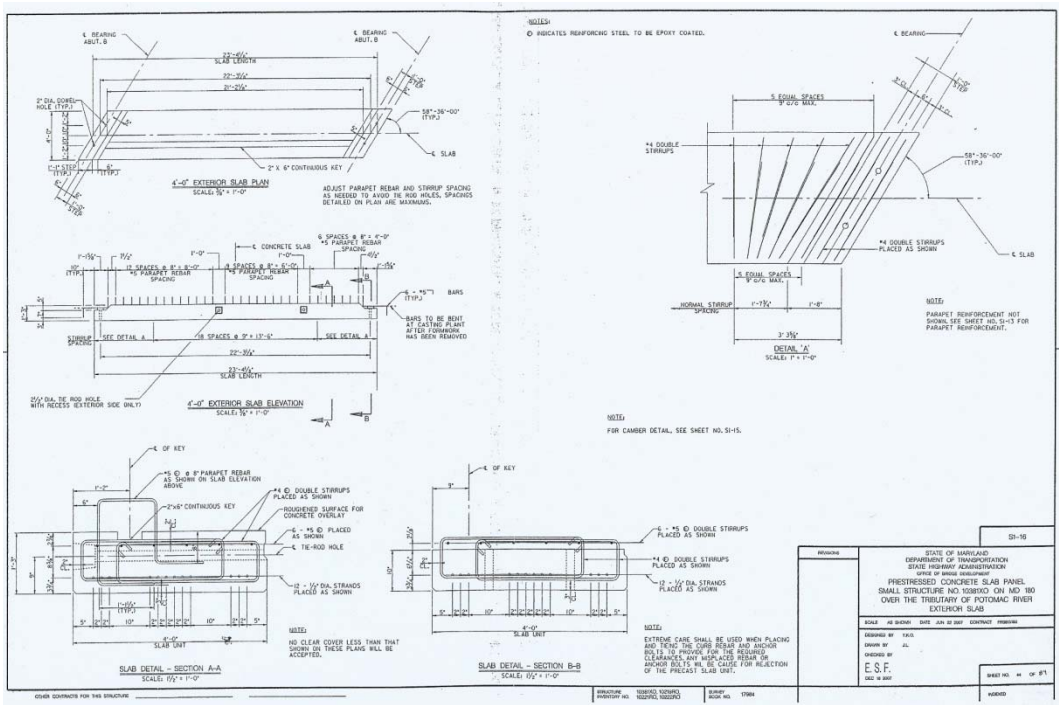

Figure B-8 Reinforcement Details of the Knoxville, MD, Bridge

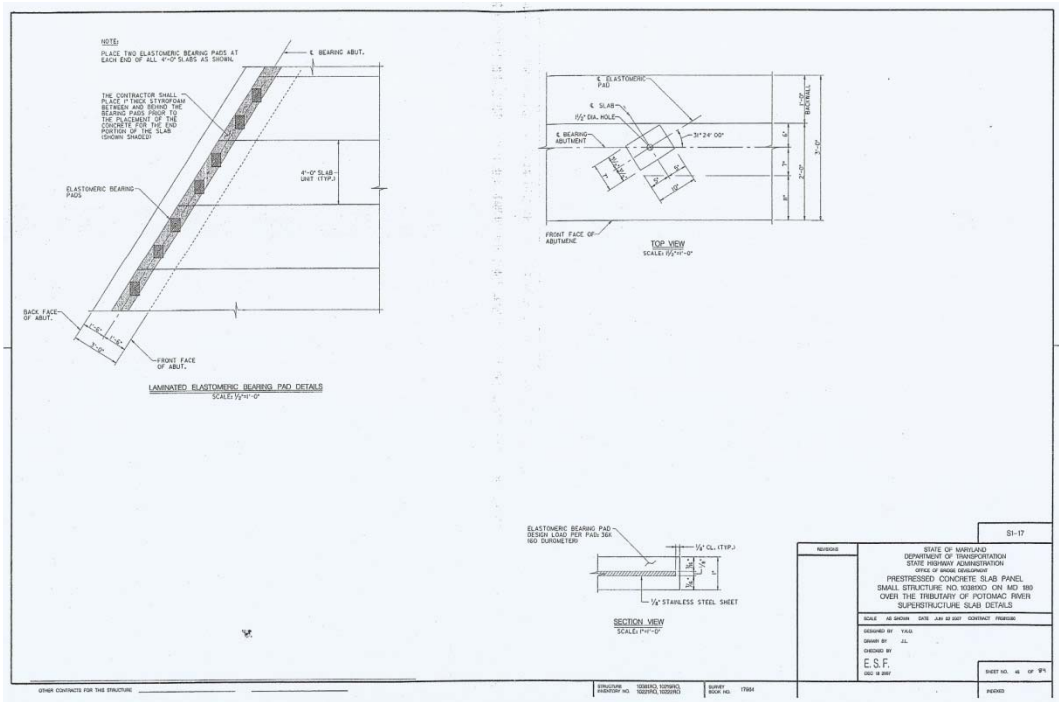

Figure B-9 Bearing Details of the Knoxville, MD, Bridge

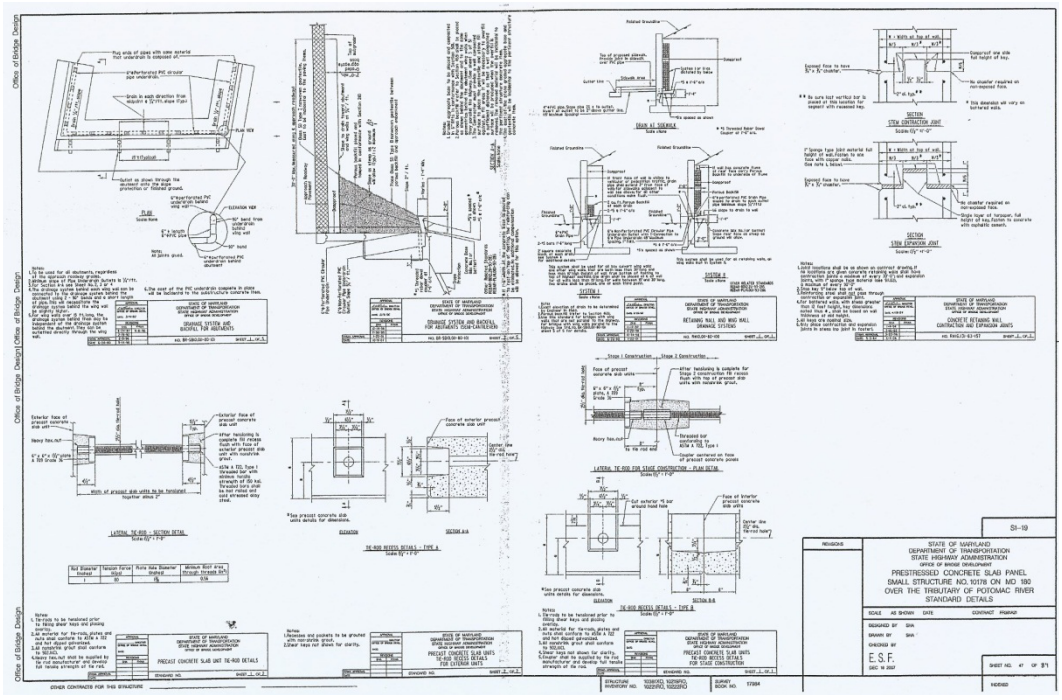

Figure B-10 Transverse Post-Tensioning Details of the Knoxville, MD, Bridge

Appendix C: Full Results from Parametric Study

C.1 Twenty-Five Foot, Fifteen Degree Skewed Bridge – One Truck Loading

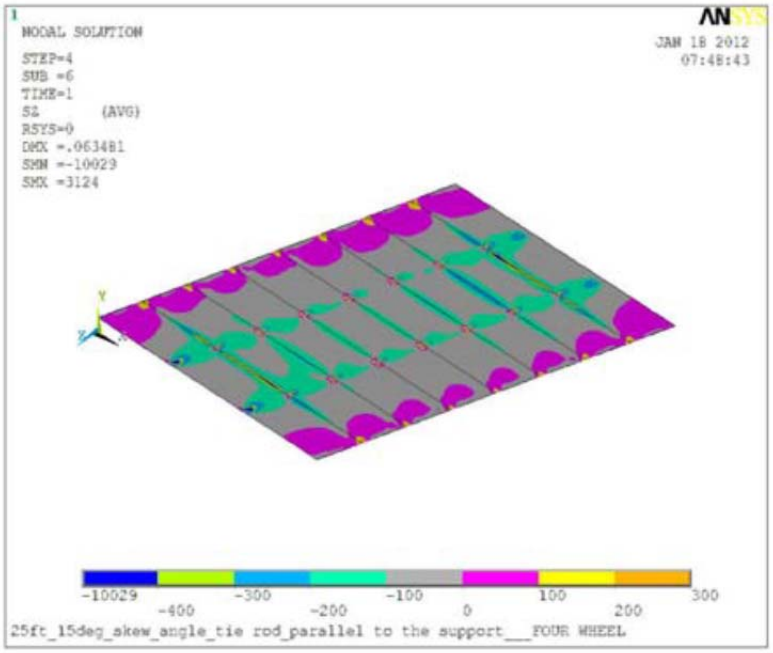

Figure C-1 Transverse Stress at the Slab-Deck Interface

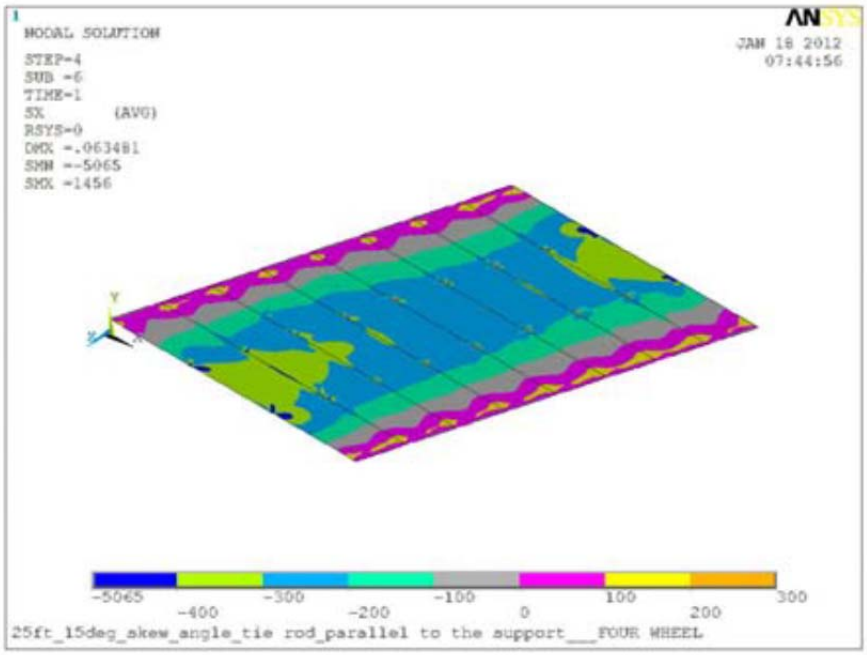

Figure C-2 Longitudinal Stress at the Slab-Deck Interface

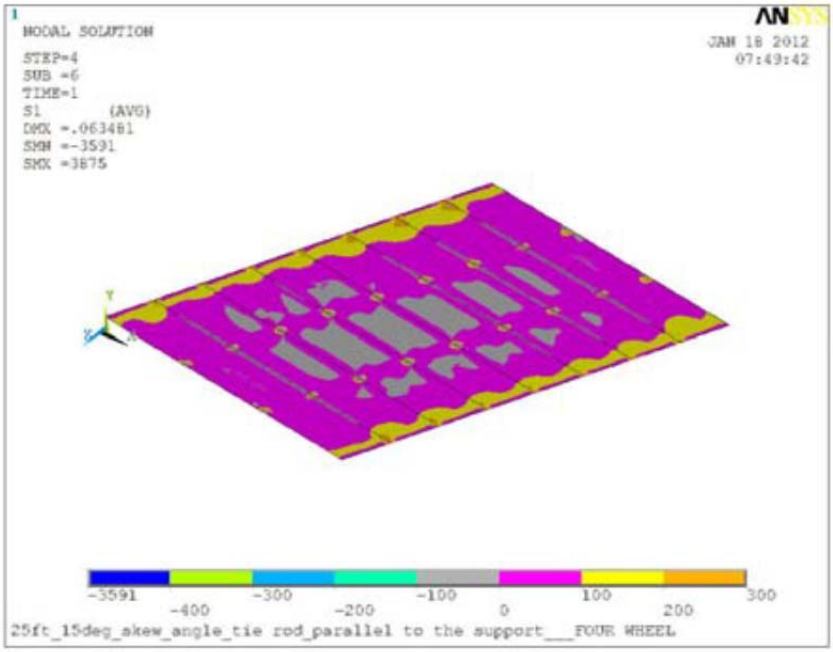

Figure C-3 First Principal Stress at the Slab-Deck Interface

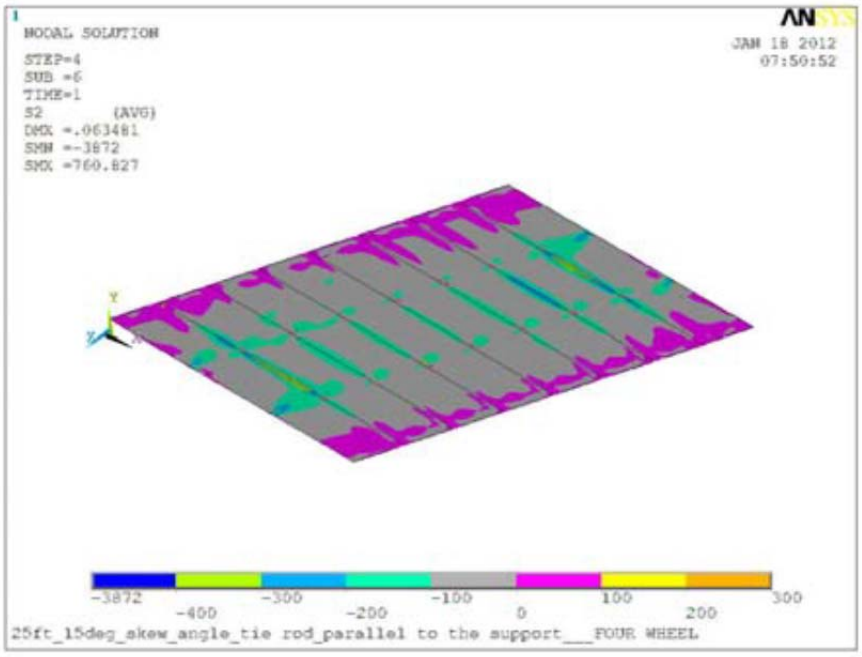

Figure C-4 Second Principal Stress at the Slab-Deck Interface

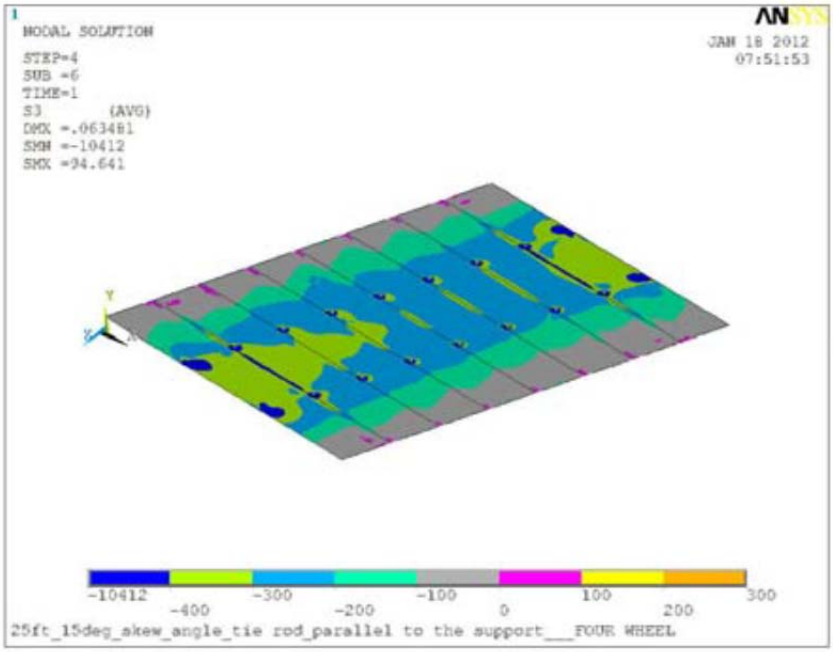

Figure C-5 Third Principal Stress at the Slab-Deck Interface

C.2 Twenty-Five Foot, Fifteen Degree Skewed Bridge – Two Truck Loading

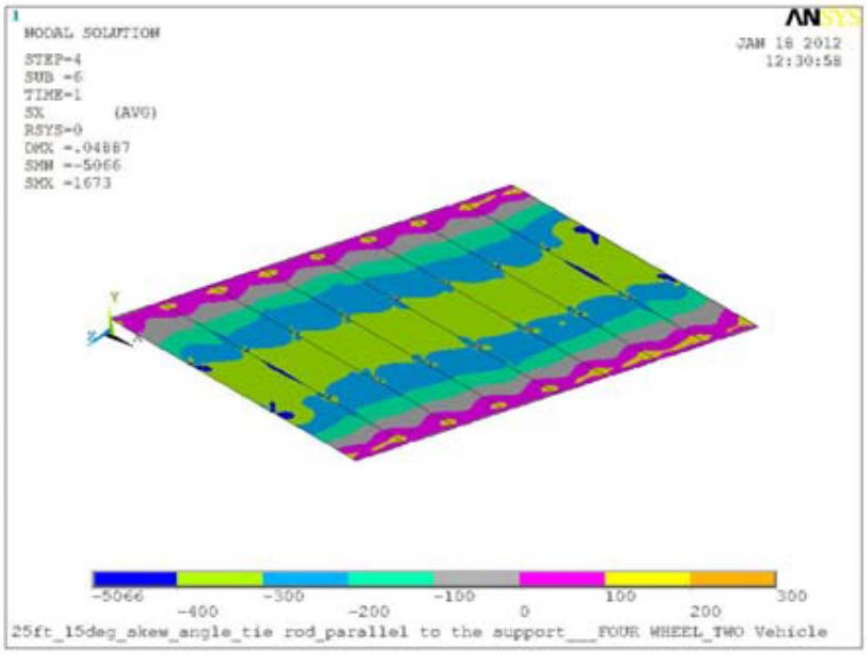

Figure C-6 Longitudinal Stress at the Slab-Deck Interface

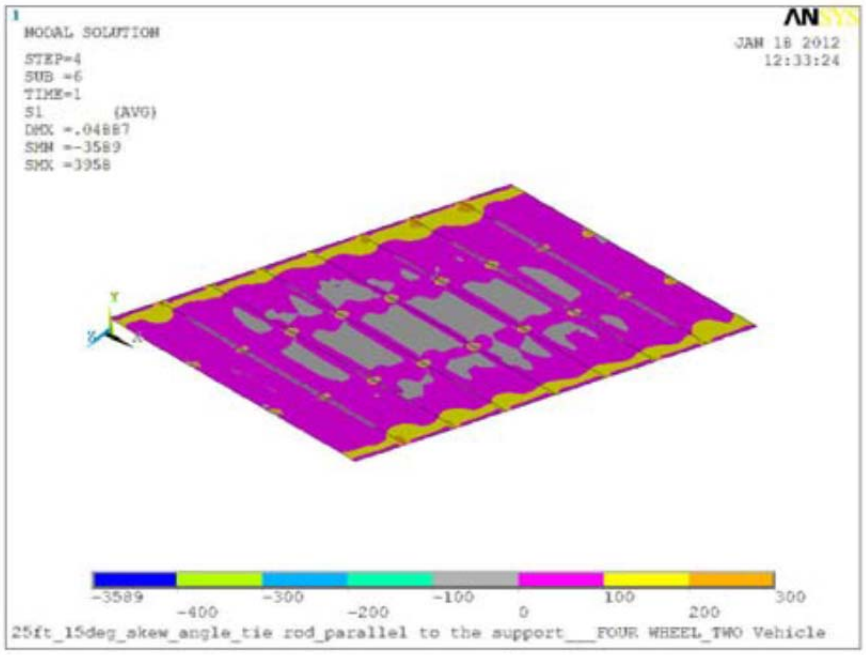

Figure C-7 First Principal Stress at the Slab-Deck Interface

C.3 Twenty-Five Foot, Fifteen Degree Skewed Bridge – Four Normal and Staggered

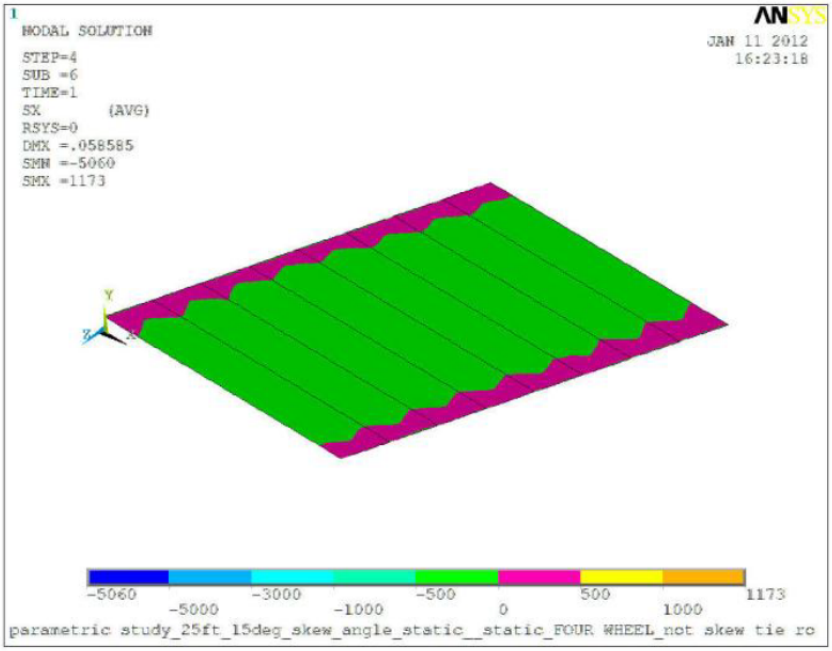

Figure C-8 Longitudinal Stress at the Slab-Deck Interface

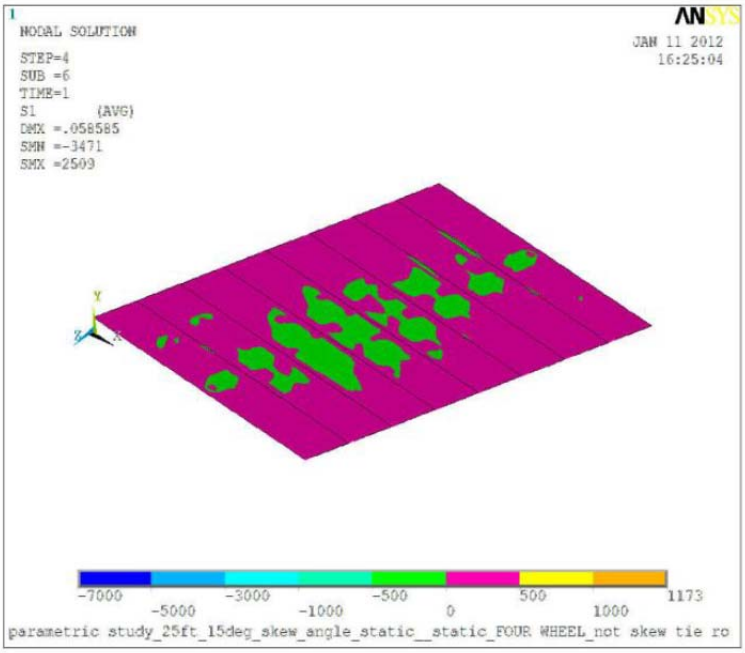

Figure C-9 First Principal Stress at the Slab-Deck Interface

C.4 Twenty-Five Foot, Fifteen Degree Skewed Bridge – Third Points Skewed

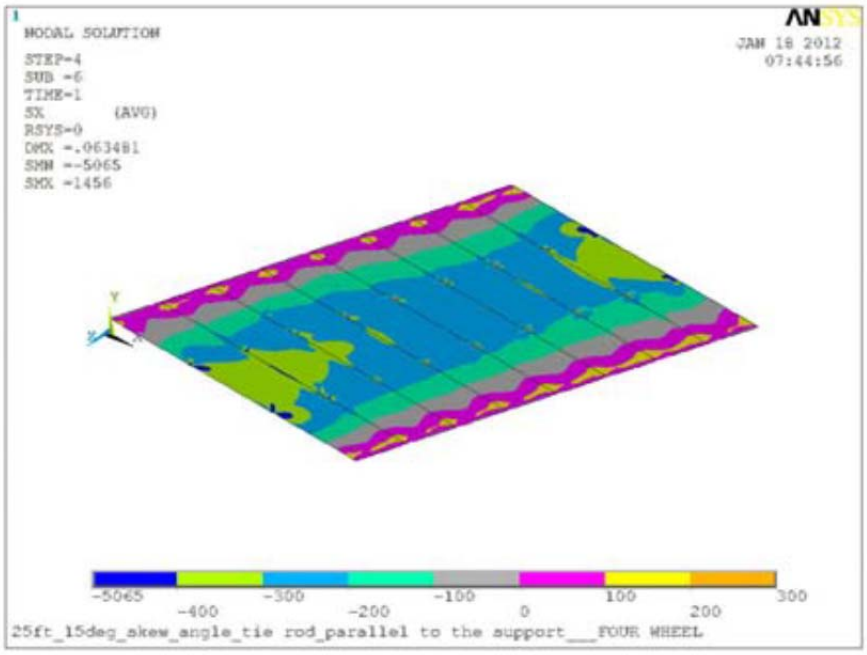

Figure C-10 Longitudinal Stress at the Slab-Deck Interface

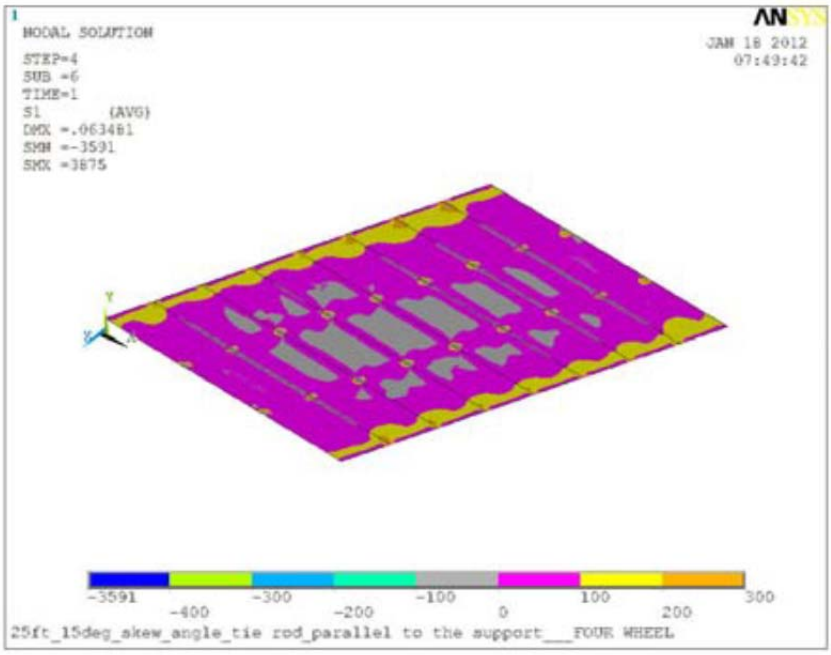

Figure C-11 First Principal Stress at the Slab-Deck Interface

C.5 Twenty-Five Foot, Fifteen Degree Skewed Bridge – Ends Skewed

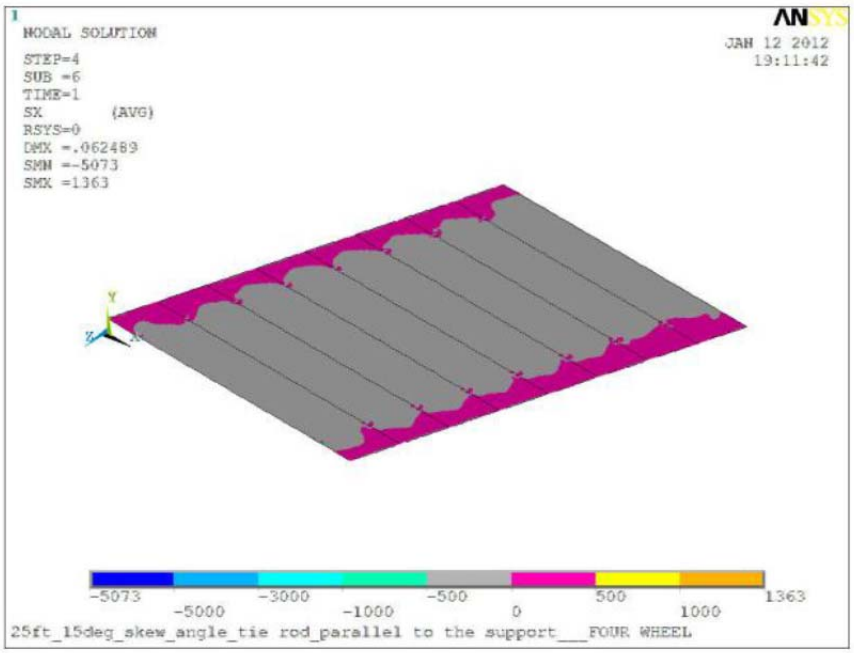

Figure C-12 Longitudinal Stress at the Slab-Deck Interface

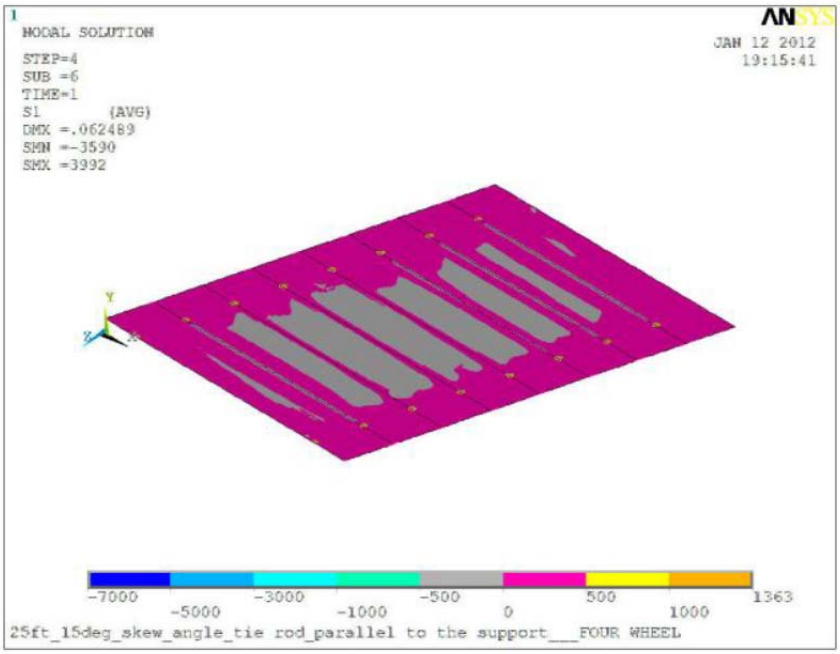

Figure C-13 First Principal Stress at the Slab-Deck Interface

C.6 Twenty-Five Foot, Fifteen Degree Skewed Bridge – Ends and Midspan Skewed

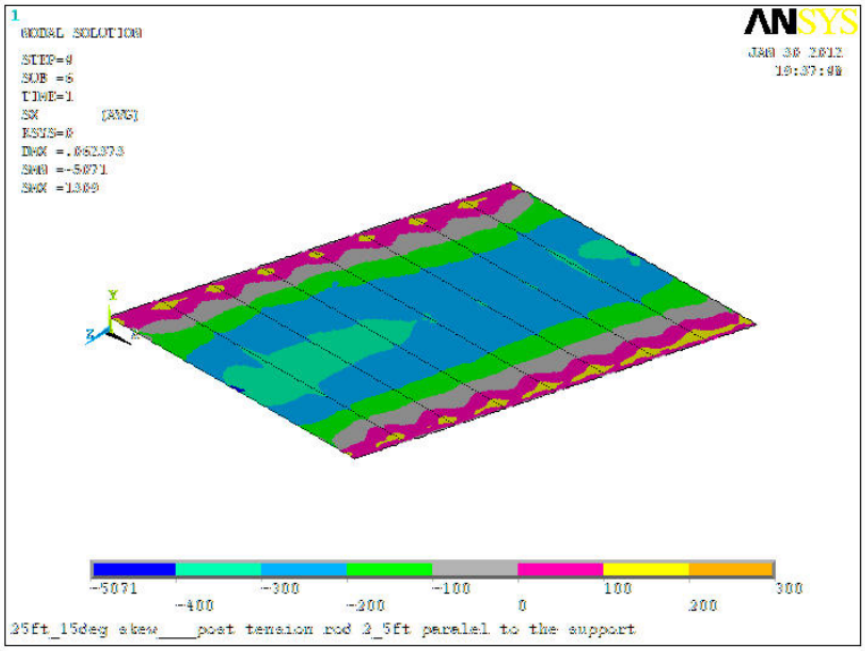

Figure C-14 Longitudinal Stress at the Slab-Deck Interface

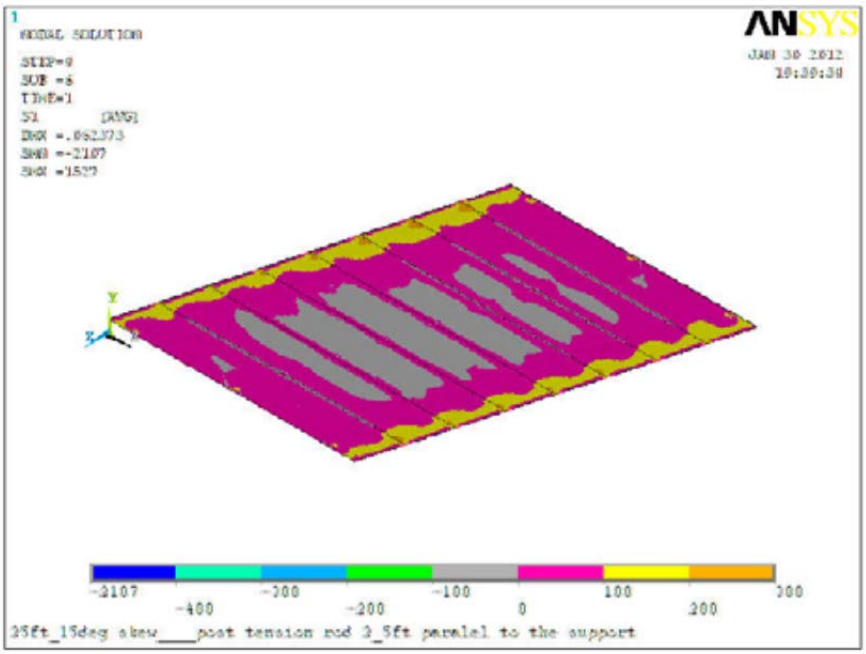

Figure C-15 First Principal Stress at the Slab-Deck Interface

C.7 Twenty-Five Foot, Thirty Degree Skewed Bridge – Four Normal and Staggered

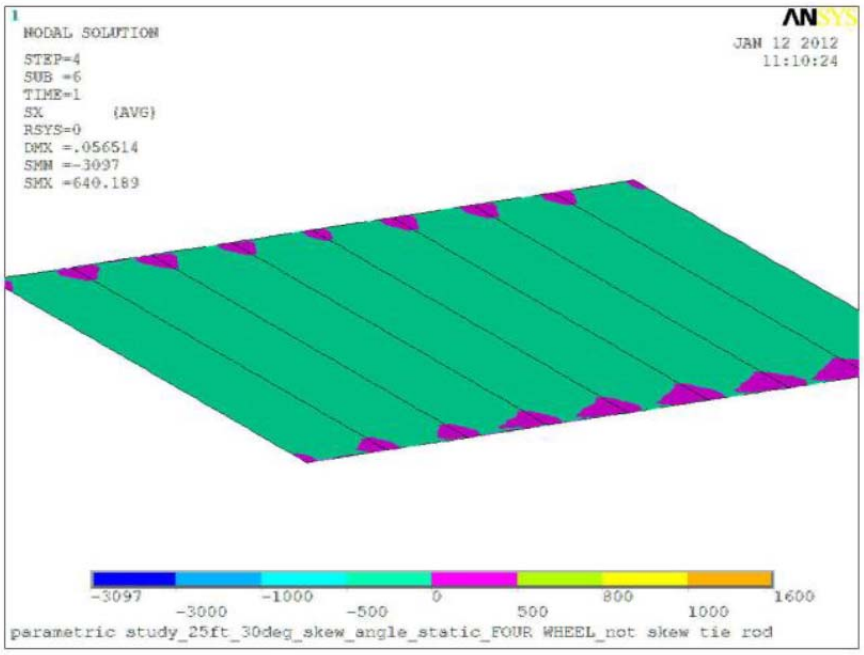

Figure C-16 Longitudinal Stress at the Slab-Deck Interface

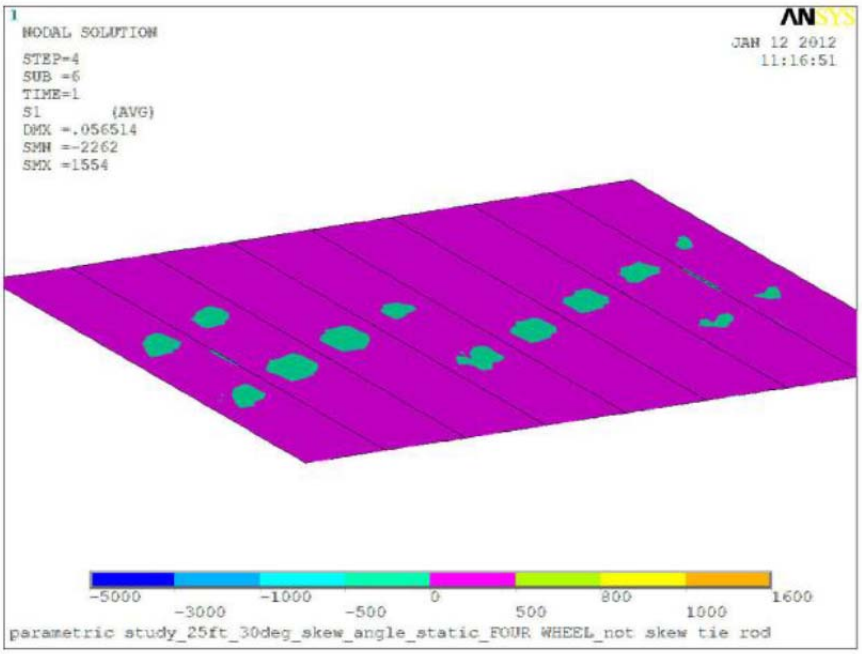

Figure C-17 First Principal Stress at the Slab-Deck Interface

C.8 Twenty-Five Foot, Thirty Degree Skewed Bridge – Third Points Skewed

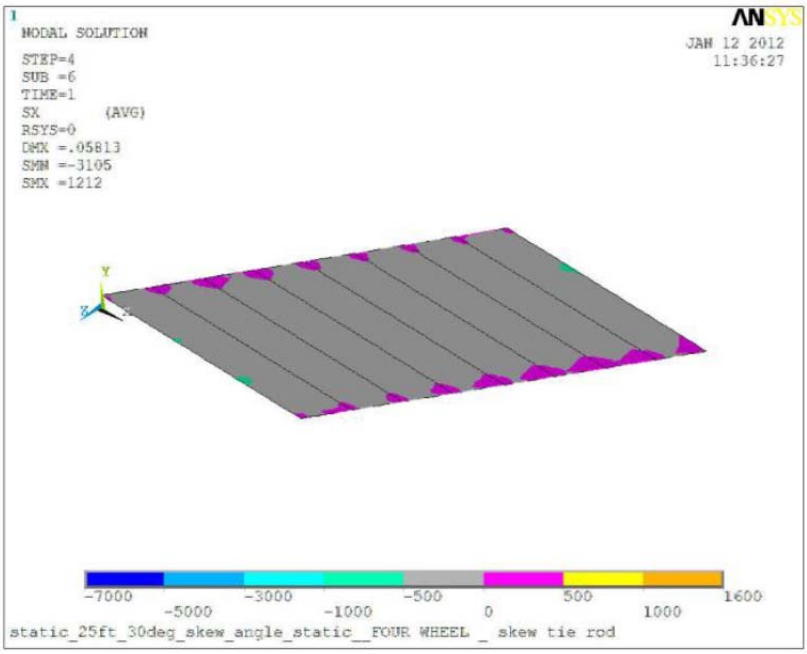

Figure C-18 Longitudinal Stress at the Slab-Deck Interface

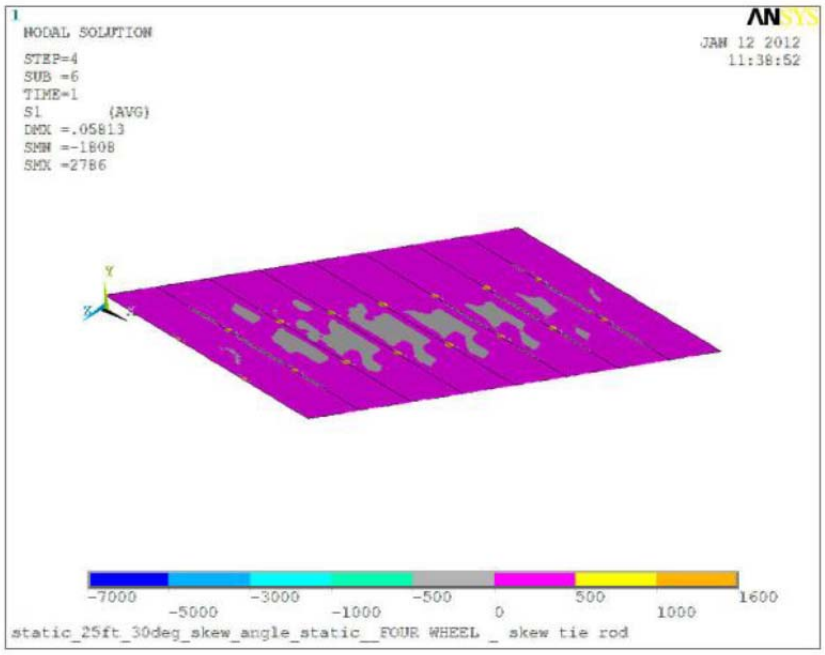

Figure C-19 First Principal Stress at the Slab-Deck Interface

C.9 Forty Foot, Fifteen Degree Skewed Bridge – Four Normal and Staggered

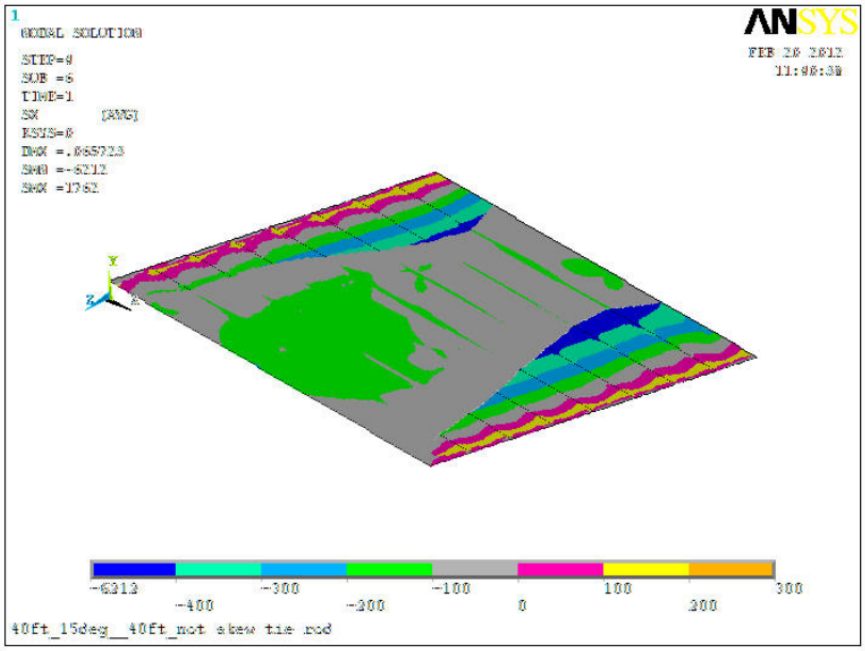

Figure C-20 Longitudinal Stress at the Slab-Deck Interface

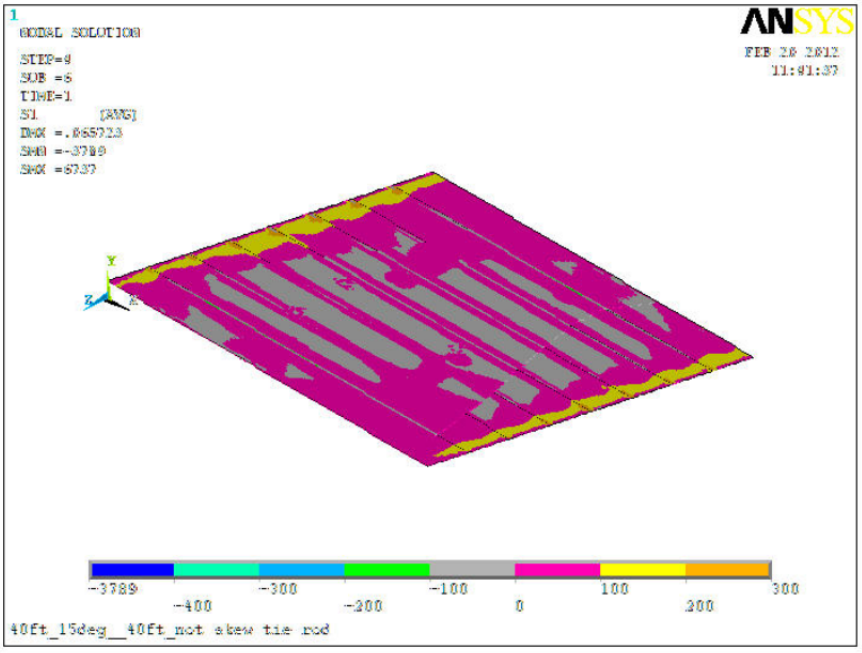

Figure C-21 First Principal Stress at the Slab-Deck Interface

C.10 Forty Foot, Fifteen Degree Skewed Bridge – Third Points Skewed

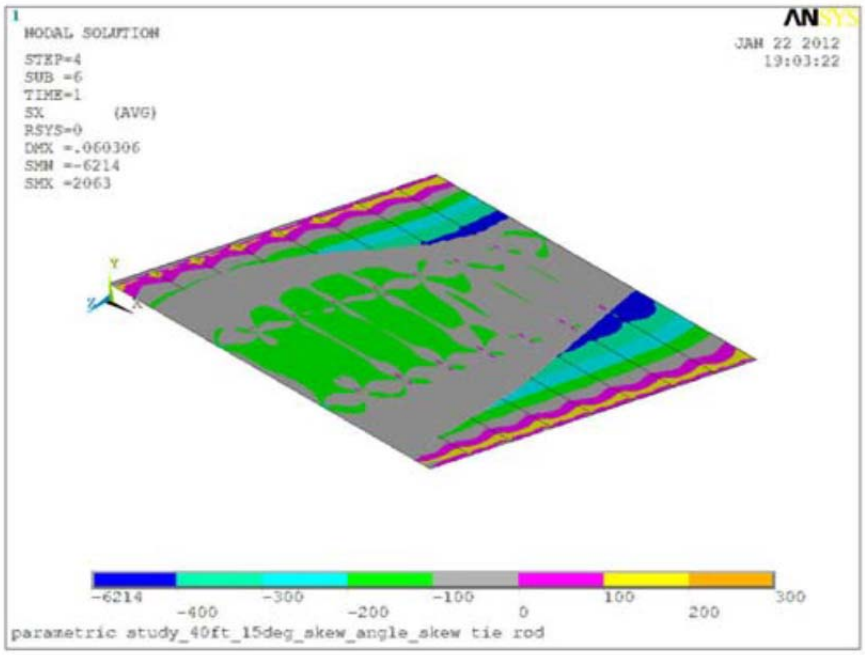

Figure C-22 Longitudinal Stress at the Slab-Deck Interface

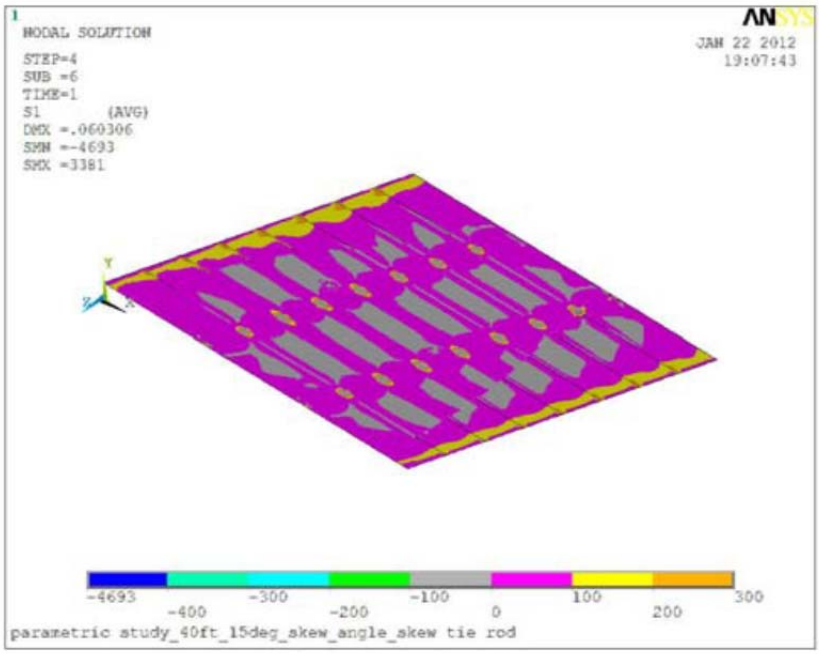

Figure C-23 First Principal Stress at the Slab-Deck Interface

C.11 Forty Foot, Fifteen Degree Skewed Bridge – Ends and Midspan Skewed

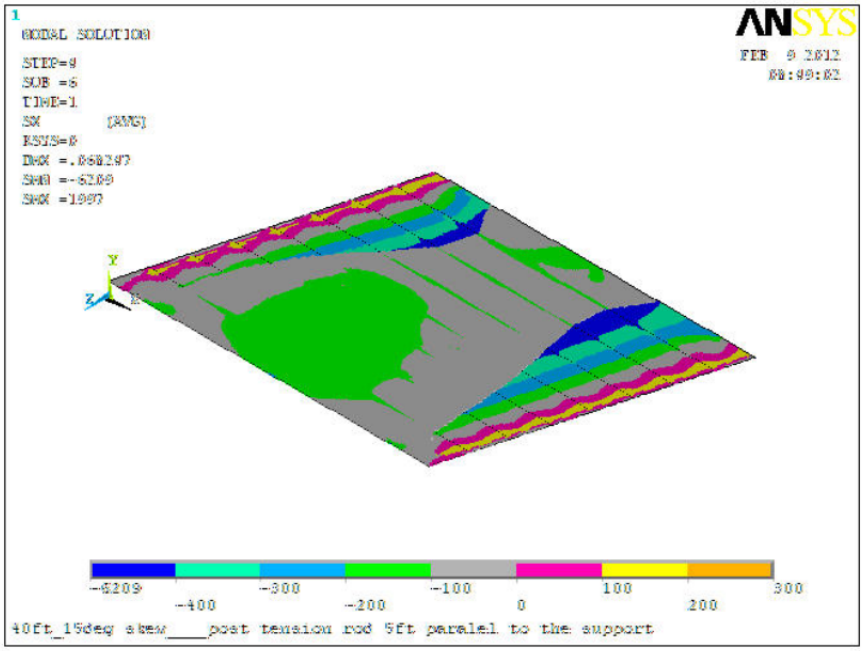

Figure C-24 Longitudinal Stress at the Slab-Deck Interface

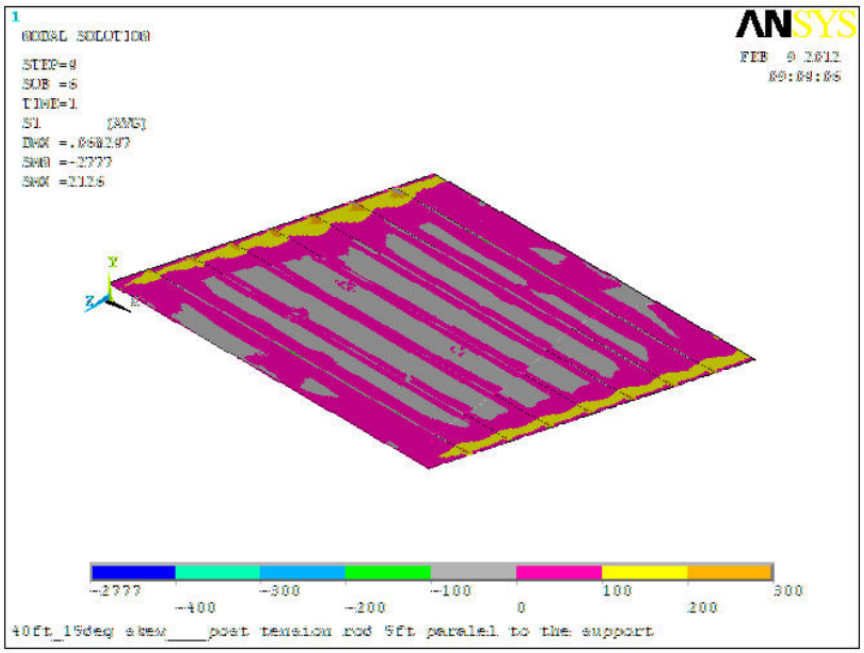

Figure C-25 First Principal Stress at the Slab-Deck Interface

C.12 Forty Foot, Thirty Degree Skewed Bridge – Two Normal

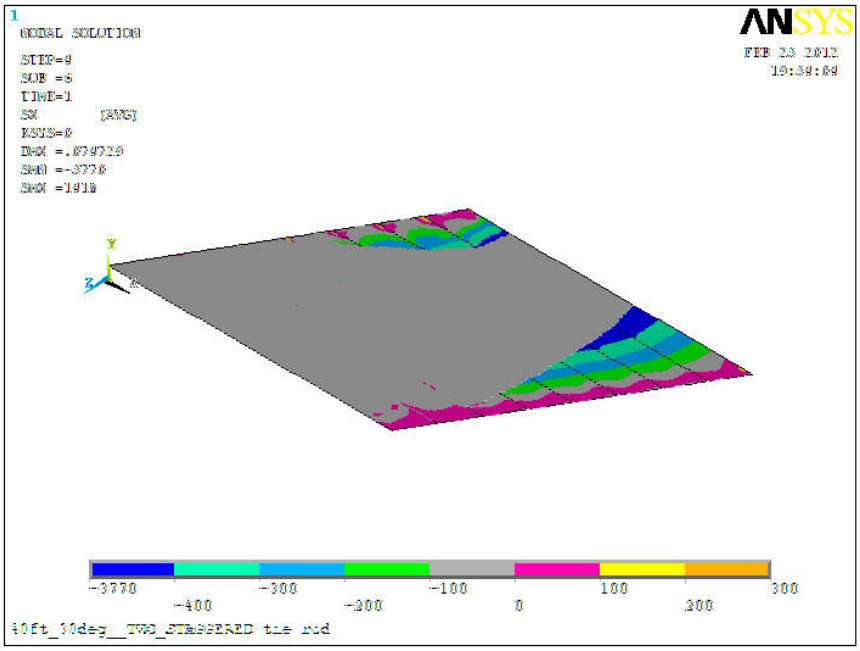

Figure C-26 Longitudinal Stress at the Slab-Deck Interface

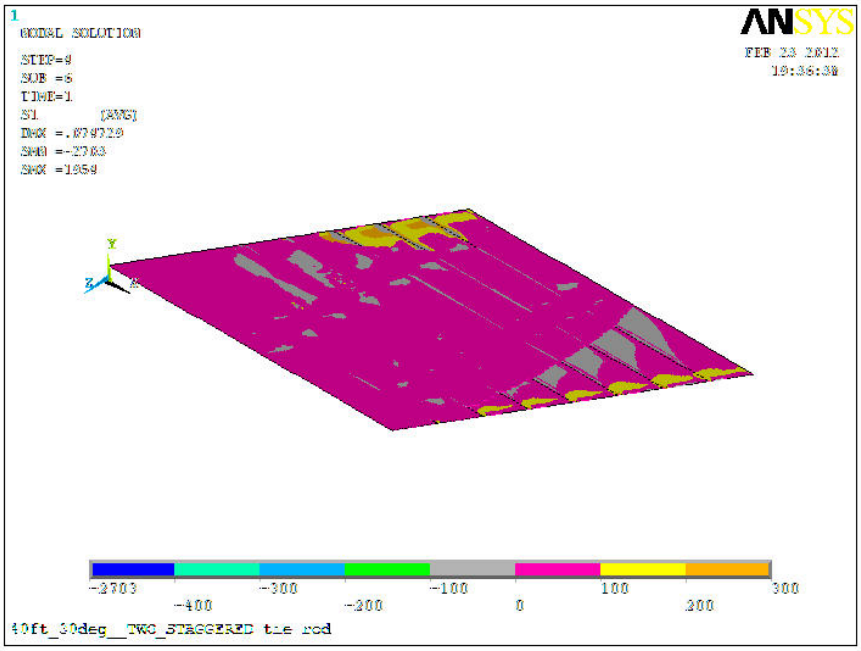

Figure C-27 First Principal Stress at the Slab-Deck Interface

C.13 Forty Foot, Thirty Degree Skewed Bridge – Four Normal and Staggered

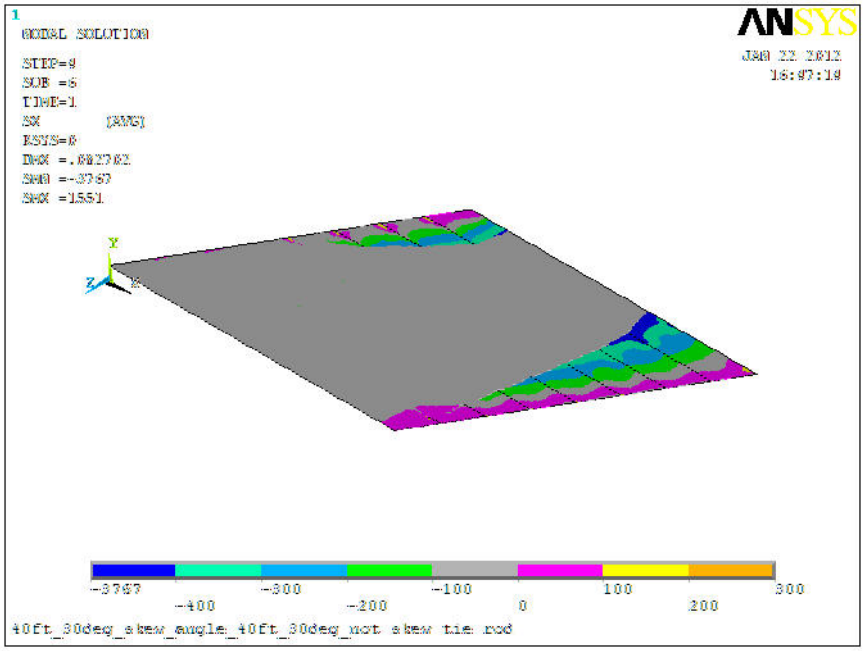

Figure C-28 Longitudinal Stress at the Slab-Deck Interface

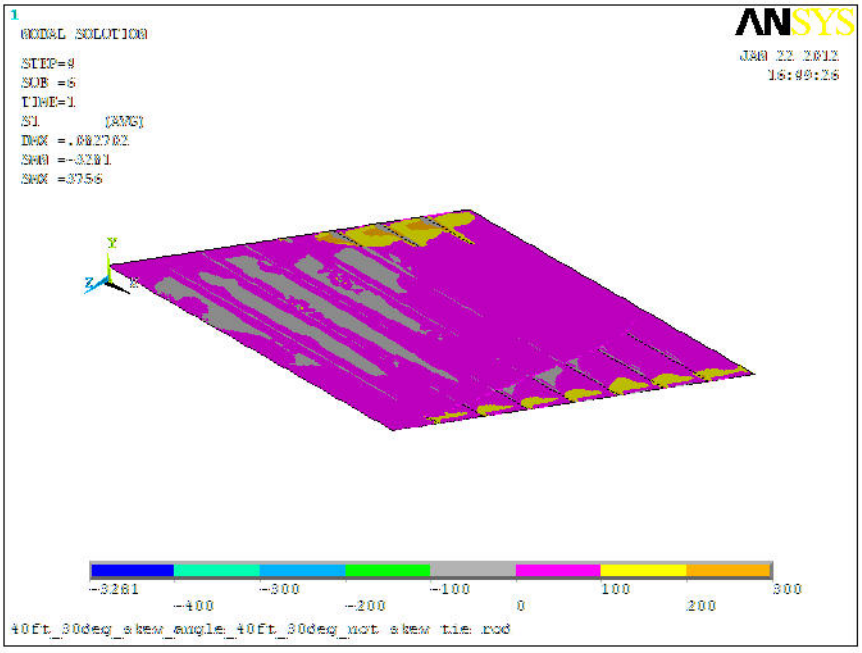

Figure C-29 First Principal Stress at the Slab-Deck Interface

C.14 Forty Foot, Thirty Degree Skewed Bridge – Third Points Skewed

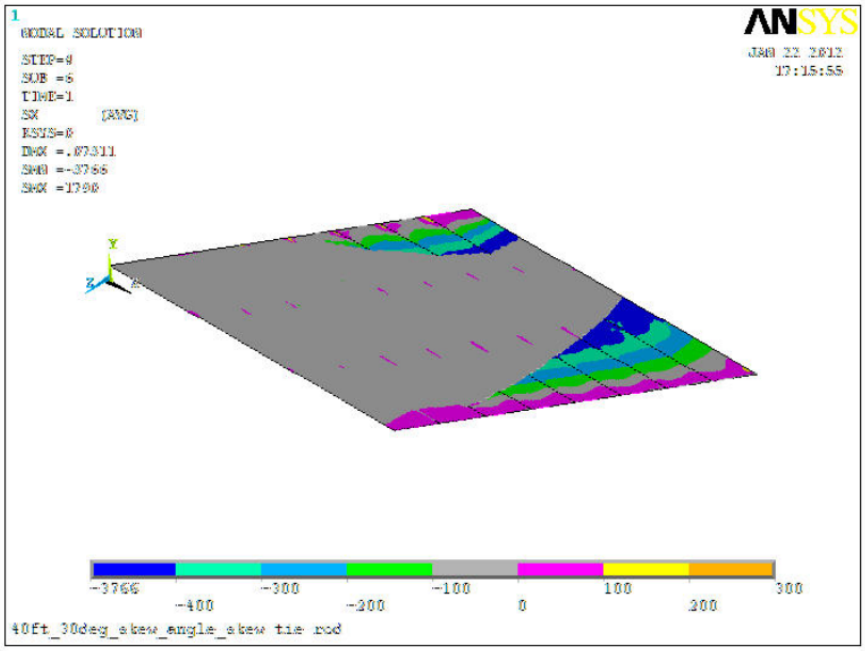

Figure C-30 Longitudinal Stress at the Slab-Deck Interface

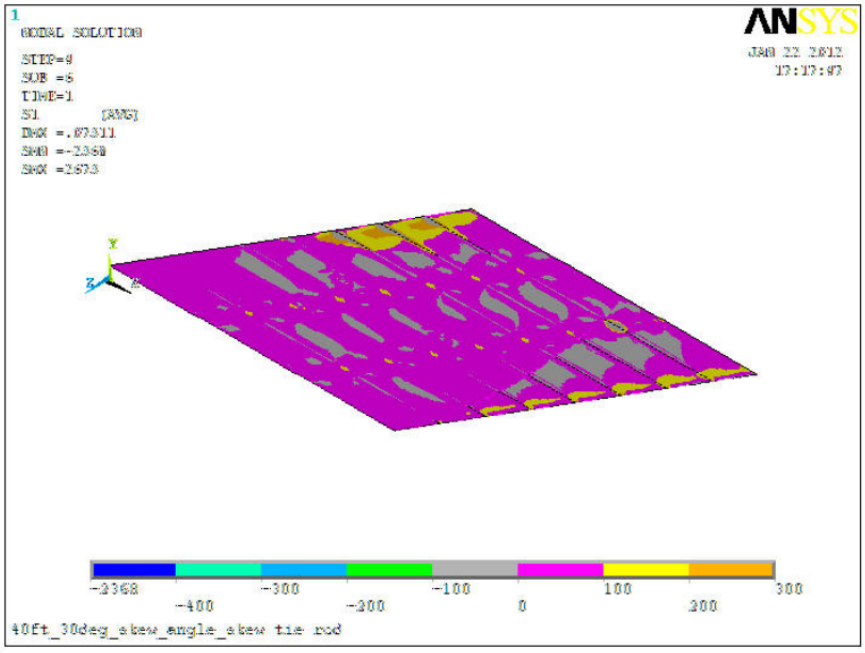

Figure C-31 First Principal Stress at the Slab-Deck Interface

C.15 Forty Foot, Thirty Degree Skewed Bridge – Ends and Midspan Skewed

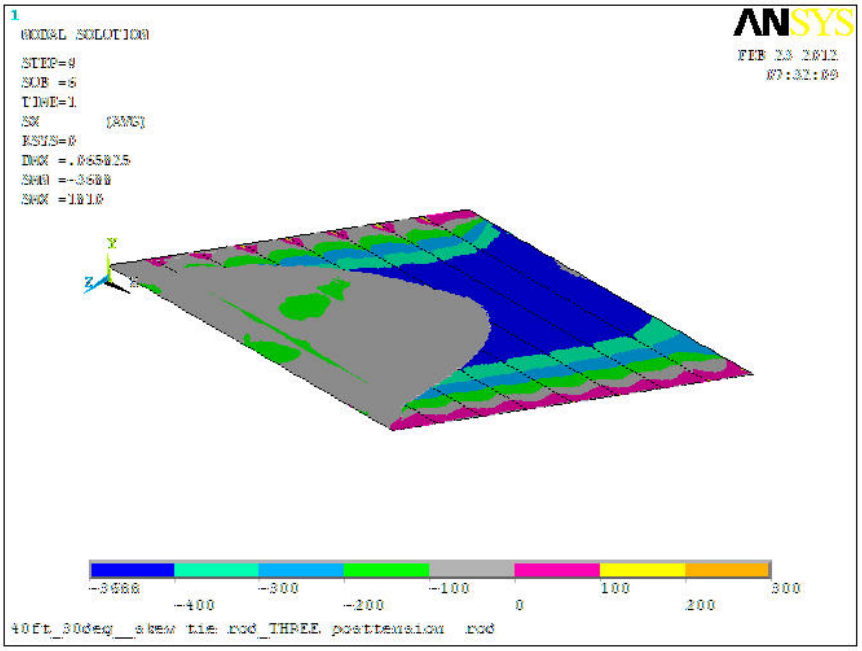

Figure C-32 Longitudinal Stress at the Slab-Deck Interface

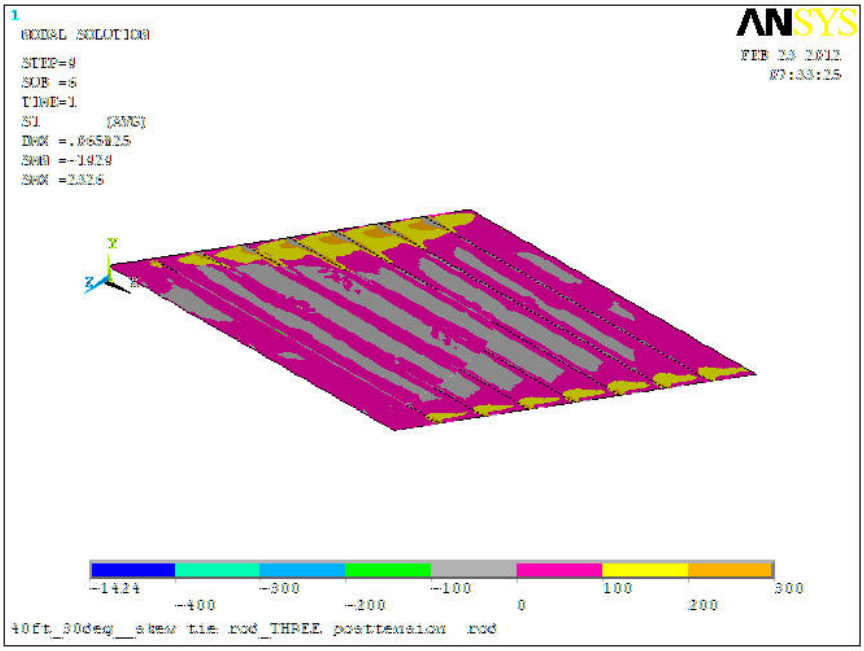

Figure C-33 First Principal Stress at the Slab-Deck Interface

C.16 Fifty-Five Foot, Fifteen Degree Skewed Bridge – Two Normal

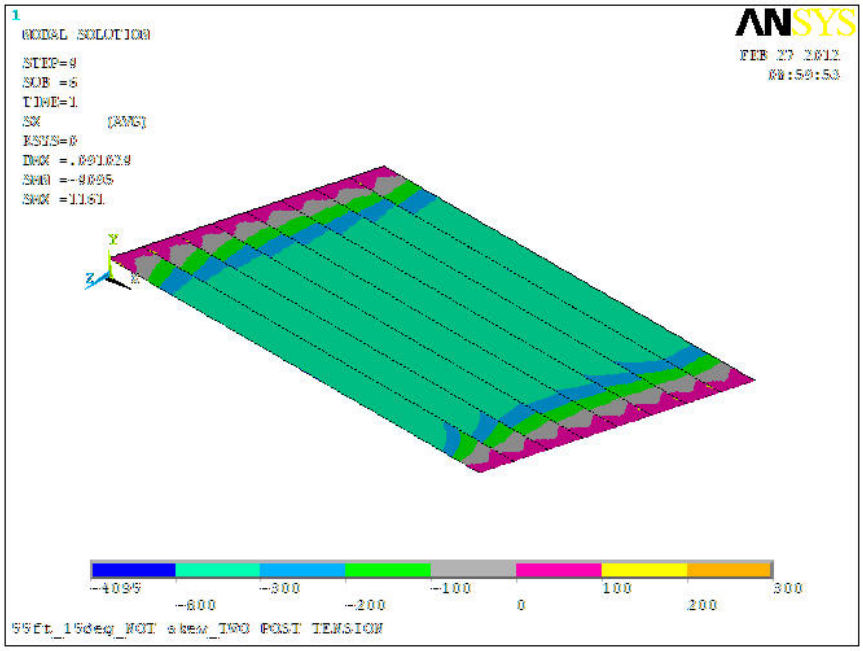

Figure C-34 Longitudinal Stress at the Slab-Deck Interface

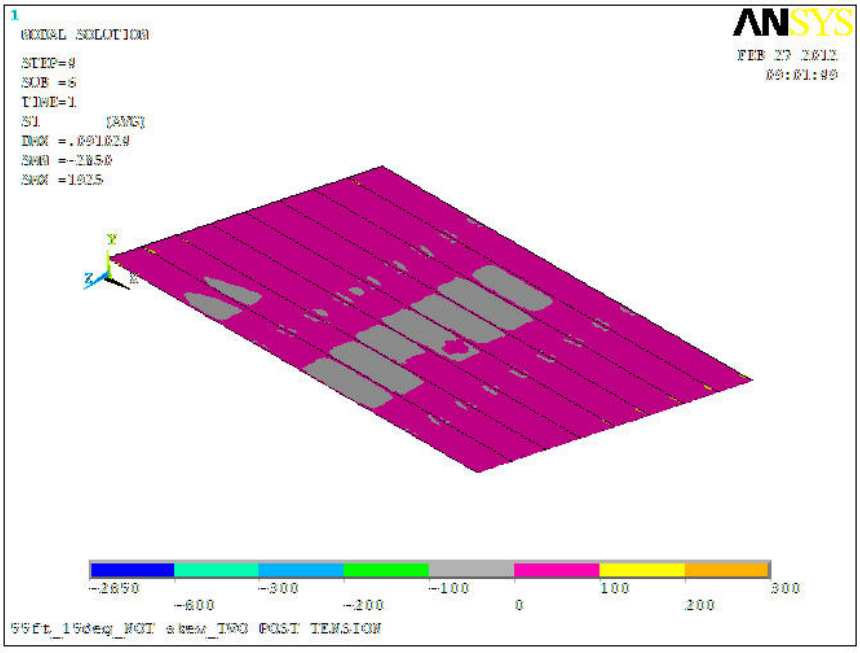

Figure C-35 First Principal Stress at the Slab-Deck Interface

C.17 Fifty-Five Foot, Fifteen Degree Skewed Bridge – Four Skewed

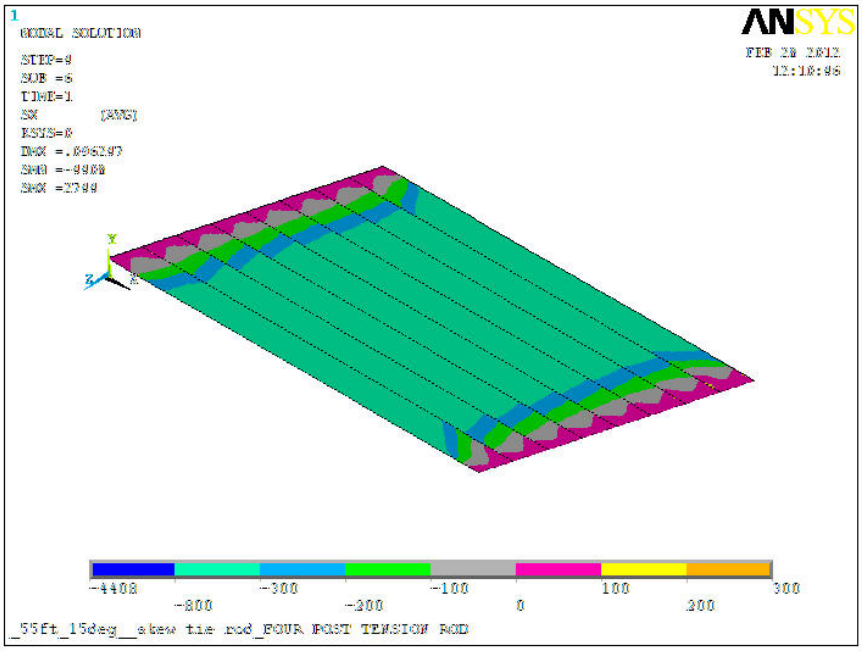

Figure C-36 Longitudinal Stress at the Slab-Deck Interface

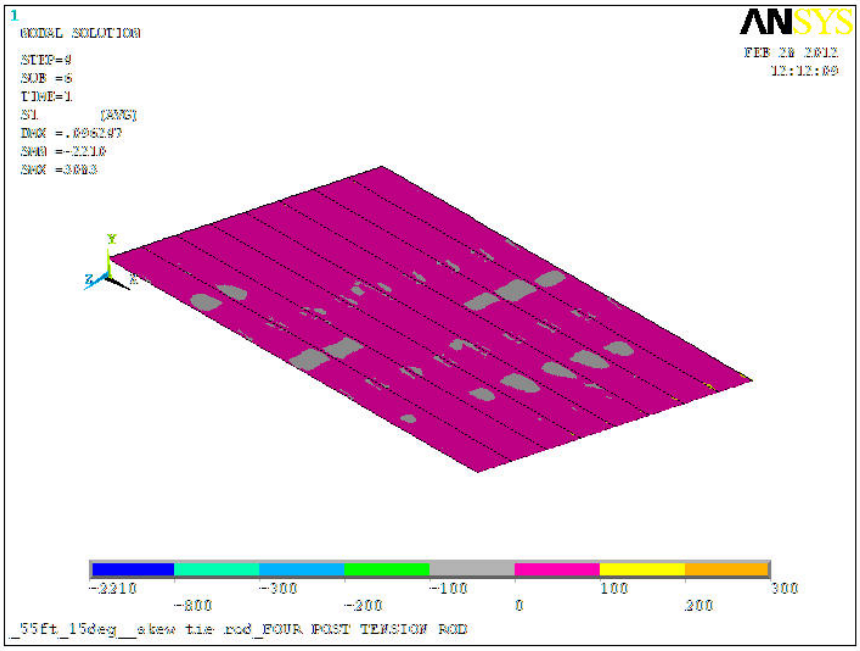

Figure C-37 First Principal Stress at the Slab-Deck Interface

C.18 Fifty-Five Foot, Thirty Degree Skewed Bridge – Two Normal

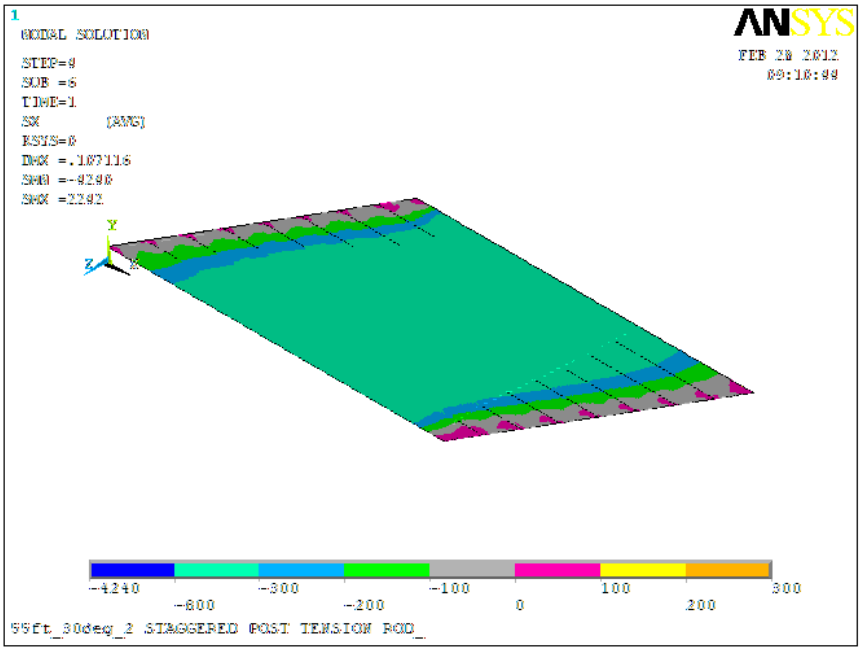

Figure C-38 Longitudinal Stress at the Slab-Deck Interface

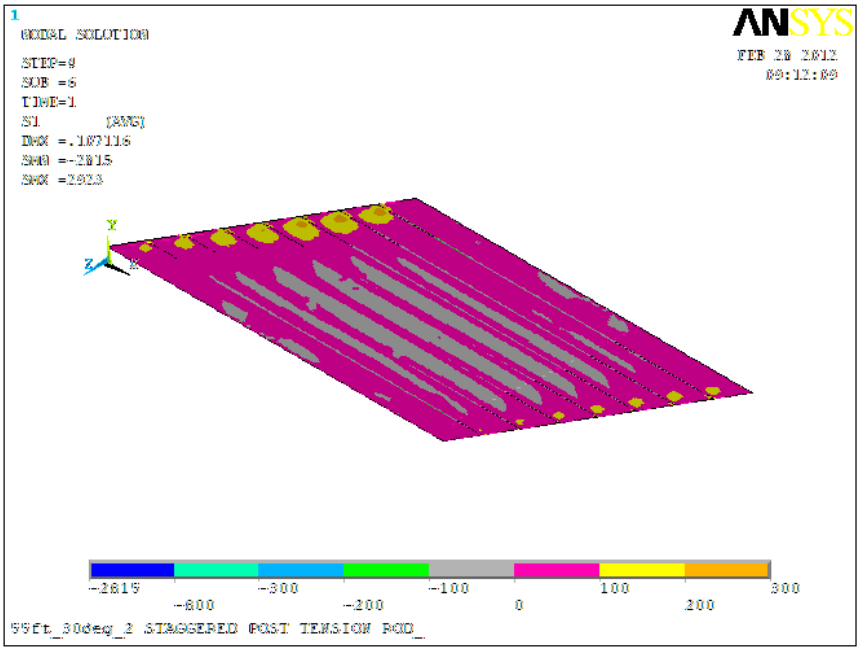

Figure C-39 First Principal Stress at the Slab-Deck Interface

C.19 Fifty-Five Foot, Thirty Degree Skewed Bridge – Three Skewed

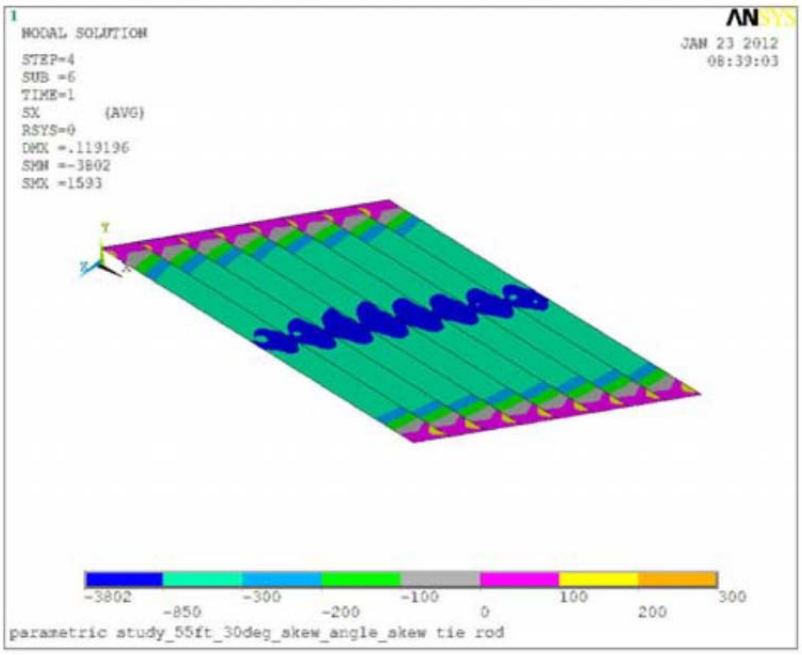

Figure C-40 Longitudinal Stress at the Slab-Deck Interface

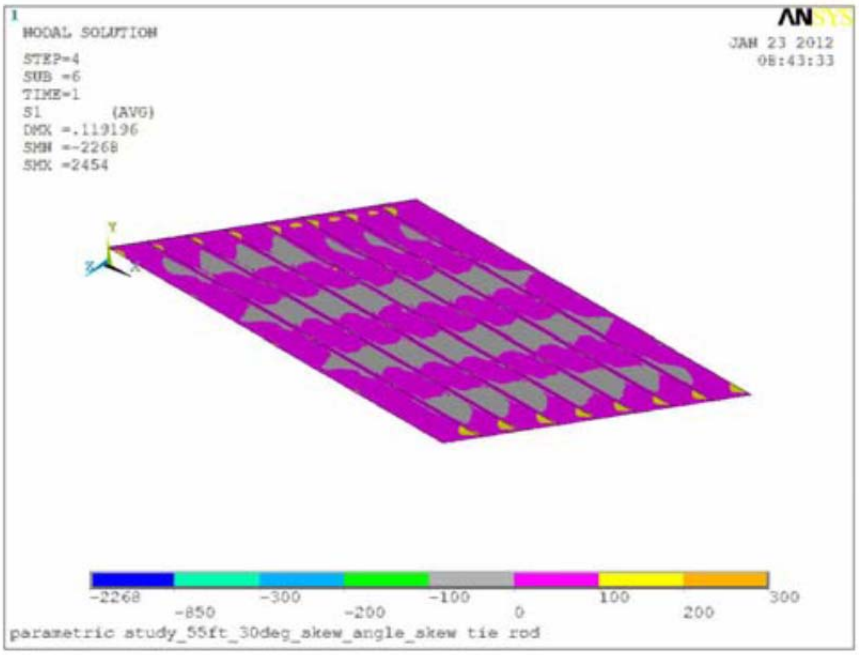

Figure C-41 First Principal Stress at the Slab-Deck Interface

C.20 Fifty-Five Foot, Thirty Degree Skewed Bridge – Four Skewed

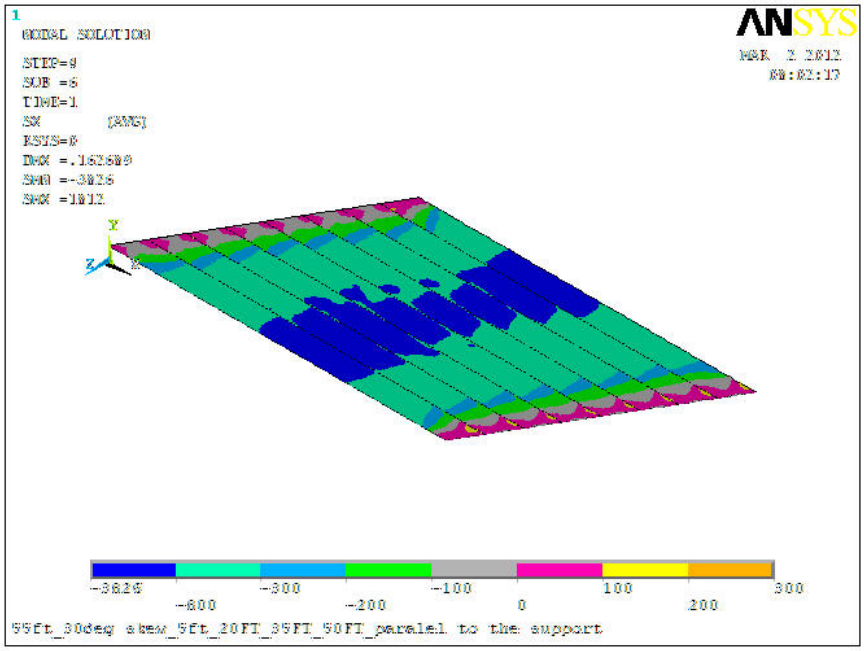

Figure C-42 Longitudinal Stress at the Slab-Deck Interface

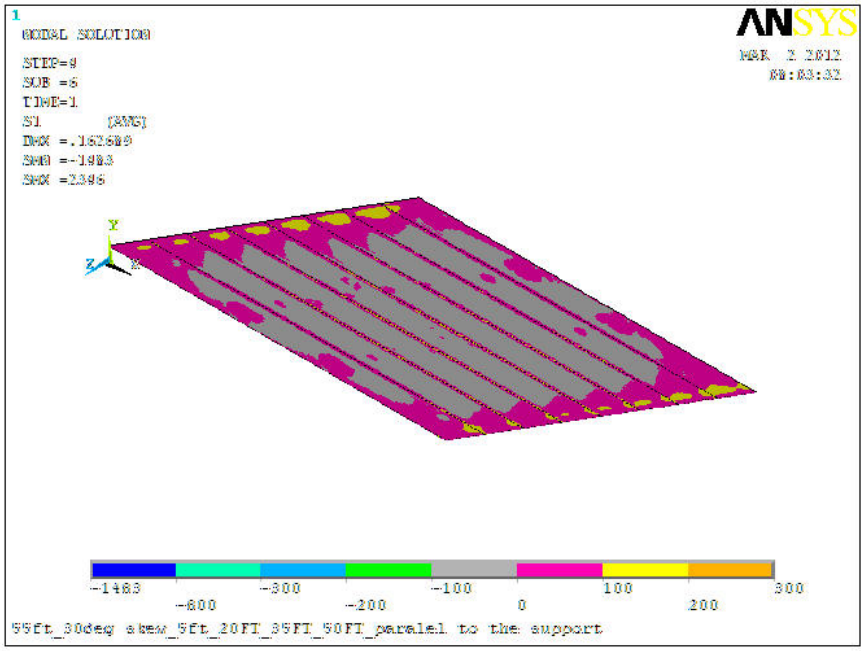

Figure C-43 First Principal Stress at the Slab-Deck Interface

C.21 Extension: Forty Foot, Fifteen Degree Skewed Bridge – Three Combined

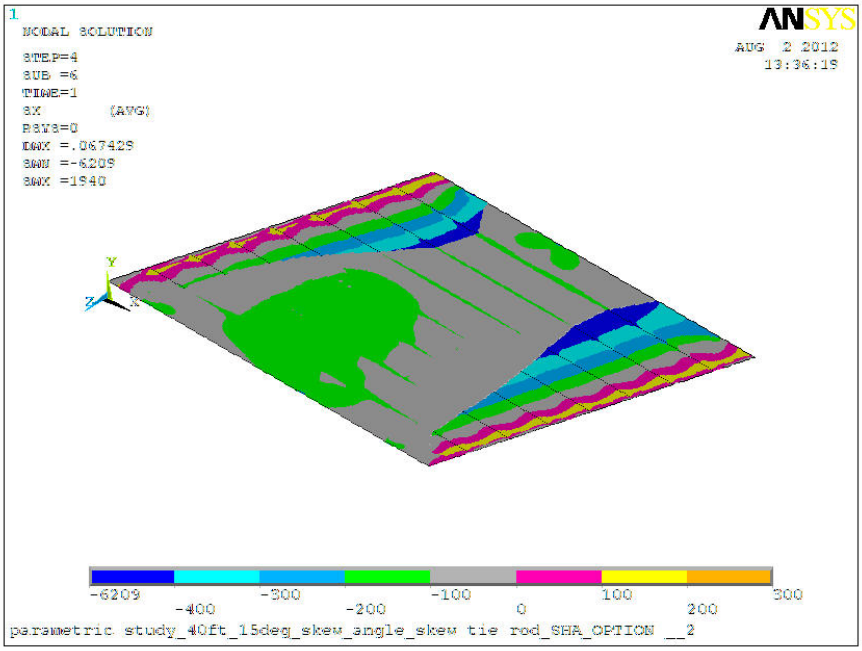

Figure C-44 Longitudinal Stress at the Slab-Deck Interface

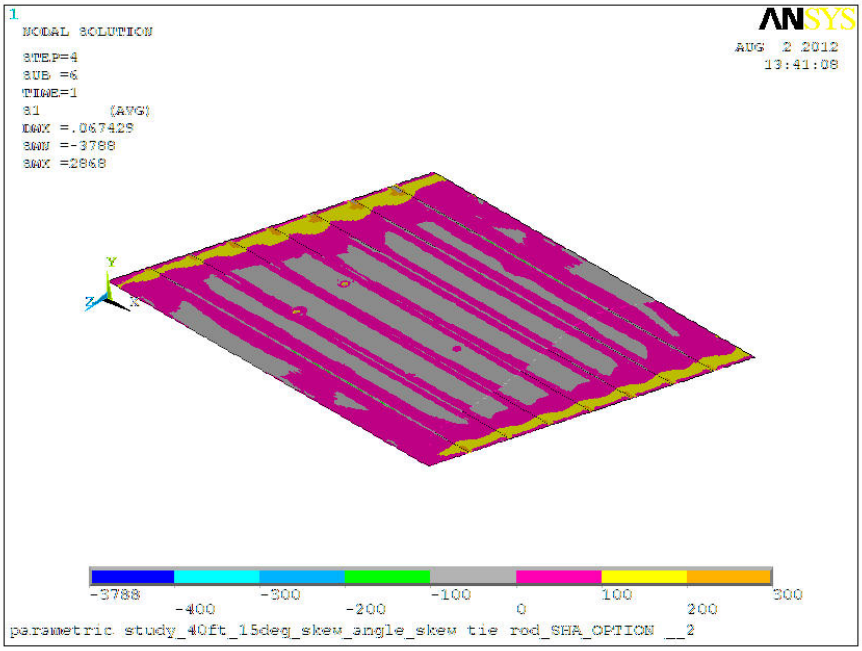

Figure C-45 First Principal Stress at the Slab-Deck Interface

C.22 Extension: Forty Foot, Thirty Degree Skewed Bridge – Three Combined

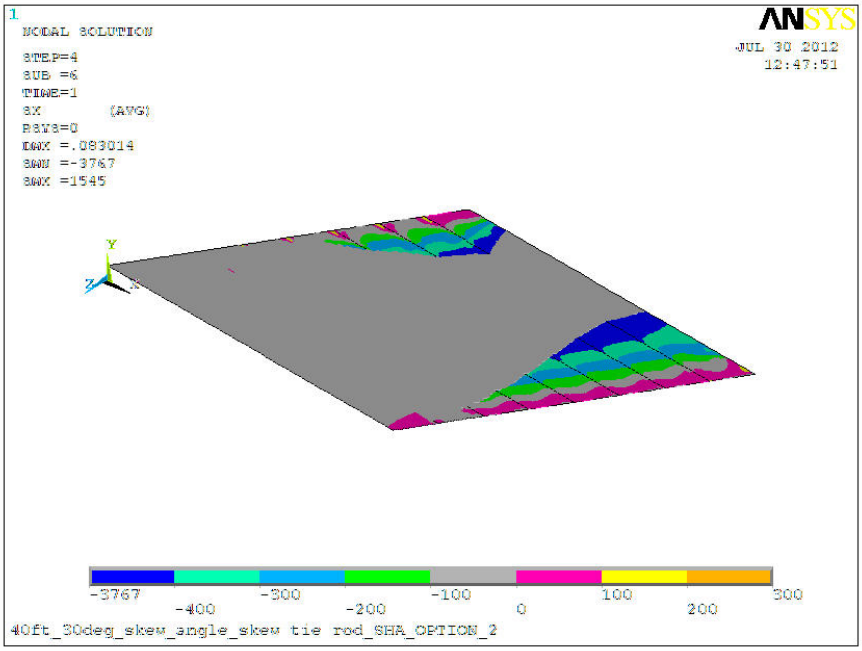

Figure C-46 Longitudinal Stress at the Slab-Deck Interface

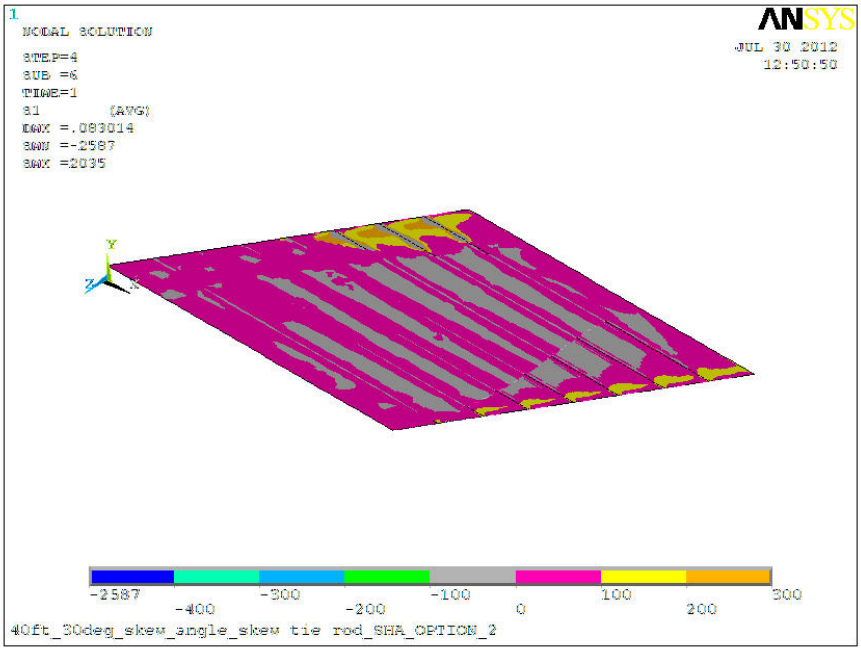

Figure C-47 First Principal Stress at the Slab-Deck Interface

C.23 Extension: Fifty-Five Foot, Fifteen Degree Skewed Bridge – Three Combined

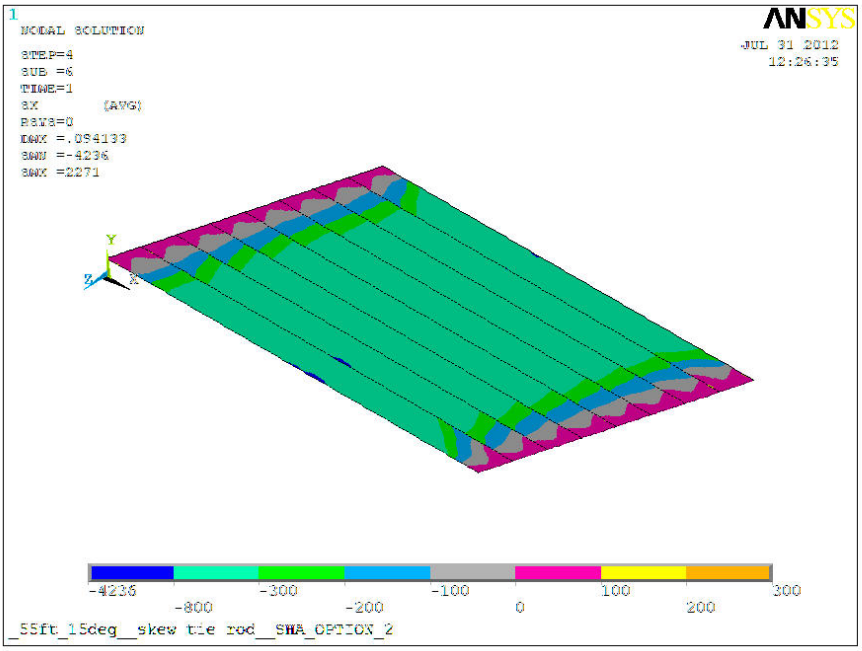

Figure C-48 Longitudinal Stress at the Slab-Deck Interface

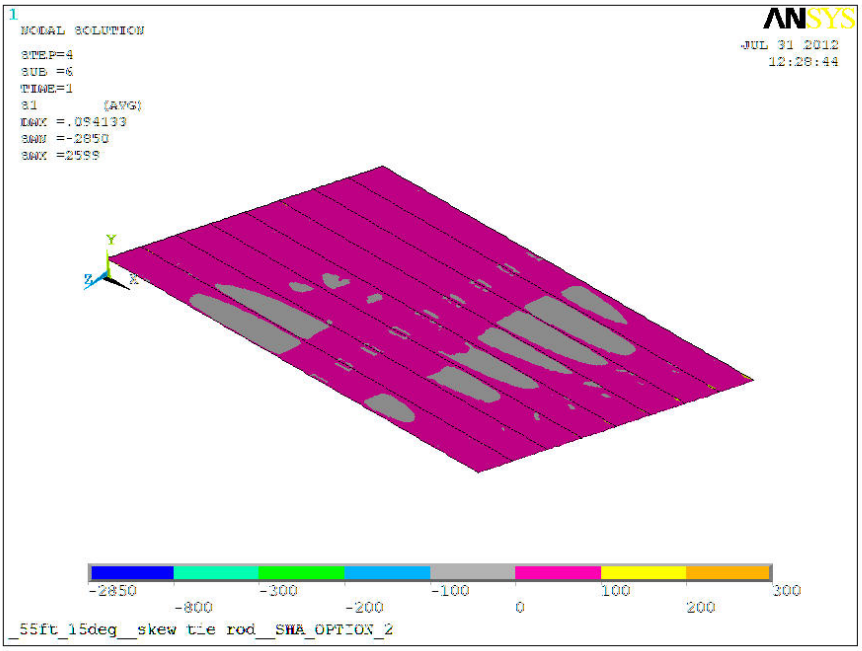

Figure C-49 First Principal Stress at the Slab-Deck Interface

C.24 Extension: Fifty-Five Foot, Fifteen Degree Skewed Bridge – Three Combined – HS-20 (Three Axle) Loading

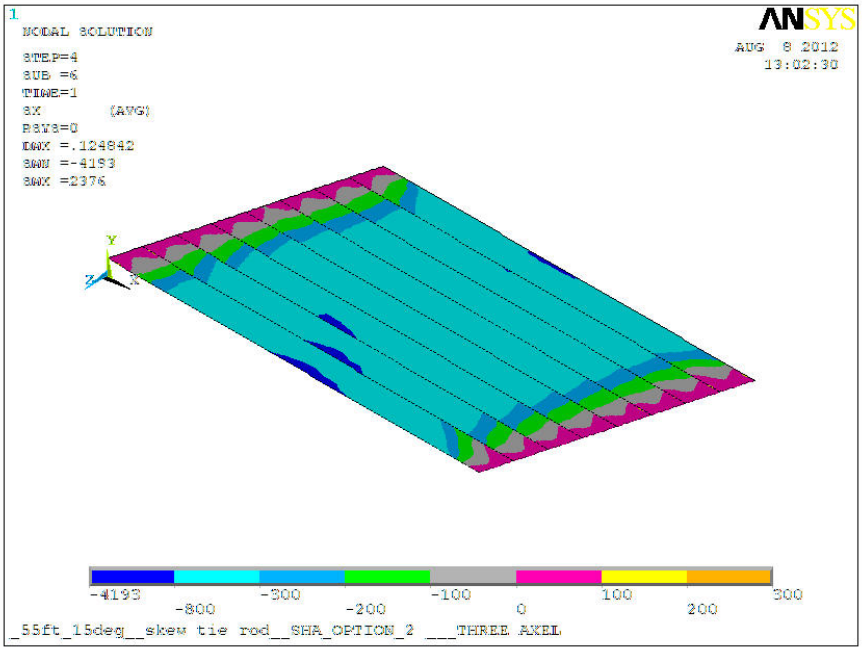

Figure C-50 Longitudinal Stress at the Slab-Deck Interface

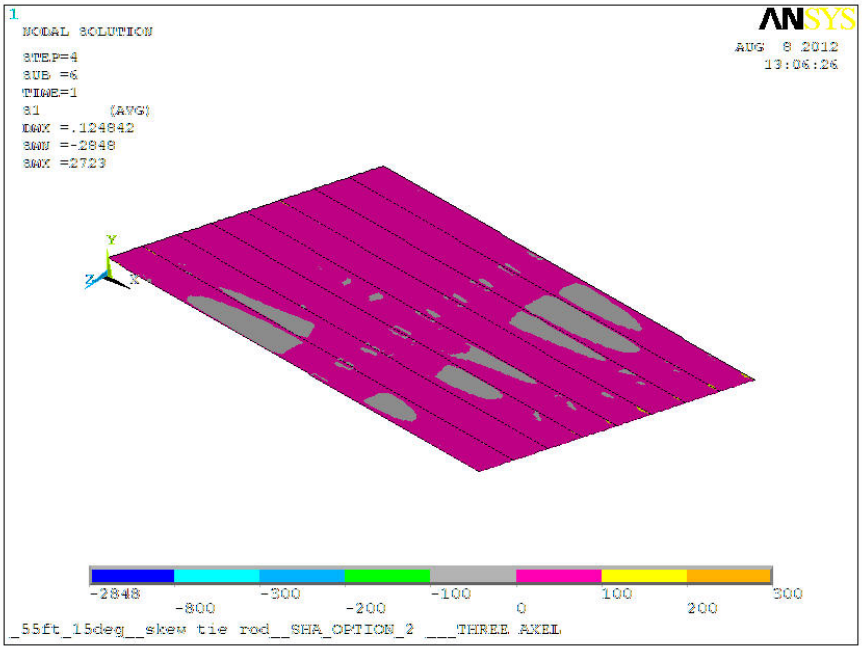

Figure C-51 First Principal Stress at the Slab-Deck Interface

C.25 Extension: Fifty-Five Foot, Fifteen Degree Skewed Bridge – Four Combined

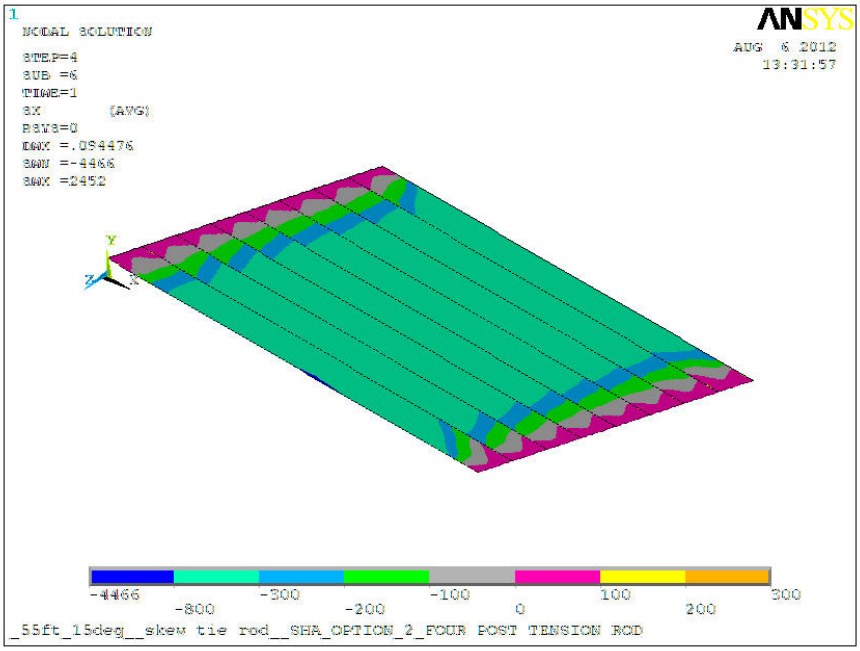

Figure C-52 Longitudinal Stress at the Slab-Deck Interface

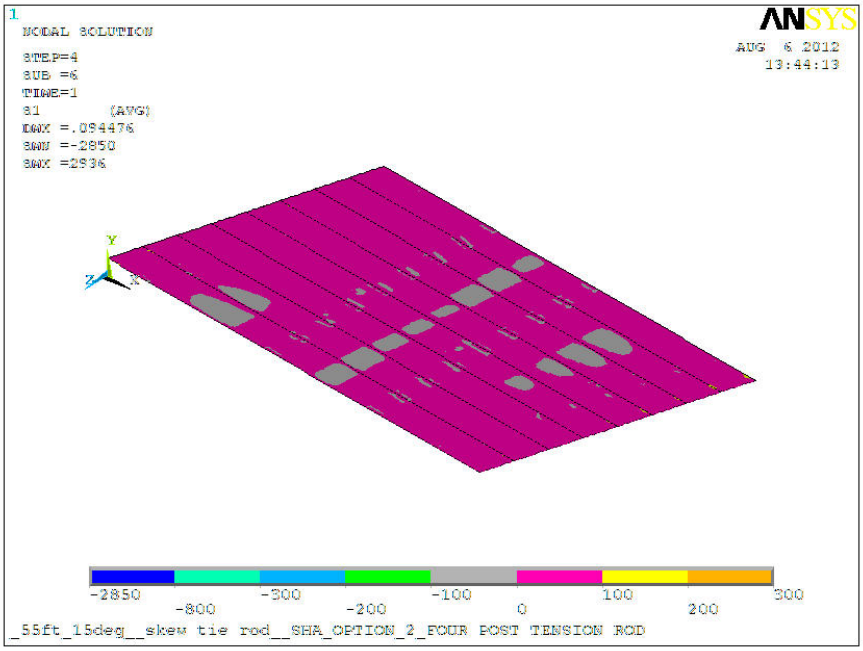

Figure C-53 First Principal Stress at the Slab-Deck Interface

C.26 Extension: Fifty-Five Foot, Thirty Degree Skewed Bridge – Three Combined

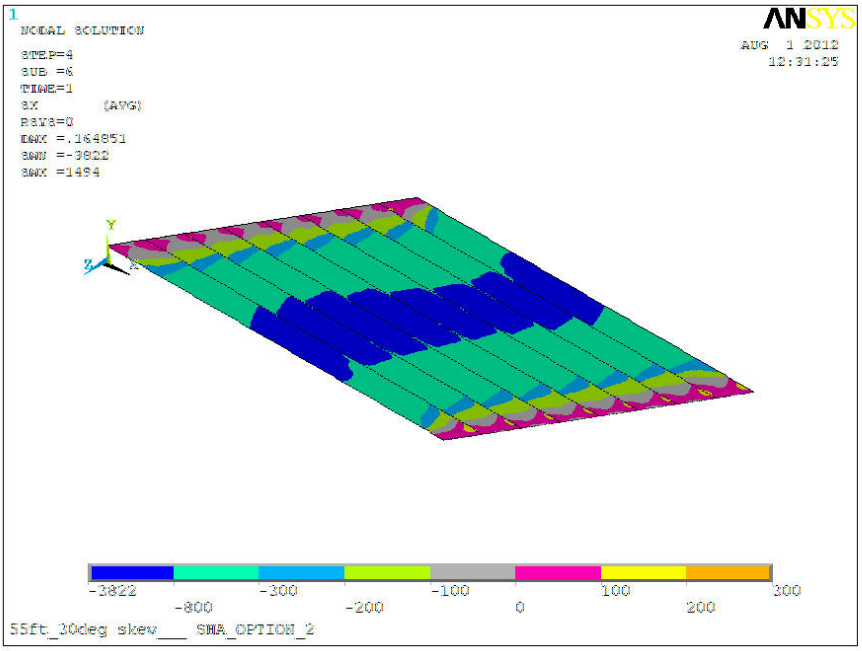

Figure C-54 Longitudinal Stress at the Slab-Deck Interface

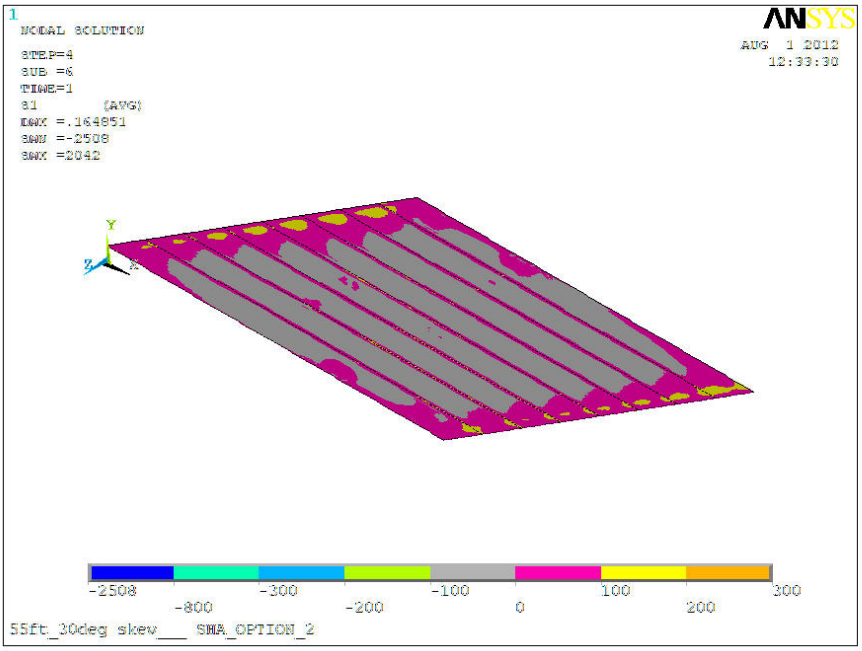

Figure C-55 First Principal Stress at the Slab-Deck Interface

C.27 Extension: Fifty-Five Foot, Thirty Degree Skewed Bridge – Four Combined

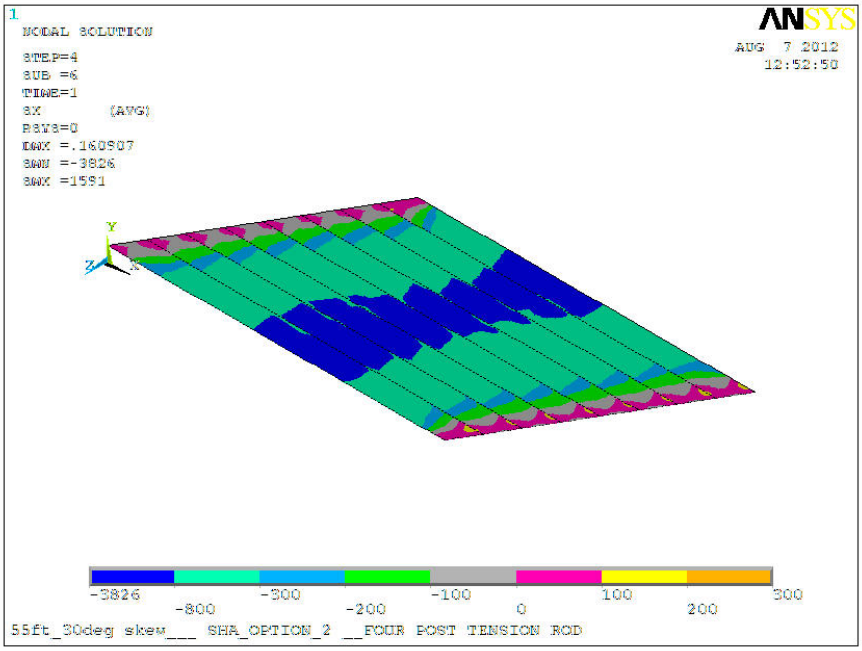

Figure C-56 Longitudinal Stress at the Slab-Deck Interface

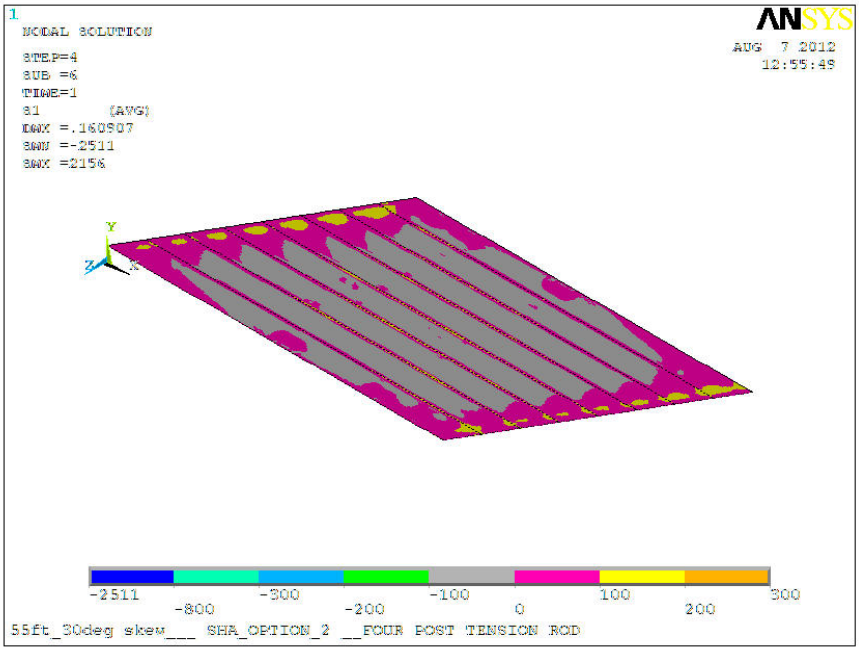

Figure C-57 First Principal Stress at the Slab-Deck Interface

References

AASHTO (2012). *AASHTO LRFD Bridge Design Specifications*, 6th Ed., American Association of State Highway and Transportation Officials, Washington, DC.

American Concrete Institute (ACI) (2011). "Building Code Requirements for Structural Concrete and Commentary." *ACI 318-11/ACI 318R-11*, Farmington Hills, MI.

ANSYS 10.0 [Computer software]. (2005). Cononsberg, PA, ANSYS.

Badwan, I. Z. and Liang, R. Y. (2007). "Performance Evaluation of Precast Posttensioned Concrete Multibeam Deck." *Journal of Performance of Constructed Facilities*, *21*(5), 368-374.

Bridge Diagnostics, Inc. (BDI). *BDI Strain Transducer Specifications*. June 13, 2012. <http://bridgetest.com/products/bdi-strain-transducers/>.

Bridge Engineering Software and Technology (BEST) Center, 2009. "Behavior and Analysis of an Instrumented MD355 over Wallace Creek Slab Bridge," Report to Maryland State Highway Administration and Federal Highway Administration (IBRC Program), Revision 0, University of Maryland, College Park.

Coletti, D., Chavel, B., and Gatti, W. (2011). "Challenges of Skew in Bridges with Steel Girders." *Transportation Research Record: Journal of the Transportation Research Board*, *2251*(5), 47-56.

Corven, J. and Moreton, A. (2004). "Post-Tensioning Tendon Installation and Grouting Manual," Report to Federal Highway Administration, Corven Engineering, Inc., Tallahassee, FL.

Federal Highway Administration (FHWA) (2011). *Deficient Bridges by State and Highway System*. February 21, 2012. <http://www.fhwa.dot.gov/bridge/deficient.cfm>.

Federal Highway Administration (FHWA) (2011). *Prefabricated Bridge Elements and Systems*. February 15, 2012. <http://www.fhwa.dot.gov/bridge/prefab/if09010/02b.cfm>.

Fu, C. C., Pan, Z., and Ahmed, M. S. (2011). "Transverse Posttensioning Design of Adjacent Precast Solid Multibeam Bridges." *Journal of Performance of Constructed Facilities*, *25*(3), 223-230.

Huang, H., Shenton, H. W., and Chajes, M. J. (2004). "Load Distribution for a Highly Skewed Bridge: Testing and Analysis." *Journal of Bridge Engineering*, *9*(6), 558-562.

Jeong, S. (2009). *Behavior and Analysis of an Instrumented Slab Bridge* (Master's thesis). University of Maryland, College Park, MD.

Marcuzzi, A. and Morassi, A. (2010). "Dynamic Identification of a Concrete Bridge with Orthotropic Plate-Type Deck." *Journal of Structural Engineering*, *136*(5), 586-602.

Mari, A. and Valdes, M. (2000). "Long-Term Behavior of Continuous Precast Concrete Bridge Model." *Journal of Bridge Engineering*, *5*(1), 22-30.

Maryland Department of Transportation State Highway Administration Office of Bridge Development (MDOT-SHA-OBD) (2006). "Slab Superstructure Details Standard Details." *Structural Standards Manual*.

Massachusetts Department of Transportation (MassDOT) (2009). *2009 LRFD Bridge Manual*. August 25, 2011. <http://www.mhd.state.ma.us/default.asp?pgid=bridge/bridgemanual_01&sid=about>.

Menassa, C., Mabsout, M., Tarhini, K., and Frederick, G. (2007). "Influence of Skew Angle on Reinforce Concrete Slab Bridges." *Journal of Bridge Engineering*, *12*(2), 205-214.

Modjeski and Masters, Inc. (2002). "Shear in Skewed Multi-beam Bridges", Report to National Cooperative Highway Research Program (Project 20-7/Task 107).

Narer, J. W. (1997). "A New Generation of Precast Prestressed Concrete Slab Bridges for Maryland's Rural Highways." *PCI Journal*, May/June, 16-20.

Oregon Department of Transportation (ODOT) (2004, rev. April 2011). *Bridge Design and Drafting Manual*. February 20, 2012. <http://www.oregon.gov/ODOT/HWY/BRIDGE/docs/BDDM/apr-2011_finals/section_1-2004_apr2011.pdf>.

Precast/Prestressed Concrete Institute (PCI) (2003). *PCI Bridge Design Manual*, 2nd Ed., Chicago, IL.

Ramirez, J. A. and Smith, J. P. (2003). *An Investigation on Transversely Prestressed Concrete Bridge Decks*. Joint Transportation Research Program, Indiana Department of Transportation and Purdue University, West Lafayette, Indiana.

Rhode Island Department of Transportation (RIDOT) (2010). *Bridge Design Standard Details*. August 29, 2011. <http://www.dot.ri.gov/documents/engineering/BlueBook/RIDOT_Bridge_Standards%202010.pdf>.

Roschke, P. N., Pruski, K. R., and Sripadanna, N. (1999). "Time-Dependent Behavior of Post-Tensioned Slab Bridge." *ACI Structural Journal*, *96*(3), 400-409.

Russell, H. G. (2009). *Adjacent Precast Concrete Box Beam Bridges: Connection Details*. National Cooperative Highway Research Program Synthesis 393, National Research Council Transportation Research Board, Washington, DC.

Russell, H. G. (2011). "Adjacent Precast Concrete Box-Beam Bridges: State of Practice." *PCI Journal*, Winter, 75-91.

Saber, A. and Alaywan, W. (2011). "Full-Scale Test of Continuity Diaphragms in Skewed Concrete Bridge Girders." *Journal of Bridge Engineering*, *16*(1), 21-28.

Schaffer, T. (1967). *Structural Response of a 45^{o} Skew Prestressed Concrete Box-Girder Highway Bridge Subjected to Vehicular Loading Brookville Bridge* (Master's thesis). Lehigh University, Bethlehem, PA.

Sharpe, G. P. (2007). *Reflective Cracking of Shear Keys in Multi-Beam Bridges* (Master's thesis). Texas A&M University, College Station, TX.

"Strain Gauge." *Wikipedia*. June 13, 2012. <http://en.wikipedia.org/wiki/Strain_gauge>.

Vermont Agency of Transportation (VTrans) (2011). *2011 Standard Specifications for Construction Book*. February 20, 2012. <http://www.aot.state.vt.us/conadmin/2011StandardSpecs.htm>.

"Wheatstone Bridge." *Wikipedia*. June 13, 2012. <http://en.wikipedia.org/wiki/Wheatstone_bridge>.